
Structures Research Report No. 716
FINAL PROJECT REPORT

August, 2001

Contract Title: Use of Grout Pads for Sign and Lighting Structures
UF Project No. 4910 4504 716 12
Contract No. BC354 RPWO #4

DESIGN GUIDELINES FOR ANNULAR BASE PLATES

Principal Investigator:

Ronald A. Cook, Ph.D., P.E.

Graduate Research Assistants:

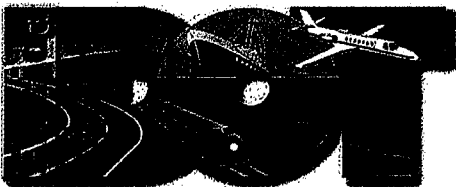
Brandon J. Bobo

Project Manager:

Marcus H. Ansley, P.E.

Department of Civil & Coastal Engineering
College of Engineering
University of Florida
Gainesville, Florida 32611

Engineering and Industrial Experiment Station



UNIVERSITY OF
FLORIDA

1. Report No. BC354 RPWO #4		2. Government Accession No.		3. Recipient's Catalog No.	
4. Title and Subtitle Design Guidelines for Annular Base Plates		5. Report Date August 2001		6. Performing Organization Code	
		8. Performing Organization Report No. 4910 45 04 716		10. Work Unit No. (TRAIS)	
7. Author(s) R. A. Cook and B. J. Bobo		9. Performing Organization Name and Address University of Florida Department of Civil Engineering 345 Weil Hall / P.O. Box 116580 Gainesville, FL 32611-6580		11. Contract or Grant No. BC354 RPWO #4	
12. Sponsoring Agency Name and Address Florida Department of Transportation Research Management Center 605 Suwannee Street, MS 30 Tallahassee, FL 32301-8064		13. Type of Report and Period Covered Final Report		14. Sponsoring Agency Code	
		15. Supplementary Notes Prepared in cooperation with the Federal Highway Administration			
16. Abstract <p>The report summarizes previous test results on 4, 6, and 8, bolt installations and provides test results for two-10 bolt installations with and without grout pads. The specimens investigated consist of tubular members welded to annular base plates and connected to a foundation with anchor bolts. The tubular members were loaded with a transverse load in order to produce a moment at the base plate-to-foundation connection. The results of this and previous projects were used to develop strength and serviceability design recommendations for annular base plates. The strength design recommendations include equations for determining the base plate thickness and the diameter of the anchor bolts. The serviceability recommendations provide a means to evaluate the rotation caused by deformation of the base plate and anchor bolts.</p>					
17. Key Words Annular Base Plates, Grout, Base Plates, Mast Arms, Traffic Signal Supports, Anchor Bolts			18. Distribution Statement No restrictions. This document is available to the public through the National Technical Information Service, Springfield, VA, 22161		
19. Security Classif. (of this report) Unclassified		20. Security Classif. (of this page) Unclassified		21. No. of Pages 114	22. Price

DISCLAIMER

"The opinions, findings, and conclusions expressed in this publication are those of the authors and not necessarily those of the Florida Department of Transportation or the U.S. Department of Transportation.

Prepared' in cooperation with the State of Florida Department of Transportation and the U.S. Department of Transportation."

DESIGN GUIDELINES FOR ANNULAR BASEPLATES

Contract No. BC 354 RPWO #4
UF No. 4910 4504 716 12

Principal Investigator:	Ronald A. Cook
Graduate Research Assistant:	Brandon J. Bobo
FDOT Technical Coordinator:	Marcus H. Ansley

Engineering and Industrial Experiment Station
Department of Civil Engineering
University of Florida
Gainesville, Florida

TABLE OF CONTENTS

	<u>Page</u>
CHAPTERS	
1 INTRODUCTION.....	1
1.1 General.....	1
1.2 Objective.....	2
1.3 Scope.....	2
2 BACKGROUND.....	4
2.1 Introduction.....	4
2.2 Strength Requirements.....	6
2.3 Serviceability Requirements.....	16
2.4 Summary.....	20
3 DEVELOPMENT OF EXPERIMENTAL PROGRAM.....	23
3.1 Introduction.....	23
3.2 Development of Test Specimens.....	23
3.2.1 Materials.....	24
3.2.2 Dimensions.....	25
3.2.2.1 Anchor Bolts.....	25
3.2.2.2 Base Plates.....	26
3.2.2.3 Grout Pads.....	27
3.2.2.4 Tubular Members.....	29
3.2.3 Test Block Design Basis.....	30
3.3 Development of Test Setup.....	30
4 IMPLEMENTATION OF EXPERIMENTAL PROGRAM.....	33
4.1 Introduction.....	33
4.2 Concrete Casting.....	25
4.3 Materials.....	34
4.3.1 Concrete.....	34
4.3.2 Anchor Bolts.....	35
4.3.3 Grout Mixtures.....	36
4.3.4 Base Plates.....	37
4.3.5 Pipes.....	38
4.4 Anchor Installation.....	38
4.5 Grout Application.....	39
4.6 Test Equipment.....	43
4.6.1 Test Setup.....	43
4.6.2 Hydraulic Loading System.....	44
4.6.3 Load Cells.....	44

4.6.4	Displacement Measurement Instrumentation.....	47
4.6.5	Data Acquisition Unit.....	49
4.7	Load and Displacement Reduction.....	49
4.8	Test Procedure.....	50
5	TEST RESULTS.....	52
5.1	Introduction.....	52
5.2	Test Observations.....	52
5.2.1	Test #1.....	52
5.2.2	Test #2.....	53
5.3	Summary of Test Results.....	53
5.4	Individual Test Results.....	54
6	DESIGN CONSIDERATIONS.....	58
6.1	Introduction.....	58
6.2	Strength.....	58
6.2.1	Base Plate Moment Capacity.....	58
6.2.2	Anchor Bolts Loads.....	61
6.3	Serviceability.....	62
6.3.1	Stiffness Evaluation.....	63
6.3.2	Analysis of Connection Rotation.....	65
6.3.3	Serviceability Evaluation.....	66
6.4	Summary – Design Recommendations.....	69
6.4.1	Required Base Plate Thickness.....	69
6.4.2	Required Effective Anchor Bolt Area.....	70
6.4.3	Serviceability Checks.....	71
7	SUMMARY AND CONCLUSIONS.....	72
7.1	Summary.....	72
7.2	Conclusions.....	74
	APPENDIX A INSTRUMENTATION NUMBERING AND ORIENTATION	77
	APPENDIX B LVDT DATA.....	80
	APPENDIX C LOAD CELL DATA.....	87
	APPENDIX D LOAD-DISPLACEMENT GRAPHS.....	94
	APPENDIX E MOMENT-ROTATION GRAPHS.....	96
	APPENDIX F STIFFNESS PLOTS.....	98
	APPENDIX G DERIVATION OF EQ. (2-9).....	100
	APPENDIX H MOMENT-ROTATION GRAPHS WITH EQ. (2-9).....	103
	LIST OF REFERENCES.....	110

CHAPTER 1

INTRODUCTION

1.1 General

Base plates are structural elements used to connect structural members to their foundations. They are commonly used in conjunction with tubular high mast poles, roadway light poles, and traffic mast arms. The base plate connects the sign or lighting

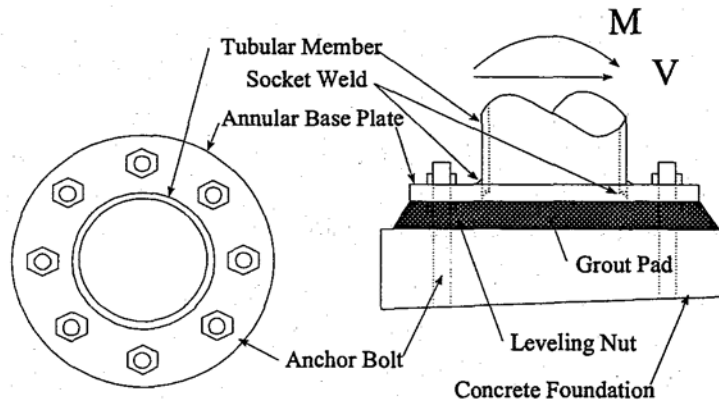


Figure 1.1 – Typical annular base plate with grout pad

Currently, the Florida Department of Transportation (FDOT) requires a grout pad beneath all signing and lighting structure base plates. Several states are eliminating this as a requirement believing that it is detrimental to the maintenance of the structures.

Based on recent failures there is evidence that grout pads are critical to the performance of these structures. The presence (or lack) of a grout pad affects both the structural response and durability of the installation. Currently, there is little information pertaining

to both the structural and serviceability benefits of placing a grout pad beneath base plates.

1.2 Objective

The primary objective of this study was to evaluate the structural behavior of sign and lighting structure base plates by performing tests on ten bolt annular plate installations and consolidating research from previous studies done at the University of Florida. Design criteria for evaluating strength and serviceability was to be developed by combining all of the research data.

1.3 Scope

This project was divided into four major tasks: 1)

- 1) Literature review.
- 2) Development of testing program.
- 3) Structural tests.
- 4) Development of strength and serviceability design guidelines.

The objective of the literature review was to determine what testing procedures were used, what results were obtained, and what had not been covered by similar studies. The second part of the project was to develop a testing program to experimentally evaluate the strength and serviceability behavior of base plates exposed to large bending moments. The program was developed to supplement previous testing. The third part of the project implemented the testing program. Construction of a test block and frame,

fabrication of base plates and anchor bolts, and grout pad placement were included in this phase. Load distribution, bolt displacements, and pipe displacement were measured after the application of a bending moment to the plate.

Analysis of recorded experimental data from this research and the results of previous research were combined to develop strength and serviceability design recommendations.

CHAPTER 2 BACKGROUND

2.1 Introduction

Studies by Cook et al. (1995) and Cook et al. (2000) involved a series of structural tests on different annular base plate configurations with and without grout pads. An analytical study by Cook et al. (1998) was performed to develop a design equation for calculating deflections. These projects have looked at several variables involved in annular base plate design as shown in Figure 2.1 and including:

- base plate thickness, t
- base plate radius, r_{pl}
- number of bolts, n
- moment, M , applied through an eccentric shear force, P • pipe radius, r_p
- distance to applied shear force from bottom of base plate, L
- distance between outside of pipe and the centerline of anchor bolt, r_d
- distance from center of pipe to centerline of anchor bolts, r_b

Cook et al. (1-995) tested annular base plates without grout pads. The tests were performed using several different combinations of the design variables. The test dimensions for the Cook et al. (1995) study are listed in Table 2.1. Cook et al. (2000) tested base plates using grout pads. The plates were first tested ungrouted through the elastic range. After the initial test grout pads were put in place and then the specimens were tested to failure. Each of the tests was designated by the nominal diameter of the

tube, the thickness of the base plate, the number of anchors in the plate, and whether or not a grout pad was present. For example, 8-3/4-10-U refers to a 3/4 inch thick plate with a nominal eight inch diameter tube, a ten anchor pattern and no grout pad. The test dimensions for the Cook et al. (2000) are listed in Table 2.2.

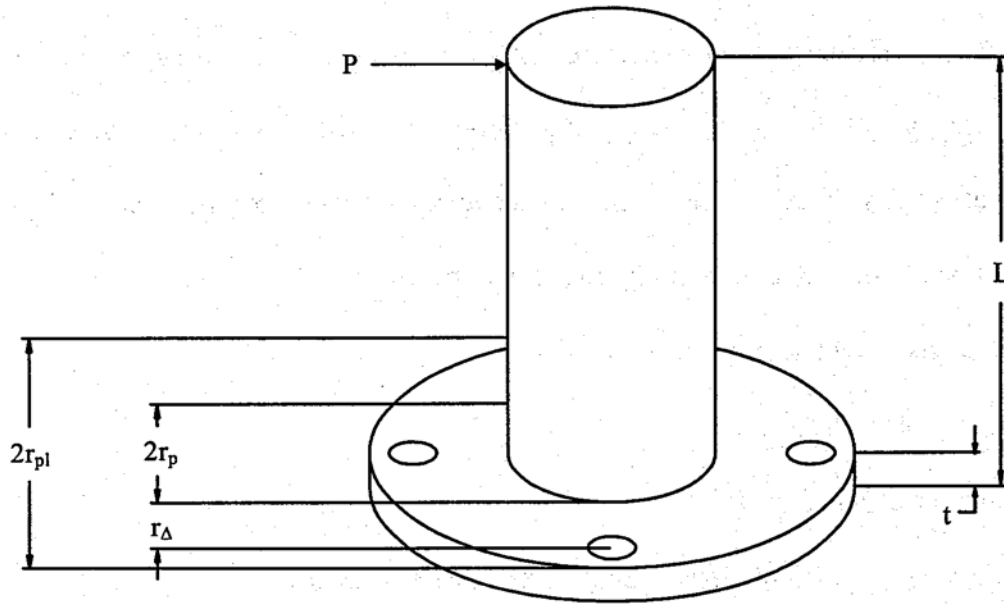


Figure 2.1 Base plate and pipe dimensions

Table 2.1 Test specimen dimensions from Cook et al. (1995)

Test #	Bolt Circle Diam. inches	Pipe Diam. inches	Bolts	Plate Thickness inches	r_{Δ}/t
6-1-4d	11.5	6.63	4	1.0	2.44
6-1-4s	11.5	6.63	4	1.0	2.44
6-1-6	11.5	6.63	6	1.0	2.44
6-1-8	11.5	6.63	8	1.0	2.44
6-3/4-4d	11.5	6.63	4	0.75	3.25
6-3/4-8	11.5	6.63	8	0.75	3.25
8-3/4-4d	11.5	8.63	4	0.75	1.92
8-3/4-6	11.5	8.63	6	0.75	1.92
8-3/4-8	11.5	8.63	8	0.75	1.92

Table 2.2 Test specimen dimensions from Cook et al. (2000)

Test #	Bolt Circle Diam. inches	Pipe Diam. inches	Bolts	Plate Thickness inches	r_d/t
8-3/4-8-U	11.5	8.63	8	0.75	1.92
8-3/4-8-G	11.5	8.63	8	0.75	1.92
8-3/4-4s-U	11.5	8.63	4s	0.75	1.92
8-3/4-4s-G	11.5	8.63	4s	0.75	1.92
6-3/4-4sW-U	11.5	6.63	4s	0.75	3.25
6-3/4-4sW-G	11.5	6.63	4s	0.75	3.25
6-3/4-4sW-GS	11.5	6.63	4s	0.75	3.25
6-3/4-4s-U	11.5	6.63	4s	0.75	3.25
6-3/4-4s-G	11.5	6.63	4s	0.75	3.25
6-3/4-4s-GS	11.5	6.63	4s	0.75	3.25

2.2 Strength Requirements

The results of the Cook et al. (1995) and Cook et al. (2000) studies yielded design equations for both plate thickness and bolt diameter. Various design models were investigated during these projects including both elastic models and yield line models. Although some yield line models exhibited a slightly better fit to test data they were abandoned due to their complexity.

The recommended equation for determining the required base plate thickness was based on a combination of the elastic distribution of loads to anchors in annular base plates subjected to an applied moment coupled with studies' by Westergaard (1930) on the maximum moments sustained by cantilevered plates subjected to concentrated loads. The following presents a summary of the derivation of the recommended equation for plate thickness.

From Westergaard (1930) the maximum unit moment (m) in a cantilevered plate subjected to a concentrated load (P) is given by Eq. (2-1):

(2-1)

The load (P) on any anchor in a bolt group subjected to an applied moment based on an elastic distribution of loads to the bolts is given by Eq. (2-2):

$$P = \frac{Mc}{I_{boltgroup}} \quad (2-2)$$

where:

P = the force in an anchor bolt due to the applied moment (M)

M = the applied moment

c = distance from the center of the bolt group to the bolt considered

$I_{boltgroup} = \frac{n}{2} r_b^2$, moment of inertia of the bolt group

The maximum load is experienced by the outermost anchor when $c = rb$ and is reflected in Eq. (2-3):

$$P = \frac{2M}{nr_b} \quad (2-3)$$

Combining Eq. (2-1) and Eq. (2-3) yields Eq. (2-4):

$$m = \frac{2M}{\pi nr_b} \quad (2-4)$$

All annular base plates tested in these studies experienced significant yielding at the maximum applied load therefore the unit moment capacity of the plate (m) is evaluated as:

$$m = \frac{F_y t^2}{4} \quad (2-5)$$

Substituting the unit moment (m) from Eq. (2-5) into Eq. (2-4) yields Eq. (2-6) for predicted moment capacity (M). Eq. (2-6) is rearranged to determine plate thickness (t) in Eq. (2-7).

$$M = \frac{n\pi r_b t^2 F_y}{8} \quad (2-6)$$

$$t = \sqrt{\frac{8M}{n\pi r_b F_y}} \quad (2-7)$$

where:

M = applied moment

n = number of bolts

r_b = distance from center of plate to center of bolt

t = base plate thickness

F_y = yield stress of the base plate

Table 2.3 shows the Cook et al. (1995) study results for predicted moment capacity and base plate thickness. Table 2.4 shows the Cook et al. (2000) results. As shown in these tables, the test results indicate that although the resulting plate thickness is

reasonable there is a large variation in the maximum applied moment compared to the predicted moment.

Table 2.3 Measured and predicted moments with design plate thickness (Cook et al., 1995)

Test #	Maximum Applied Moment kip-in	Predicted Moment Eq. (2-6) kip-in	$M_{\text{predicted}}/M_{\text{applied}}$	Actual Thickness in	Design Thickness Eq. (2-7) in
6-1-4d	534	474	0.89	1.0	1.06
6-1-4s	647	474	0.73	1.0	1.17
6-1-6	688	711	1.03	1.0	0.98
6-1-8	706	948	1.34	1.0	0.86
6-3/4-4d	351	281	0.80	0.75	0.84
6-3/4-8	405	563	1.39	0.75	0.64
8-3/4-4d	562	281	0.50	0.75	1.06
8-3/4-6	863	422	0.49	0.75	1.07
8-3/4-8	962	563	0.59	0.75	0.98

Table 2.4 Measured and predicted moments with design plate thickness for connections with grouted plates and grouted plates with stiffeners (Cook et al., 2000)

Test #	Maximum Applied Moment kip-in	Predicted Moment Eq. (2-6) kip-in	$M_{\text{predicted}}/M_{\text{applied}}$	Actual Thickness in	Design Thickness Eq. (2-7) in
8-3/4-8-G	889	562	0.63	0.75	0.94
8-3/4-4s-G	970	281	0.29	0.75	1.39
6-3/4-4sW-GS	753	281	0.37	0.75	1.23
6-3/4-4s-GS	756	281	0.37	0.75	1.23

These studies also included measurement of the actual bolt loads during testing. Measured bolt loads at ultimate were compared to the loads predicted by Eq. (2-3). Table 2.5 shows the Cook et al. (1995) results while Table 2.6 shows the Cook, et al. (2000) results. Table 6.5 in Cook et al. (2000) shows that the distribution of load to the anchor

bolts is also valid under service loads with a mean of 0.96 and coefficient of variation of 0.14 for nine different tests that included ungrouted, grouted, and stiffened base plates.

Table 2.5 Measured and predicted bolt loads at ultimate (Cook et al., 1995)

Test #	Measured Bolt Load kips	Predicted Bolt Load Eq. 2-3 kips	Predicted $P_{bolt}/$ Measured P_{bolt}
6-1-4d	49.9	47.3	1.05
6-1-4s	40.7	58.6	1.43
6-1-6	34.4	39.2	1.14
6-1-8	29.3	30.6	1.04
6-3/4-4d	29.1	30.0	1.03
6-3/4-8	19.7	18.0	0.91
8-3/4-4d	38.7	48.2	1.25
8-3/4-6	43.5	49.8	1.14
8-3/4-8	33.5	41.6	1.24
		Mean:	1.13

Table 2.6 Measured and predicted bolt loads at ultimate for connections with grouted plates and grouted plates with stiffeners (Cook et al., 2000)

Test #	Measured Bolt Load kips	Predicted Bolt Load Eq. (2-3) kips	Predicted $P_{bolt}/$ Measured P_{bolt}
8-3/4--8-G	N/A	38.7	N/A
8-3/4-4s-G	67.6	59.6	0.88
6-3/4-4sW-GS	39.5	46.3	1.17
6-3/4-4s-GS	41.2	46.5	1.13
		Mean:	1.06

During the review period for this project, Mr. Marcus H. Ansley, the Project Manager for the FDOT, developed a yield line analysis that varied from those considered previously in the Cook et al. (1995) study. The yield line analysis is based on the observation that the final deformed shape of the annular base plates was essentially the

same for previously tested six and eight bolt arrangements and the ten bolt arrangement reported in this study. Figures 2.2 and 2.3 show base plate displacement contours for six and eight bolt tests in the Cook et al. (1995) study.

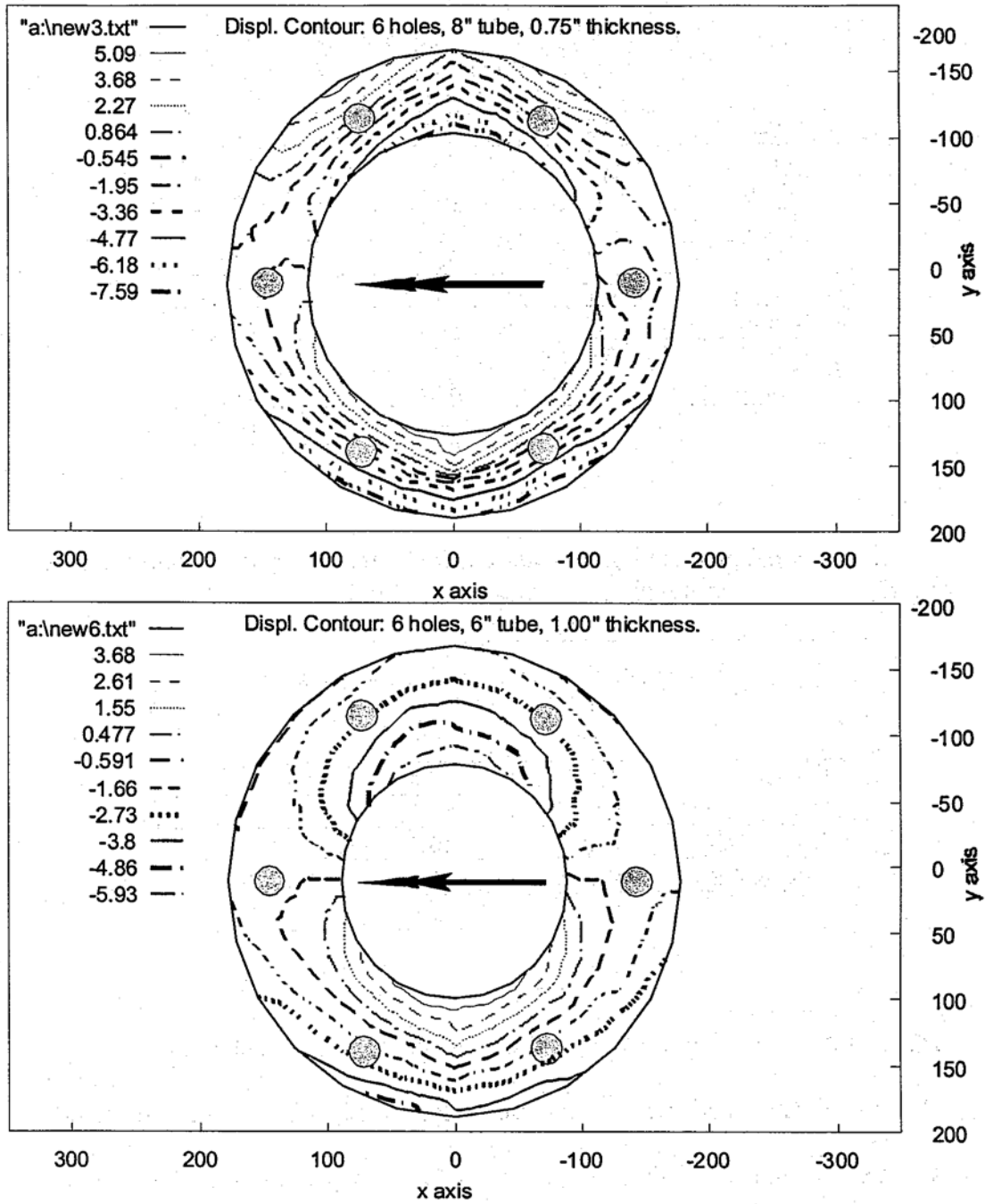


Figure 2.2 – Base plate contours for the six-bolt pattern (Cook et al. (1995))

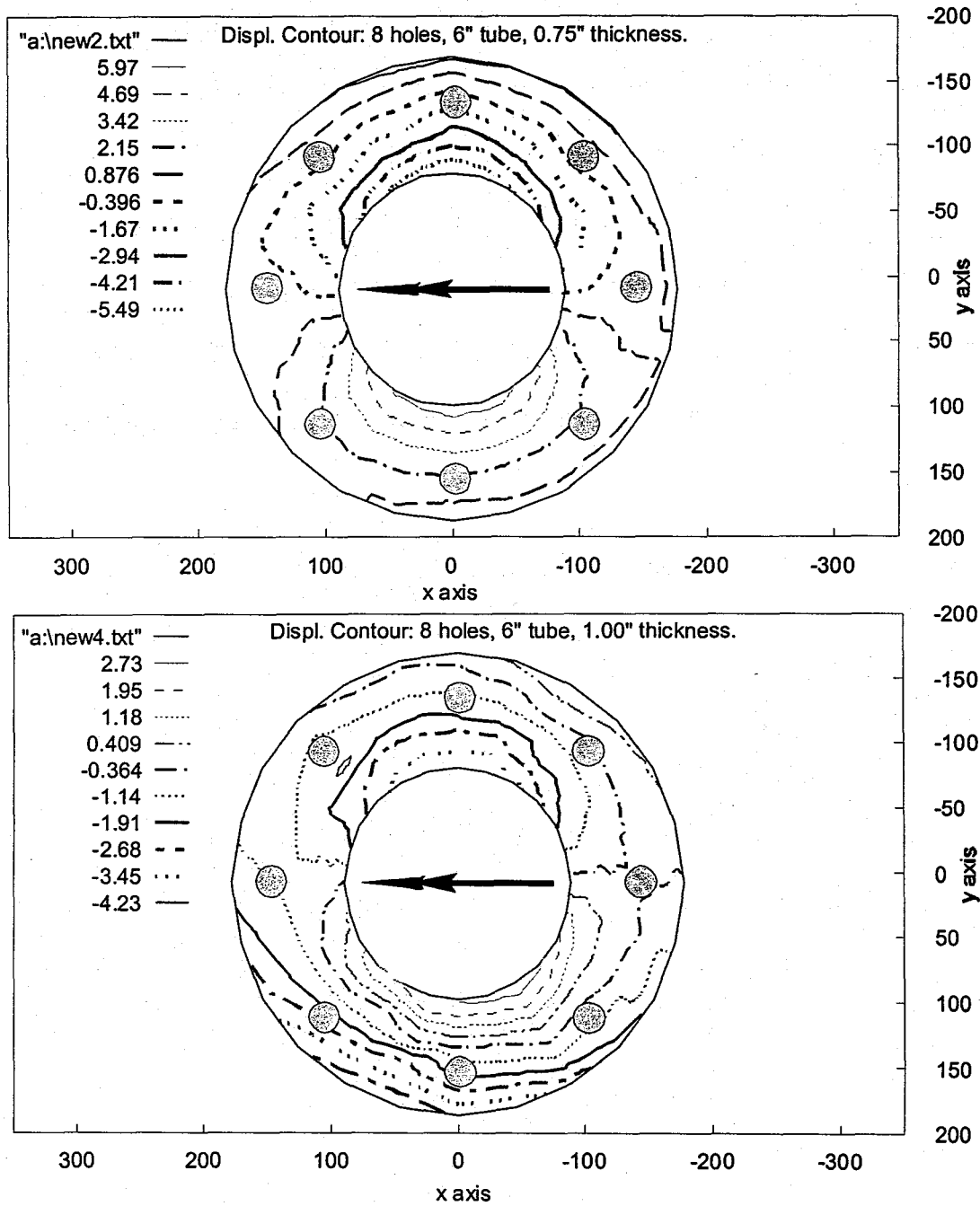


Figure 2.3 – Base plate contours for the eight-bolt pattern (Cook et al. (1995))

The consistency of the deformed shapes for the six and eight bolt tests regardless of the number of anchors led to the development of the yield line mechanism represented

by Fig. 2.4. Fig. 2.4 shows a polygon with 12 sides at the pipe/plate intersection. By increasing the number of sides to infinity the pipe/plate intersection will be represented by a circle and the final deformed shape will reflect that observed in the tests. Eq. (2-8) provides the results of the evaluation of the yield line mechanism after the number of sides is allowed to approach infinity. Full details of the calculations are provided in Appendix G. Although the development of the model for the yield line mechanism is complex as shown in Appendix G, the resulting equation is quite simple to apply.

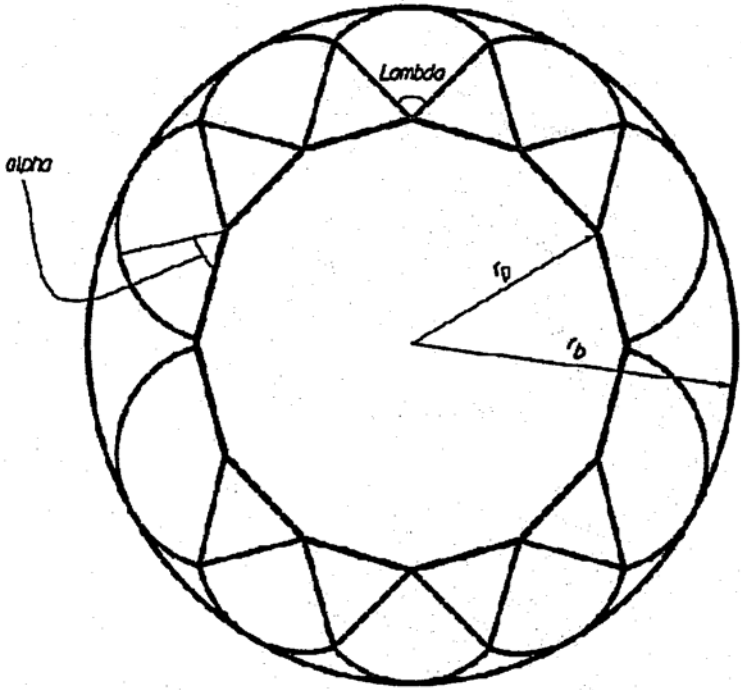


Figure 2.4 Yield line mechanism

$$M = 4 m r_p \frac{r_b}{r_b - r_p} \tag{2-8}$$

Substituting Eq. (2-5) for unit moment (m) into Eq. (2-8) yields Eq. (2-9).

$$M = F_y t^2 \frac{r_p r_b}{r_b - r_p} \quad (2-9)$$

It should be noted that the deformed shapes for four bolt arrangements with both square and diamond bolt patterns are different than those exhibited by the six and eight bolt tests. Typical deformed shapes for the four bolt square and diamond patterns from Cook et al. (1995) are shown in Fig.2.5.

Another item of consideration raised during the project review was whether it would be better to assess strength design equations based on the ultimate strength or yield strength of the tested annular base plate assemblies. Previous studies by Cook et al. (1995) and Cook et al. (2000) based the evaluation of proposed strength design equations on the maximum moment sustained by the annular base plate test specimen. From a purely strength design perspective this seems acceptable, however, based on the importance of the base plate remaining in the elastic range under design loads, it was determined that comparison of design equations to the performance of the test specimens in the range of initial yielding would be appropriate. This is discussed further in Chapter 6. Given the complexity of the equation developed for serviceability checks as discussed below, it seems prudent to base design on performance in the elastic range since this could preclude the need for separate serviceability calculations.

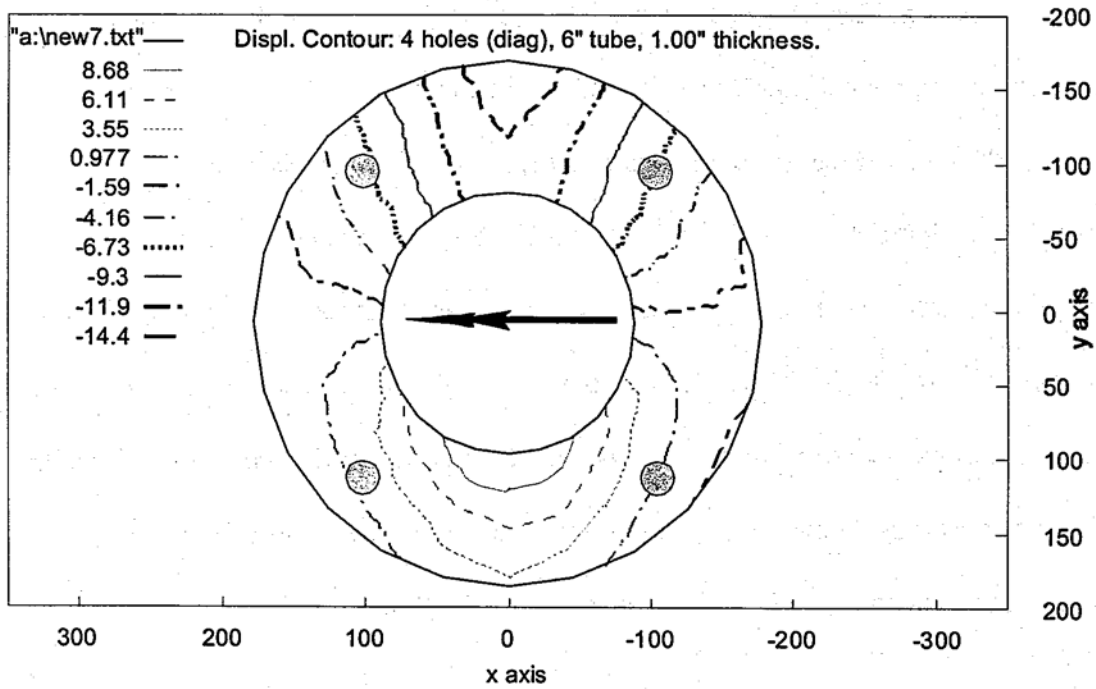
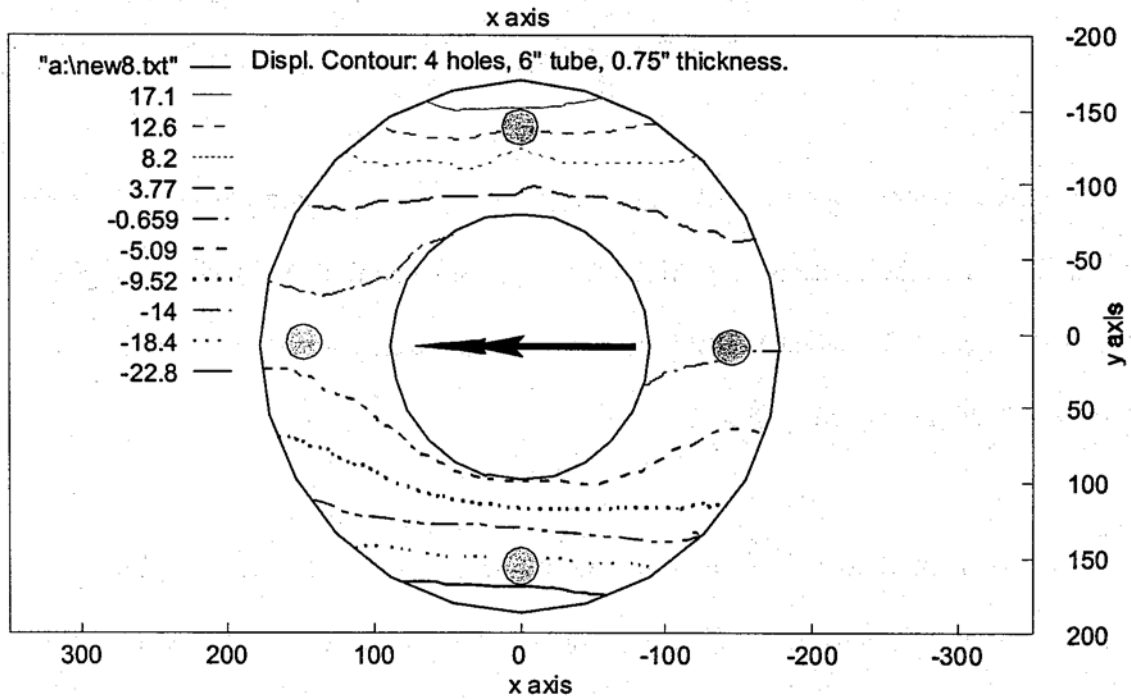


Figure 2.5 – Base plate contours for the four-bolt pattern (Cook et al. (1995))

2.3 Serviceability Requirements

The serviceability performance of annular base plate installations was first investigated by Cook et al. (1995). The primary finding of this study was that the deflection of annular base plate structures could not be accurately determined by considering only the deflection of the structural member (i.e., the additional deflection caused by rotation associated with loading of the anchor bolts and base plate need to be addressed). This study was followed by an analytical finite element study reported in Cook et al. (1998) and an experimental study reported in Cook et al. (2000) that addressed ungrouted, grouted, and stiffened base plates. Figure 2.5 illustrates the source of the different components of deflections.

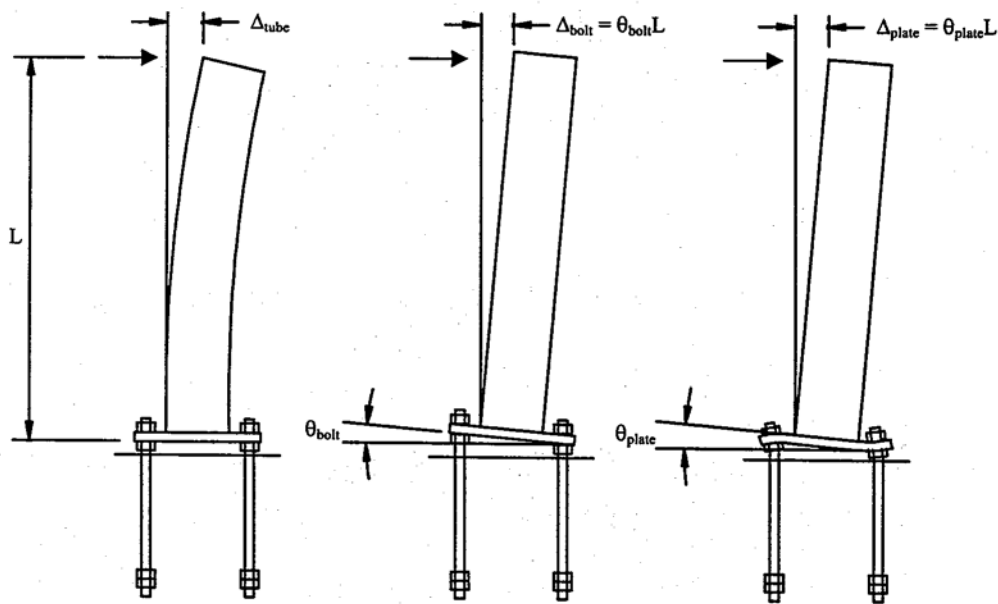


Figure 2.5 Components of total deflection

Based on the Cook *et al.* (2000) study that incorporated results of the previous studies, the recommended equation to account for the rotation due to loading of the anchor bolts and base plate is given by Eq. (2-10) The first term in Eq. (2-10) accounts for rotation due to loading of the anchor bolts and is based on elastic deformation of the anchor bolts under the applied moment. The second term accounts for rotation of the base plate and is based on a rationally developed equation that was initially presented by Cook *et al.* (1998) and that was empirically adjusted to reflect both the finite element results (Cook *et al.* 1998) and test results from Cook *et al.* (2000).

$$\theta_{bolt+plate} = \theta_{bolt} + \theta_{plate} \quad (2-10)$$

$$\theta_{bolt} = \frac{2ML_b}{nr_b^2 A_b E_b} \quad (2-11)$$

$$\theta_{plate} = \frac{45M}{Er_b^2} \left(\frac{r_b - r_p}{t} \right)^{1.23} \quad (2-12)$$

where:

M = applied moment

L_b = length of bolt from top of plate to embedded head of anchor bolt

n = number of anchor bolts

A_b = cross-sectional area of anchor bolt

E_b = modulus of elasticity of bolt

E = modulus of elasticity of plate

r_b = distance from center of plate to center of bolt

r_p = radius of pipe

t = thickness of base plate

$$b = 2\sqrt{r_b^2 - r_p^2}$$

Table 2.7 presents the results a comparison of Eq. (2-12) for plate rotation to the predicted plate rotation from the finite element analysis normalized by assuming a value of 1.0 for the applied moment and modulus of elasticity for the base plate.

Table 2.7 Evaluation of plate rotation using Eq. (2-12) based on FEM analysis

Designation	Calculated FEM	Eq. (2-12)	Measured/ Eq. (2-12)	r_d/t
10-3/4-6	0.4500	0.3912	1.1504	1.67
10-1-6	0.2620	0.2311	1.1339	1.25
10-1.75-6	0.1730	0.1536	1.1263	1.00
25-2-8	0.0258	0.0273	0.9457	2.00
25-2.375-8	0.0186	0.0199	0.9337	1.68
25-3-8	0.0112	0.0130	0.8621	1.33
24-1-1.75	0.0337	0.0339	0.9930	2.00
24-1.75-12	0.0207	0.0214	0.9656	1.56
24-1.75-12	0.0129	0.0148	0.8718	1.27
6-1-4d	0.7738	0.7394	1.0466	2.44
6-1-4s	0.7907	0.7394	1.0694	2.44
6-1-6	0.7110	0.7394	0.9616	2.44
6-1-8	0.6813	0.7394	0.9215	2.44
6-3/4-4d	1.2878	1.2517	1.0288	3.25
6-3/4-4s	1.5567	1.2517	1.2438	3.25
6-3/4-8	1.0767	1.2517	0.8601	3.25
8-3/4-4d	0.7238	0.5885	1.2299	1.92
8-3/4-4s	0.4693	0.5885	0.7974	1.92
8-3/4-6	0.5681	0.5885	0.9653	1.92
8-3/4-8	0.2243	0.2599	0.8627	1.92
		Mean:	0.998	
		COV:	0.166	

Table 2.8 shows a comparison of the actual test results for ungrouted base plates from Cook et al. (2000) based on an applied moment of 124 kip-in that was determined to

be in the elastic range for the tests compared to Eq. (2-10) that includes both rotation due to the anchor bolts and rotation due to deformation of the base plate.

Table 2.8 Evaluation of rotation from anchor bolts and base plate using Eq. (2-10) for ungrouted base plates based on Cook et al. (2000) test results

Test #	θ_{measured}	$\theta_{\text{predicted}}$	$\theta_{\text{measured}}/\theta_{\text{predicted}}$
8-3/4-8-U	0.00130	0.00336	0.388
8-3/4-4s-U	0.00274	0.00420	0.651
6-3/4-4sW-U	0.00583	0.00704	0.828
6-3/4-4s-U	0.00711	0.00704	1.01
		Mean:	0.719
		COV:	0.319

It should be noted that test #8-3/4-8-U exhibited an unusually high stiffness that was likely due to bond developed by the anchor bolts (i.e. the anchor bolts did not exhibit deformation over their entire embedded length). When this test is not considered, the results of the ungrouted tests from Cook et al. (2000) provide a mean of 0.83 and coefficient of variation of 0.22.

Cook et al. (2000) observed that the addition of grout pads stiffened the connections and that Eq. (2-10) resulted in an overprediction of the rotations. For grouted base plates, the measured rotations were on average 66% of the rotation predicted by Eq. (2-10). Eq. (2-10) was modified with an adjustment factor to yield Eq. (2-13),

$$\theta_{\text{bolt +grouted plate}}^B = 0.66\theta_{\text{bolt+plate}} \quad (2-13)$$

It was also observed that the use of both a grout pad and stiffeners significantly increased the connection stiffness of the base plates. Analysis revealed that the measured values were an average of about 39% of the predicted values. An adjustment factor of 0.39 was applied to the original form of Eq. (2-10). The result was Eq. (2-14).

$$\theta_{\text{bolt+ grouted stiffened plate}} = 0.39\theta_{\text{bolt+plate}} \quad (2-14)$$

2.4 Summary

The Cook et al. (1995) study was initiated to evaluate the strength and general behavior of annular base plate connections subjected to an applied moment. The primary purpose of this study was to develop a method to determine the required base plate thickness. Several behavioral models were investigated during this study including both elastic models based on plate theory and models based on yield line analysis. Overall structural rotations due to deformations of both the anchor bolts and base plate were not a primary consideration during the course of this study. Based on the results of the Cook et al. (1995), it was determined that the overall deflection of the annular base plate structure was dependent on both anchor bolt and base plate deformations as well as that of the attached structural member, this led to the Cook et al. (1998) finite element study. This study investigated annular base plate systems representative of the size of systems typically specified by the MOT and the size of those tested in the Cook et al. (1995) study. This resulted in recommendations for evaluating the contribution of both the anchor bolt and base plate deformations to the overall displacement of the annular base plate system.

In the study reported by Cook et al. (2000); the effect of grout pads relative to both structural behavior and protection from corrosion were investigated. The results of this study, indicated that protection from corrosion is significantly improved with the addition of a grout pad. The study also resulted in recommendations for evaluating both strength and serviceability behavior of ungrouted and grouted annular base plates.

As a result of these studies, it can be concluded that both the strength and serviceability evaluations of the annular base plate are highly indeterminate. From a strength perspective, the distribution of load to the anchor bolts seems fairly straightforward as exhibited by Table 2.5 and Table 2.6 that are based on an elastic distribution of load to the anchor bolts (Eq. For the determination of the required base plate thickness, several approaches are possible. The most promising: of these is the yield line method presented by Mr. Marcus Ansley presented above and compared to test data in Chapter 6. From a serviceability perspective (i.e., structural rotation due to deformation of both the anchor bolts and base plate), the prediction of rotation is extremely difficult to determine from experimental results due to the fact that the anchors may or may not be de-bonded over their entire length and that the behavior of the base plate is influenced by the performance of the socket weld between the base plate and the structural member.

Based on the results of the previous studies, it is recommended that the design of the base plate and anchor bolts be determined based on service loads in order to minimize the need for calculating the additional deflections caused by rotation of the base

plate/anchor bolt system. If the base plate thickness were determined based on ultimate capacity, additional serviceability checks would certainly be necessary.

CHAPTER 3 DEVELOPMENT OF EXPERIMENTAL PROGRAM

3.1 Introduction

This section describes the objectives of the experimental program, the reasons for selection of test specimens and their dimensions, a description of the test setup, and the purpose of each test.

3.2 Development of Test Specimens

The experimental program was conducted by performing two tests on one unique base plate set-up. Many of the characteristics of this study were chosen to duplicate a studies by Cook et al. (1995) and Cook et al. (1999). These two studies tested annular base plates with and without grout pads by varying plate thickness, pipe diameter, and number of bolts. These tests were only performed on four, six, and eight bolt patterns. The FDOT has based recent design guidelines for patterns involving larger numbers of bolts. This study was performed on a ten-bolt pattern to see if previous design criteria still worked for patterns with larger numbers of bolts. The test specimens and procedure; were purposely selected to conform to those of the previous studies. This was done because the set-ups had been proven effective and to provide a direct means of comparison of the test data.

The following subsections provide descriptions of the selected test specimens and materials.

3.2.1 Materials

The basis for selecting the particular concrete, particular grout, anchor bolt material, base plate material and pipe material used in this study are given below:

- 1) Concrete: The concrete chosen for the experimental program was a ready-mix concrete designed to meet Florida DOT Specifications for Class II concrete. This is typical of FDOT structures. The minimum design compressive strength of Class II concrete is 3400 psi at 28 days.
- 2) Grout: The grout was chosen directly from the FDOT approved product list for use in FDOT structures. Master Builders Technologies's Masterflow 928 Grout was the grout selected. This is a high precision, nonshrink, natural aggregate grout. This Masterflow 928 grout was selected because of its quick set time and favorable compressive strength. The FDOT specifications for sign and lighting fixtures require a minimum 28-day compressive strength of grout to be 5075 psi.
- 3) Anchor Bolts: The anchor bolts were fabricated at a local shop in accordance with ASTM F1554.
- 4) Base Plates: The base plate material was ASTM A36 clean mill steel. FDOT uses galvanized plates consistent with ASTM 123. However, since galvanization would have no bearing on the outcome of the experimentation, these plates were left black.
- 5) Pipes: Structural steel pipes were used to model the tubular sections used by FDOT for their sign and lighting structures. The pipes were ASTM A53 Type E, Grade B, Extra Strong. The pipes were socket-welded to the base plates in accordance with FDOT specifications.

3.2.2 Dimensions

The typical dimensions of the anchor bolts, base plates, grout pads, and tubular members used in the experimental program are presented in the following subsections.

3.2.2.1 Anchor Bolts

The anchor bolts dimensions and depth of embedment were chosen to conform directly to the 1995 study by Cook et al. (1995) and the 1999 study by Cook et al. (1999). The anchor bolts were one-inch diameter cold-rolled structural steel rods that were threaded on each end. The bolts were 29.5 inches long with 3.5 inches of thread on the embedded end and 9 inches of thread on the- exposed end (see Figure 3.1). The length of threading was determined from typical shop drawings of base plate connections supplied by the FDOT. Additional threaded length was added to the bolts to support the' load cells on the exterior of the base plates.

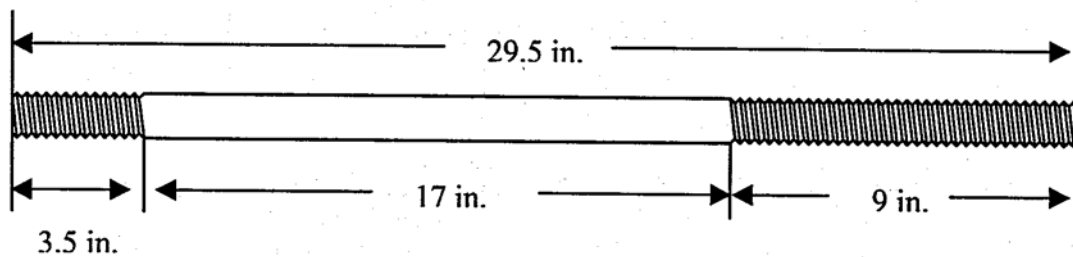


Figure 3.1 Anchor bolt detail

One inch diameter heavy hex nuts were used with two inch outer-diameter hardened steel washers. The embedded end of the bolt was fitted with two heavy hex nuts to simulate the effects of a headed anchor. The use of two nuts reduced the

possibility of the nuts moving during concrete placement. The length of the bolt from the bottom of the base plate to the top of the uppermost embedded nut was 19.5 inches.

3.2.2.2 Base Plates

The base plates examined in this study were chosen to be 0.75 inch thick because of what was learned during the testing in the study by Cook et al. (1995). The tests in that study were all originally performed with base plates one inch thick. However, it became obvious during testing that both the plate and the pipe were yielding. Thus, the remainder of the tests were conducted on plates 0.75 inch thick in order to have initial yielding occur in the plate. The same base plate thickness was chosen throughout this study to increase chances of the base plates failing before the pipe:

The base plates were round with a circular hole in the middle. Base plate rigidity was also modeled after the studies by Cook et al. (1995) and by Cook et al. (1999). By varying the thickness of the base plate and the diameter of the pipe, the plate rigidity was varied by increasing or decreasing the rdt ratio. A smaller rdt ratio gave a more rigid base plate.

It was decided that for this study a more rigid base plate would be studied. The rdt ratio used in the tests was in the allowable range used by FDOT. The most rigid base plate setup would use an 8 inch nominal diameter pipe. The number of bolts was kept the same for the two tests, both using a ten-bolt arrangement.

Two tests were conducted on the somewhat rigid specimens. One was tested with a grout pad while the second was tested without a grout pad. Both tests were loaded to failure.

None of the anchors used for testing in this study had a preload applied. This decision was considered to be conservative since preload cannot be guaranteed in the field and because it is eliminated at ultimate load. Since it is eliminated at ultimate load, the lack of anchor preload would not affect the ultimate strength. The choice to forgo any anchor preloading allowed a clearer understanding of the load distribution between the grout pad and the anchors and more conservative results for the deflection analysis.

Each of the tests was designated by the nominal diameter of the tube, the thickness of the base plate, the number of anchors in the plate, and whether or not a grout pad was present. For example, 8-3/4-10-U refers to a 3/4 inch thick plate with a nominal eight inch diameter tube, a ten anchor pattern and no grout pad. Table 3.1 lists the tests performed and their rdt ratios. A typical base plate shop drawing is shown in Figure 3.2.

Table 3.1 Test dimensions

Test #	Bolt ϕ inches	Pipe ϕ inches	Bolts	Plate Thickness inches	r_d/t
8-3/4-10-U	11.5	8.63	10	0.75	1.88
8-3/4-10-G	11.5	8.63	10	0.75	1.88

3.2.2.3 Grout Pads

The gap between the bottom of the base plates and the exterior face of the test block was 1.5 inches. This entire region had to be filled with grout and evacuated of all air voids. The MOT design specifications for the foundations of cantilever signal structures require that the grout pad be flush against the bottom of the base plate. In addition, the grout pad is required to extend away from the plate to the foundation, making a 45 degree angle with the horizontal (see Figure 3.3). Thus, the base of the

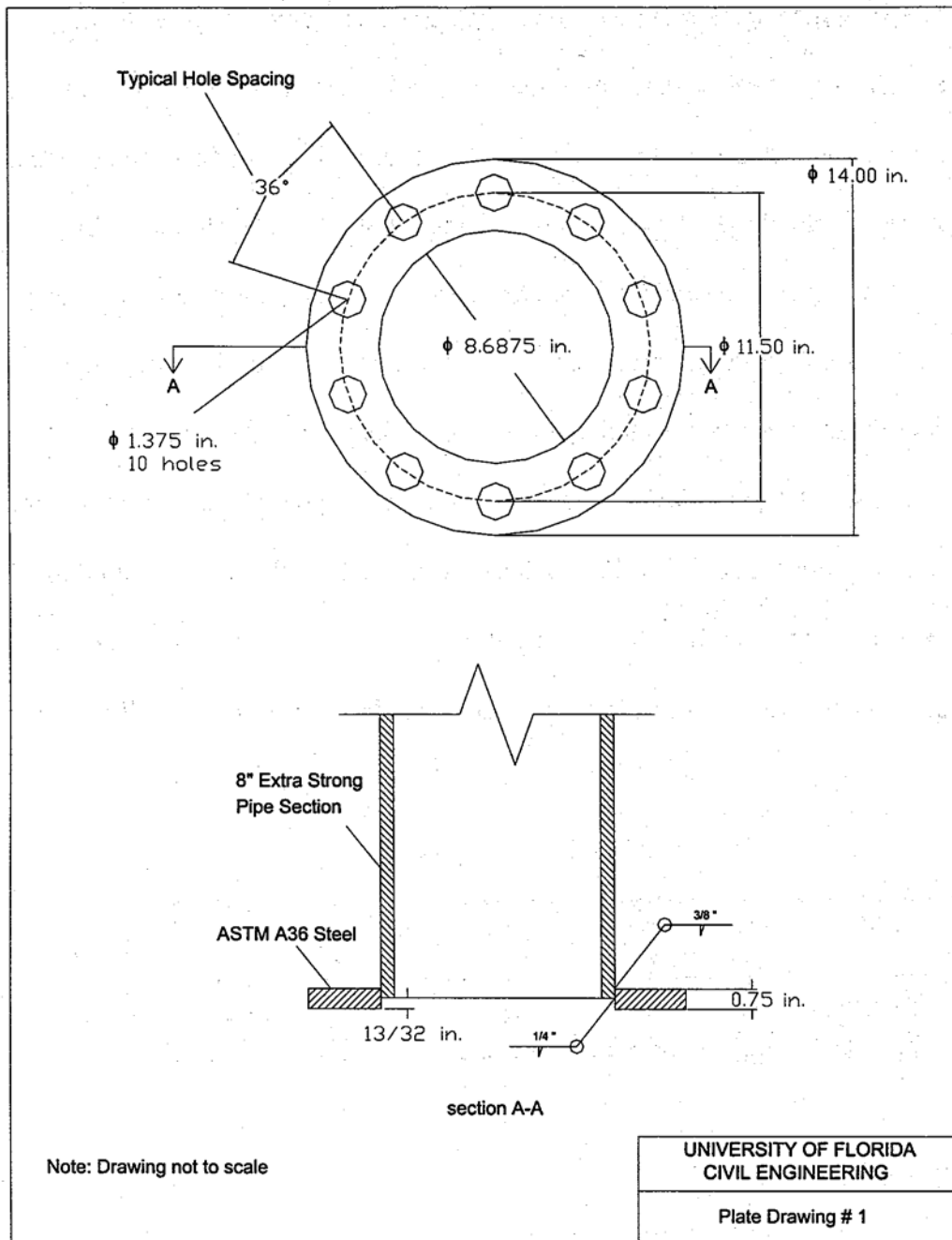


Figure 3.2 Typical shop drawing

grout pad would extend 1.5 inches out from the bottom of the base plate. However, for this project the grout pads were constructed flush with the edge of the plate. This was modeled after the study by Cook et al. (1999). This was considered to be conservative

because it would now be more sensitive to an edge failure from bearing. Thus, the objective of understanding the structural benefits of placing a grout pad beneath a base plate would not be altered.

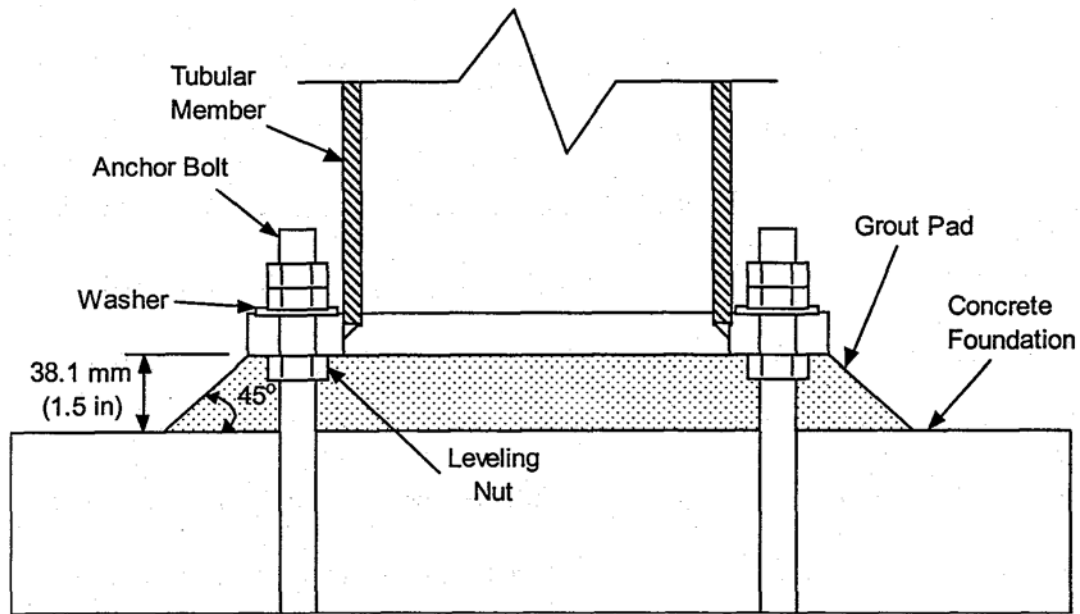


Figure 3.3 FDOT grout pad requirement

3.2.2.4 Tubular Members

The pipe dimensions and moment arm were selected based on the study by Cook et al. (1995). The member length was determined using atypical length-to-diameter ratio obtained from MOT drawings for tubular structures. The ratio was taken as 12 for the test program. This ensured that shear was not over represented in the connection. A nominal pipe diameter of eight inches was chosen to model a base plate with more rigidity. Using the length-to-diameter ratio calculated above, the pipe was loaded at eight feet. The overall length of the pipe was 9.5 feet. The additional 1.5 feet of pipe beyond the loading point permitted an allowance for the loading mechanism.

3.2.3 Test Block Design Basis

The test block dimensions and orientation were chosen to conform to the base plate study by Cook et al. (1995). As shown in Figure 3.4, the test blocks were 24 inches wide by 48 inches long by 48 inches deep, and were reinforced with eight #4 hoops with four perpendicular to the other four to create a cage. The maximum width of the largethroat 400-kip screw tight universal testing machine which confined the testing block was a little more than 24 inches. Calculations of concrete pullout strength and side blowout determined the other two block dimensions. Because of the depth of the blocks, they were cast on their sides to reduce the pressure on the bottom of the forms. Cast-in-place anchors were installed in the blocks on one side surface and inserts were situated in what would be the top surface during testing. After curing, hooks were screwed into the inserts and the blocks were tilted to their resting position.

3.3 Development of Test Setup

The test setup was developed to apply bending moments to the base plate-pipe connection through an eccentric shear force applied to the pipe. The setup was chosen to duplicate the test setup used in the Cook et al. (1995) and Cook et al. (1999) studies. The test setup is illustrated schematically in Figure 3.5.

The test setup consisted of the following components:

- 1) A large-throat 400-kip universal testing machine which confined the test block during testing.
- 2) The test block.

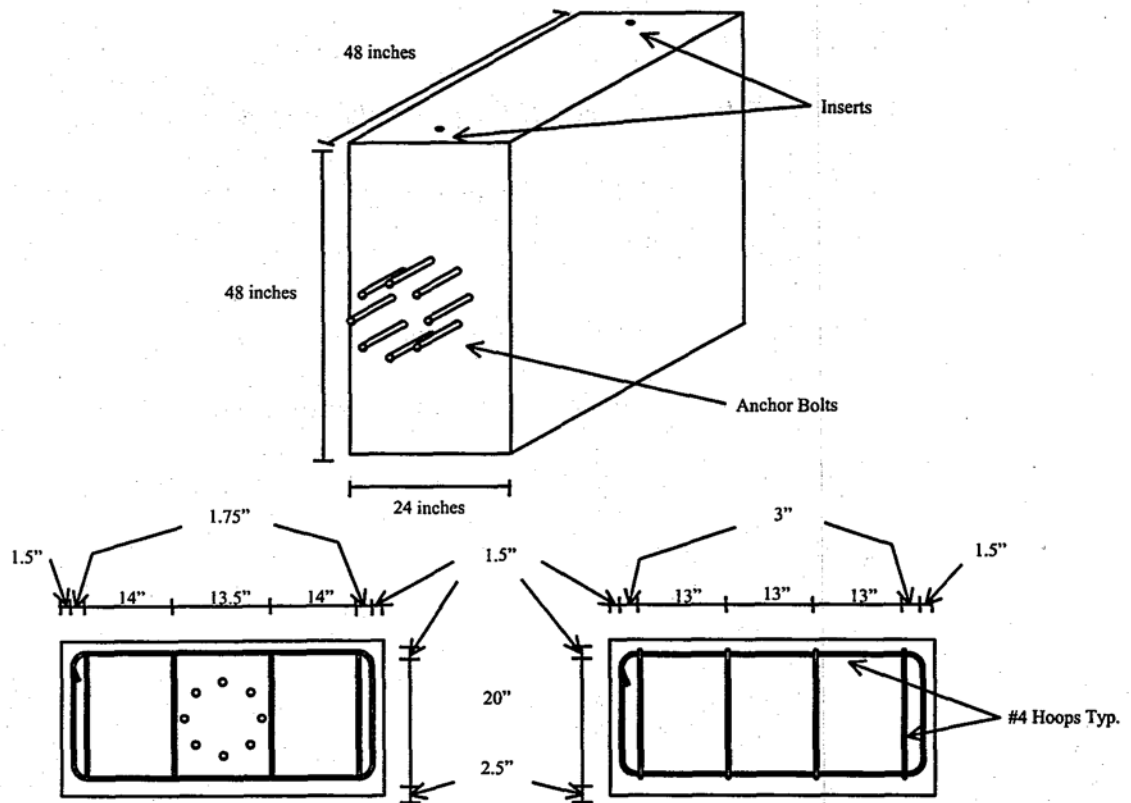


Figure 3.4 Typical test block

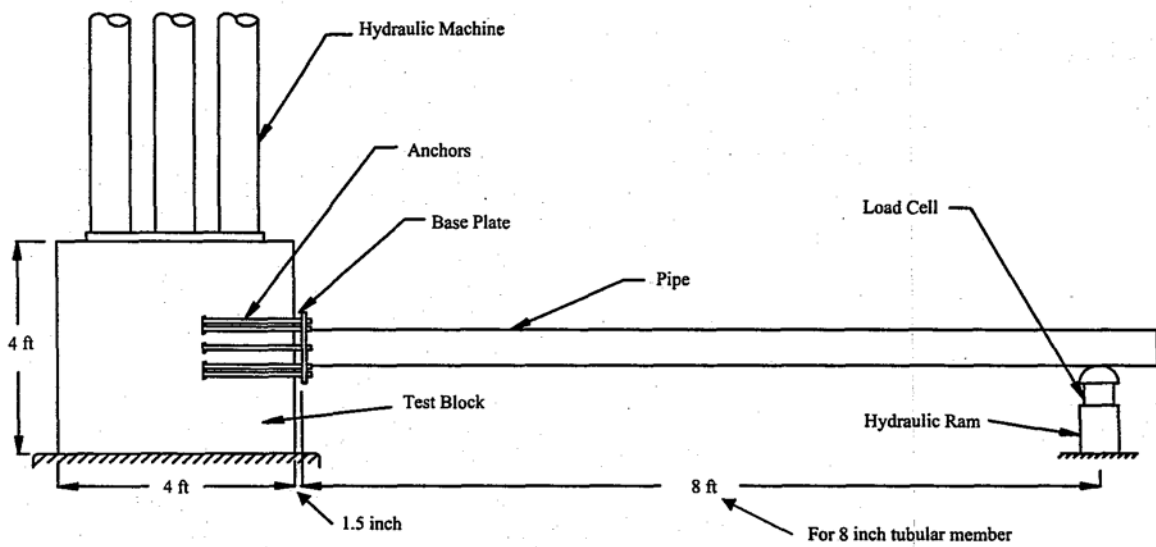


Figure 3.5 Schematic diagram of typical test setup

- 3) A steel pipe that acted as the moment arm for the applied moment at the plate/pipe connection.
- 4) A hydraulic ram at the end of the pipe with a load cell to measure the applied load. Moments were applied to the connection by raising the ram with a hand pump.
- 5) Load cells were embedded in the, grout between the bottom of the base plate and the outer face of the test block to measure the bolt loads. The bolt displacements were recorded by LVDTs located on the outer exposed face of the bolts.

CHAPTER 4 IMPLEMENTATION OF EXPERIMENTAL PROGRAM

4.1 Introduction

All tests were conducted in the Structural Engineering Laboratory in Weil Hall at the University of Florida. This chapter contains a discussion of the concrete casting procedures, the material properties, the testing equipment, and the testing procedure.

4.2 Concrete Casting

All test blocks were cast indoors using ready-mix concrete (Figure 4.1). As the concrete was placed it was consolidated using a hand-held mechanical vibrator. After the forms were filed, the surfaces were screeded, floated, trowelled, and covered with a polyethylene sheet to aid in curing. Cylinders were poured at the same time as the blocks, consolidated with a small vibrating table, and cured beside the formwork under the same conditions as the test specimen. The formwork was oiled prior to pouring to aid in the removal of the forms. The formwork was stripped and the test blocks were moved within seven days after casting. The test blocks were not used until well over 28 days after casting. Cylinders were broken at 7, 14, 21, and 28 days to determine a strength curve for the concrete. Two test blocks were cast during the concrete pour.

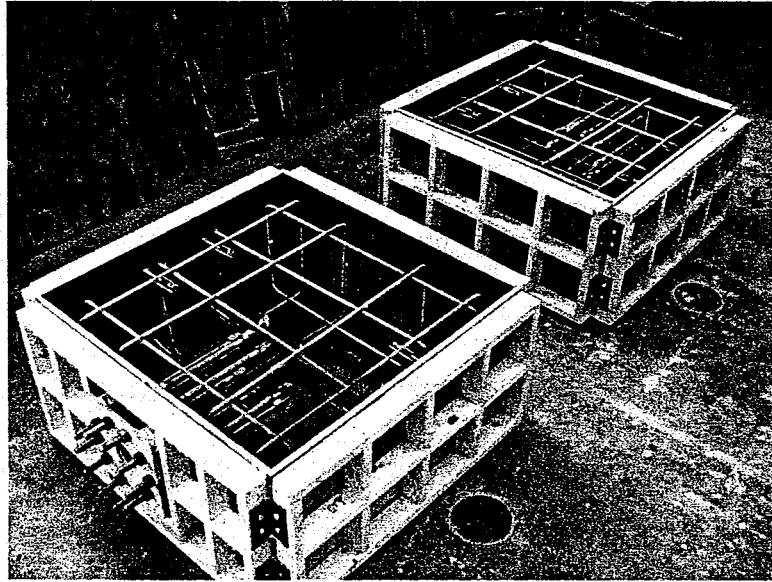


Figure 4.1 Test block formwork

4.3 Materials

A description of the materials used and results of tests performed on the materials for the concrete, anchor bolts, grout mixtures, base plates, and pipes are presented *in* the following subsections.

4.3.1 Concrete

The concrete used was a ready-mix concrete designed to meet FDOT Specifications for Class II concrete. The compressive strengths of the six inch diameter by 12 inch cylinders at 28 days are shown in Table 4.1. Since three cylinders were broken, the average compressive strength was computed.

Table 4.1 Concrete cylinder strengths at 28 days

Cylinder #	Compressive Strength 28 days psi	Compressive Strength 28 days (average) psi
1	7425	7235
2	7130	
3	7151	

4.3.2 Anchor Bolts

The anchor bolts were fabricated at a local shop according to ASTM F1554. The Grade 380 (55) bolts had a thread designation of 8UNC and a diameter of one inch. This is the same strength designation used for the bolts in the base plate study performed by Cook et al. (1995). The same strengths obtained in that study were used again for this study since the material generally has minimal differences between heat numbers. The anchor bolt tensile strengths in the study by Cook et al. (1995) were determined by failing three smooth rods and three threaded rods in tension using a 400-kip universal Tinius Olsen machine. The rods were all made from the same stock used to make the anchor bolts. The results of the tensile strength tests are shown in Table 4.2.

Table 4.2 Anchor bolt tensile strengths

Type of Rod	Sample #	Tensile Strength kips	Average Tensile Strength kips	Average Tensile Stress ksi
Smooth	1	72.53	70.13	89.29
	2	68.90		
	3	68.97		
Threaded	1	57.00	56.44	95.82
	2	56.21		
	3	56.10		

4.3.3 Grout Mixtures

The grout used was required to meet the MOT requirements for a minimum 28day compressive strength of 5080 psi. Testing was to begin at 14 days since the compressive strength at that time far exceeded the required 28-day minimum. The compressive strengths of the two-inch square grout cubes are shown in Table 4.3. The grout cubes were made after the grout pad was poured using the standard steel forms. Since two cubes were broken, the average compressive strength was computed.

Table 4.3 Grout cube strengths

Cube #	Compressive Strength 14 days psi	Compressive Strength 14 days (average) psi
1	7263	7027
2	6375	
3	7444	



Figure 4.2 Mixing grout

The grout was initially mixed according to the mixture to water ratio -recommended by the manufacturer. The manufacturer's recommendations for mixing were approximately 37.5 pounds of grout mixture and 0.93 gallons of water. The mixture and water were blended with a mechanical mixer in a large container for five minutes. The flow of the grout mixture was then tested using a flow cone as described by ASTM C 939. A flow time of 20 to 25 seconds was desired. A slower time indicated that the water to mix ratio was too low. More water was added and blended, and the test was performed again. The proper flow was achieved with a flow time of 24 seconds.

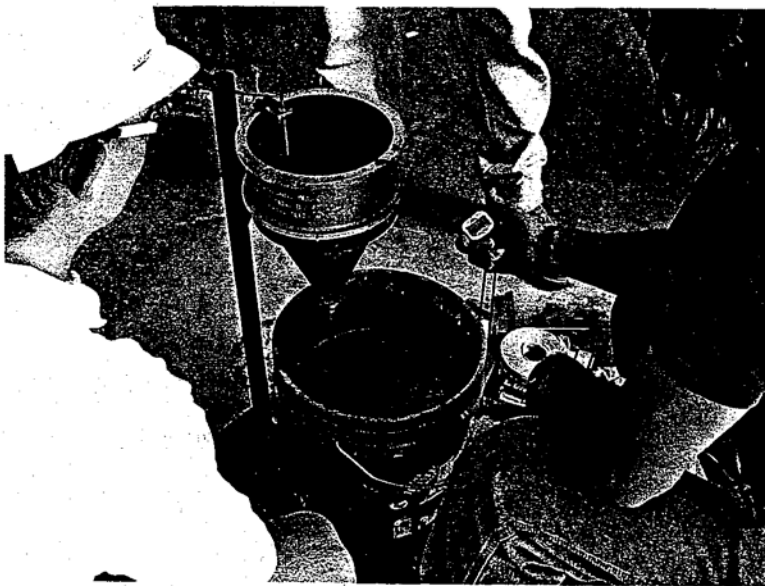


Figure 4.3 Grout flow cone

4.3.4 Base Plates

The base plates were fabricated from ASTM A36 clean mill steel and left black. The ASTM specified minimum yield stress was 36 ksi. The base plates were $\frac{3}{4}$ inch thick. The actual values of the yield stress, F_Y , and the ultimate stress, F_u , were contained

in a mill report provided by the manufacturer. The mill report stated a value of 43.5 ksi for F_y and a value of 65.0 ksi for F_u .

4.3.5 Pipes

The pipes used were ASTM A53 Type E, Grade B, Extra Strong. ASTM A53 requires a minimum yield strength of 35 ksi and a minimum tensile strength of 60 ksi. The pipe was socket welded to the base plate in a manner consistent with MOT specifications. The pipes used in this study were the same as those used by Cook et al.' (1999). A set of tensile coupons was fabricated from the pipes to determine the actual strength of the pipes. The results of the tensile strength tests are' shown in Table 4.4. An average value was calculated from the test results and used: for the pipe strengths in this study.

Table 4.4 Pipe tensile strength test results

Coupon #	Yield Stress ksi	Average Yield Stress ksi	Ultimate Stress ksi	Average Ultimate Stress ksi
1	45.9	46.0	72.1	72.3
2	45.8		71.8	
3	46.3		73.1	

4.4 Anchor Installation

All anchors were cast-in-place were installed with templates to hold the bolts in the proper position at the correct embedded length during concrete placement. The templates consisted of 3/4 inch plywood with holes 1/32 inch larger than the anchor bolts

and were attached to the forms using three-inch drywall screws. The bolts were secured to the templates with nuts on each side of the template. To create the effect of a headed, the embedded end of the bolt was double-nutted.

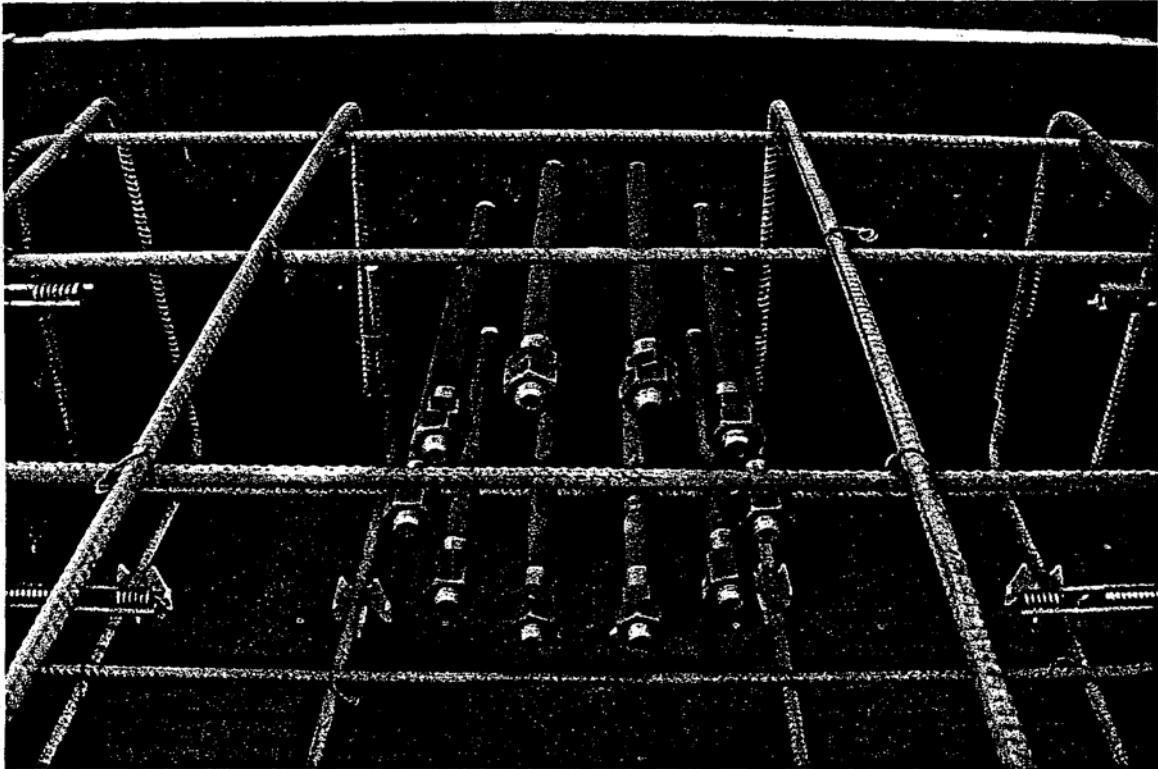


Figure 4.4 Double-nutted bolts

As mentioned in Section 3.2.2, the length of the bolt from the bottom of the base plate to the top of the uppermost embedded nut was 19.5 inches. For the 1.5 inch gap between the bottom of the base plate and the top of the concrete, this represented an effective embedment length of 18 inches for the anchor bolts.

4.5 Grout Application

The test block set-up was rotated on its side in order to pour the grout pad on a horizontal surface. The pipe and base plate were lowered onto the anchor bolts and

leveled using heavy hex nuts under the base plate. The heavy hex nuts also allowed the required 1.5 inch distance between the bottom of the base plate and the exterior face of the test block.

Formwork was constructed to fit around the base plate and flush against the face of the concrete block (see Figure 4.3). First a piece of 0.125 inch thick steel plate 2.5 in wide was selected so that the 1.5 inch grout pad thickness and 0.75 inch base plate thickness would be adequately covered. The plate was rolled to the approximate radius of the base plate. The radius was slightly larger to allow for the visual inspection of how deep the grout pad was after pouring began. Two additional pieces of the same flat plate were cut to 2.5 in by 1.5 in and a 7/16 in diameter hole was drilled in their centers. These two pieces were tack welded perpendicularly to the ends of the long piece of plate. The two ends of the plate were brought together to form a circle. A 1/4 in diameter bolt was passed through the two holes and fitted with a nut.

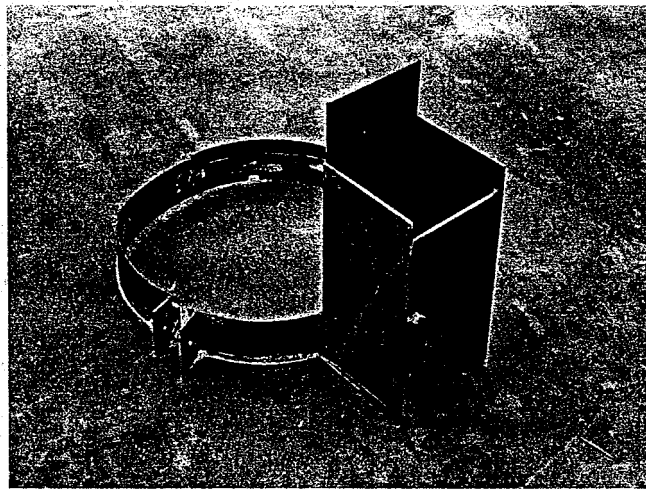


Figure 4.5 Grout application formwork

A head box was constructed to pour the grout using gravity. Four 0.125 inch thick plates were tack welded together to form the box. Three pieces were welded

perpendicularly to form a rectangular box section. The fourth piece was welded at an angle to allow the grout to flow directly into the formwork. A one inch high by five inch long hole was cut out of the original rolled plate. The head box was then tack welded to the rolled plate to form the continuous grout form.

A small 0.25 in by 0.25 in hole was cut on the bottom of one side of the rolled plate. This hole was used for the compression load cell wires to come out of the grout pad in order to read the loads after the grout was in place. Each compression load cell was caulked using silicone sealant to help preserve the wiring before being placed for use in the grout pad.

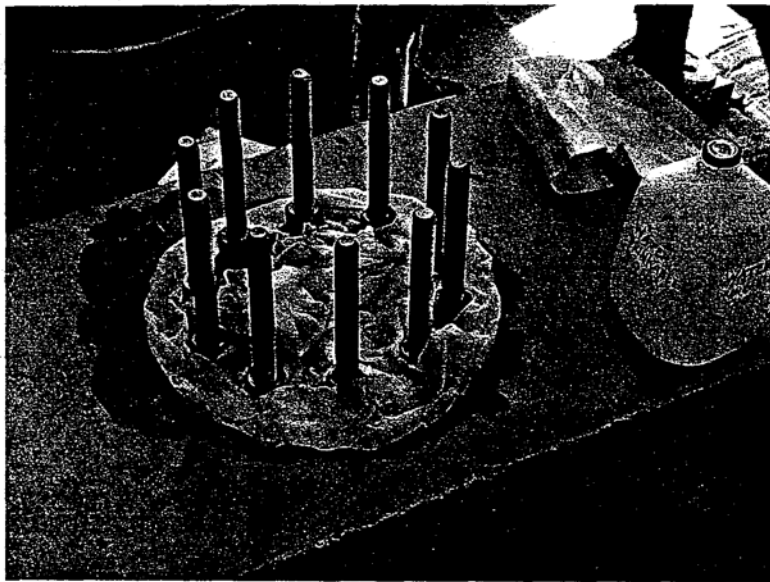


Figure 4.6 Soaking concrete

Before the formwork was put in place around the pipe and plate, the concrete was soaked with water as per the grout instructions. The formwork was then placed around the base plate and flush against the concrete face. Caulking cord was wrapped around the entire bottom of the formwork: All of the joints between the formwork and the concrete block were then sealed with silicone sealant and allowed to set for one hour.

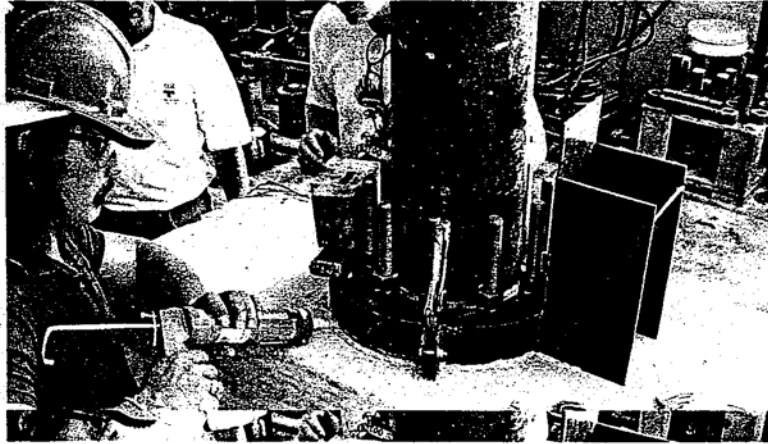


Figure 4.7 Sealing formwork

The grout was then poured into the formwork until the required 1.5 inch depth was reached. After pouring, the grout pad was cured using damp paper towels and a polyethylene sheet wrapped around the entire bottom of the piper. The grout was allowed to cure under the damp condition for seven days. After: the initial set of the grout, approximately two hours, the pad was scored flush to the face of the base plate using a putty knife. After the seven days: curing the remaining grout was chipped away from the grout pad in order to make the grout pad flush with the edge of the base plate.

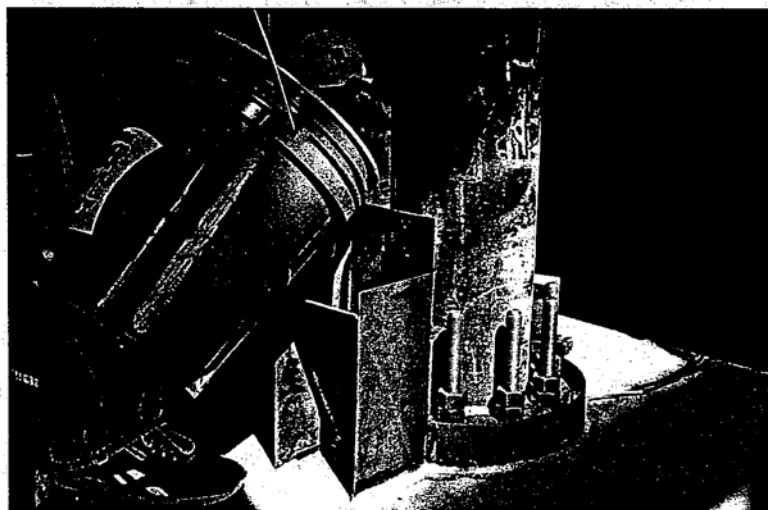


Figure 4.8 Pouring grout

4.6 Test Equipment

The following describes the test setup, hydraulic loading system, load cells displacement measurement instrumentation, and data acquisition unit used in this experimental program.

4.6.1 Test Setup

The test setup for a typical base plate test is shown in Figure 4.4.

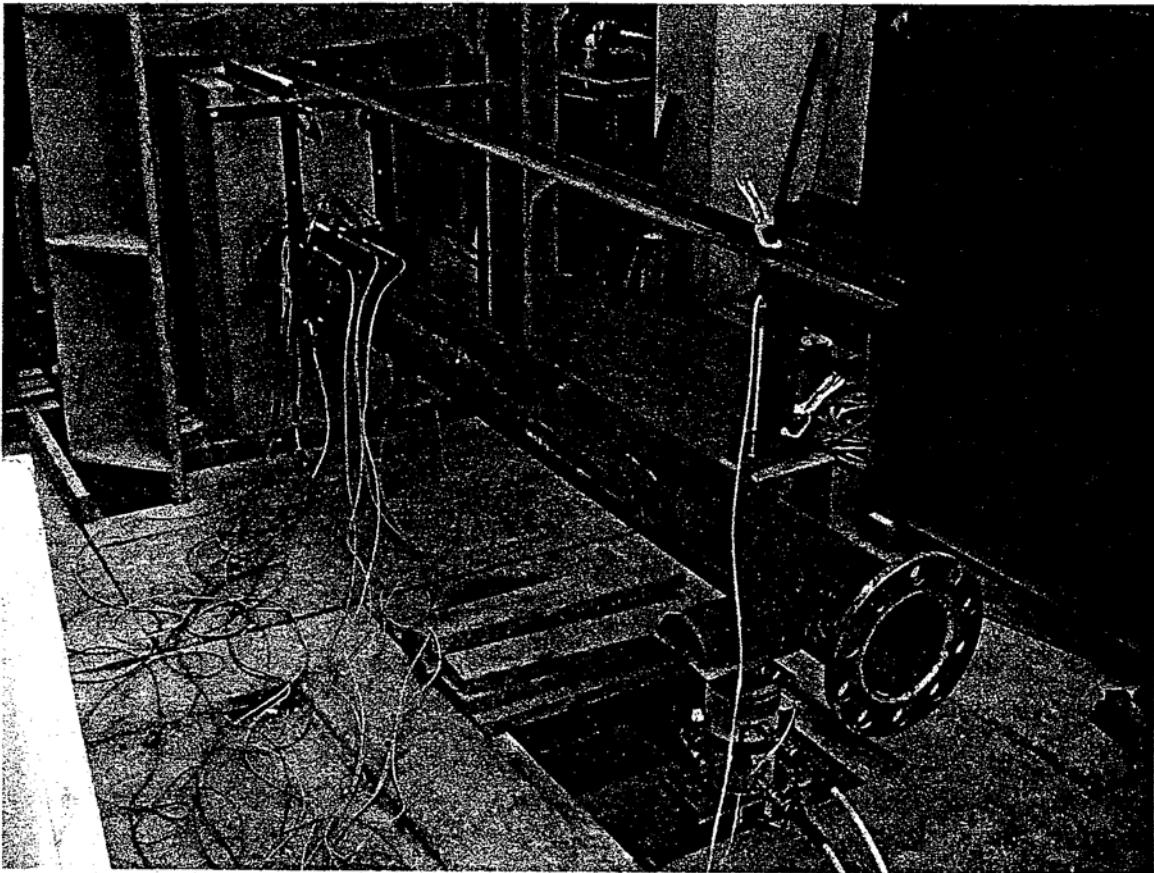


Figure 4.9 Typical test setup

4.6.2 Hydraulic Loading System

Loads were applied using a 60-ton, center-hole Enerpac hydraulic ram with a four inch stroke. A manual Enerpac hydraulic pump with a rated pressure of 10,000 psi powered it.

4.6.3 Load Cells

The load applied by the hydraulic ram at the end of the pipe was measured with a Houston Scientific center-hole 100-kip load cell. This cell was installed on top of the ram below the pipe. The load cell was calibrated in a Tinius Olsen universal testing machine.

The anchor compression beneath the base plates was measured with the bolt load cells shown in Figure 4.10. The load cells were purchased from A.L. Design, Inc. of Buffalo, NY. Waterproof load cells were ordered to ensure that the load cells were not damaged during the application of the grout. The load cells contained strain gages in a full Wheatstone bridge. The load cells were all calibrated to 40 kips with an accuracy of $\pm 0.8\%$ of full load. Each load cell was used in conjunction with a heavy hex nut machined to an overall thickness of 1/2 inch. The hex nuts were placed on the bolts, followed by the load cells, leaving a gap of 1/4 inch between the outer face of the concrete test block and the nut. This allowed for a uniform distance of 1.5 inch between the bottom of the base plate and the face of the block. Then, the base plate was placed directly against the face of the load cell. The purpose of these load cells was to determine how much of the

compressive reaction goes directly into the bolt and how much is transferred to the grout pad.

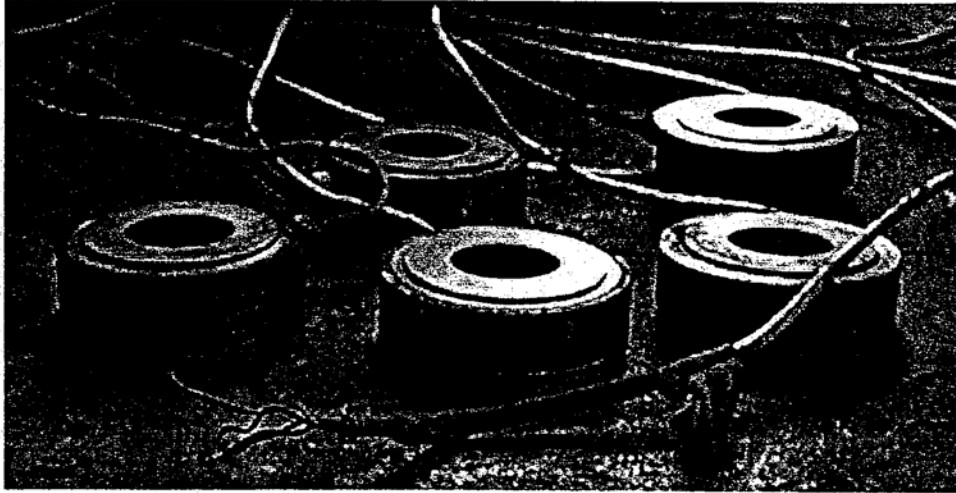


Figure 4.10 Compression bolt load cells

The anchor tension was measured with the bolt load cells shown in Figure 4.11. The load cells were constructed of high strength 2024 Aircraft Aluminum and had strain gages from Micro-Measurements Division in a full wheatstone bridge. The load cells were all calibrated to 40 kips with an accuracy of $\pm 1-0.5\%$ of full load. Each load cell was secured to the bolt by first placing a two inch outside diameter washer around the bolt and against the plate. The load cell was then set on the washer, another washer was placed on top and a one inch heavy hex nut screwed down snug by hand. These load cells were only placed on the tension load cells because they would experience no load on the compression bolts. The tension load cells, coupled with the compression load cells, provided a complete picture of the internal equilibrium of the base plate. The placement of the tension and compression anchor bolt load cells for a typical test is shown in Figure 4.12.

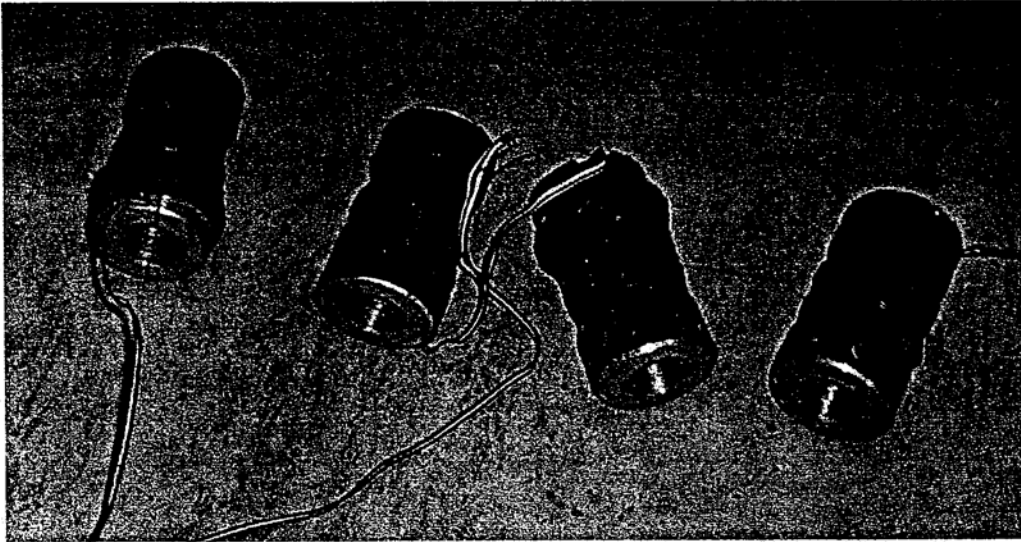


Figure 4.11 Tension bolt load cells

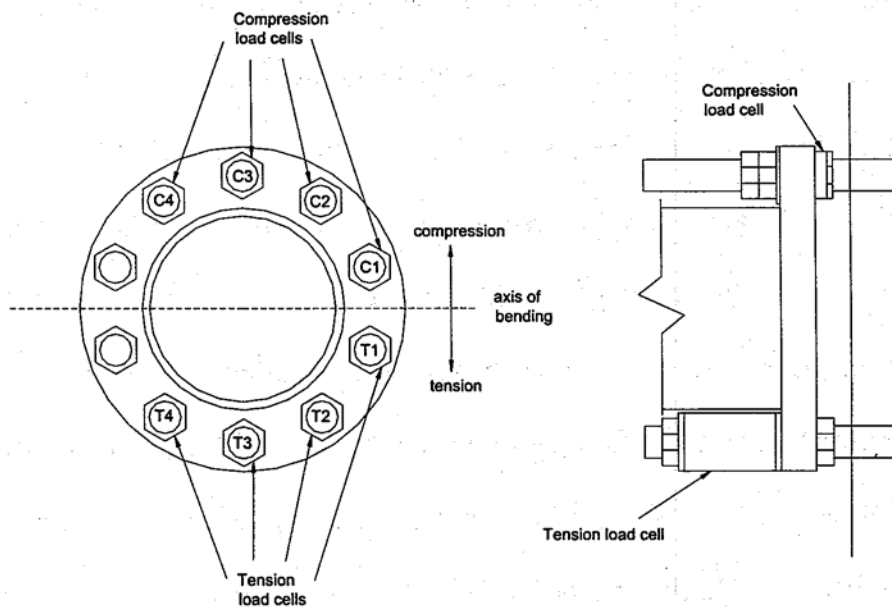


Figure 4.12 Load cell placement

4.6.4 Displacement Measurement Instrumentation

LVDTs (Linear Variable Displacement Transformers) with +/- one inch of travel were placed on the outer face of six of the ten anchor bolts (see Figure 4.13). The LVDTs were only used on the outermost bolts on each side of the neutral axis because they would show the most deformations out of the entire bolt group. These LVDTs had to be adjusted whenever the bolt rotation would cause the tip of the LVDT to fall off of the tip of the bolt. The LVDTs were held in place by a template constructed of steel channel sections and flat steel plates (see Figure 4.14):

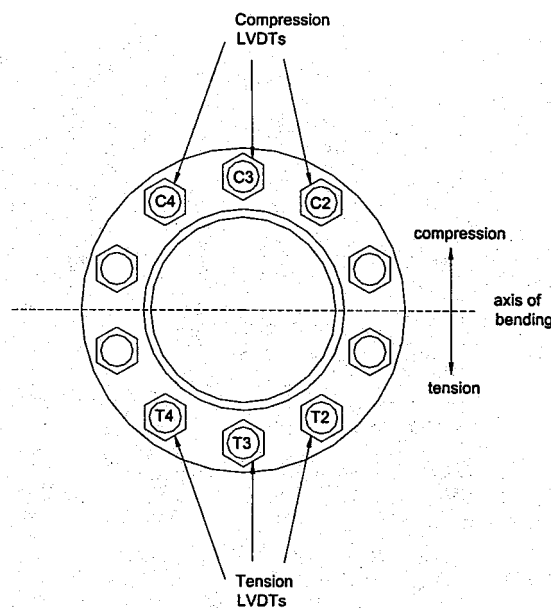


Figure 4.13 LVDT placement

The pipe displacement was measured by placing an additional LVDT on the surface of the pipe directly over the load point. During the grouted test an LVDT with +/- one inch of travel was used. This LVDT had to be adjusted each time it ran out of travel. For the ungrouted test a displacement transducer with +/- 12 in of travel was used.

This allowed for continuous loading without having to adjust the transducer over the applied load. The LVDT displacement transducer was attached to a steel angle that was in turn attached to threaded rod: embedded on the top of the test block. The anchor bolt LVDTs were attached to steel plates connected to steel angles that were in turn attached to threaded rod embedded on the top of the test block. Thus, all of the displacements measured by the LVDTs were relative to the concrete block. This was done so that any rotation of the test block within the hydraulic loading system during testing would not be recorded by any of the LVDTs.

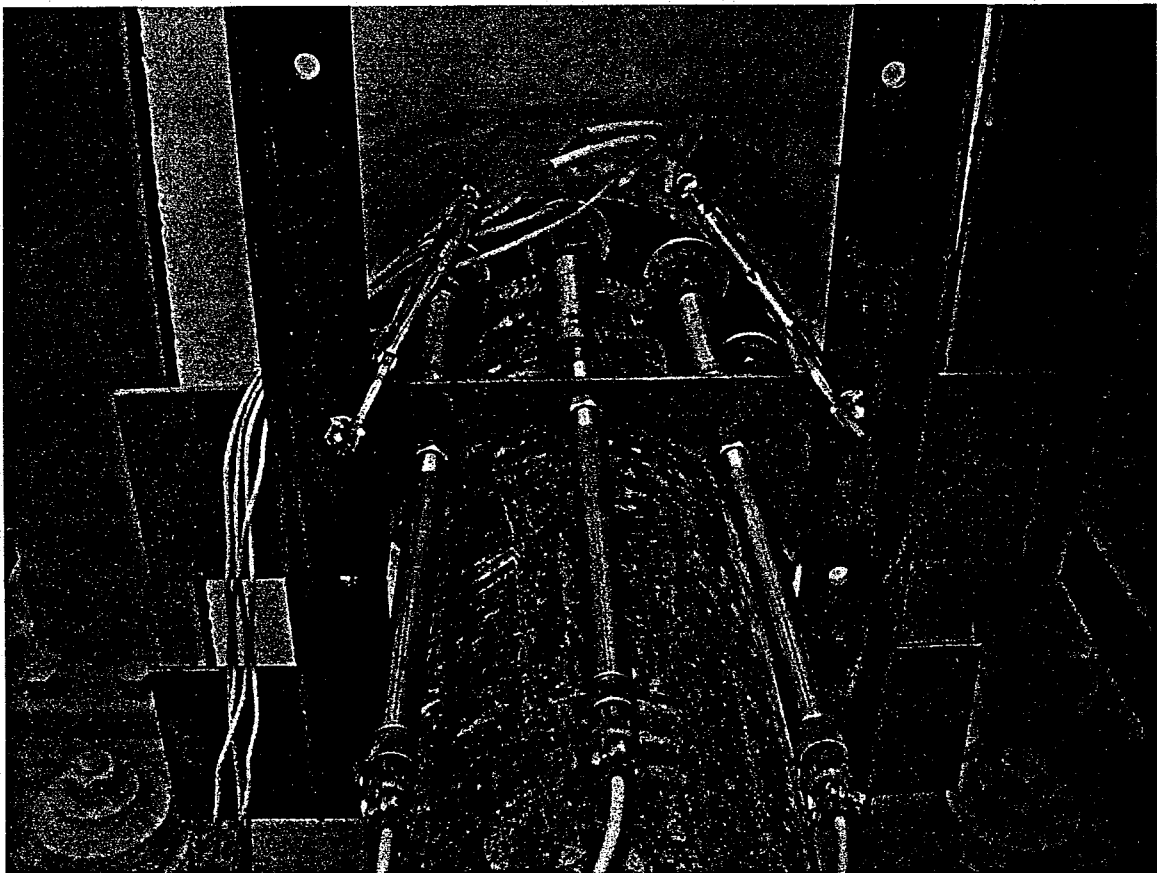


Figure 4.14 Template for LVDTs

4.6.5 Data Acquisition Unit

The load cells and LVDTs produced voltage through strain gages. All of the load cells except for two, load cells LC4 and LC3, were then run through a Vishay signal conditioning system purchased from Measurements Group, Inc. This Vishay machine was able to amplify and filter the voltages the load cells were reading in order to achieve greater precision before being read and recorded by a data acquisition card, National Instruments model PCI-6031E, located inside the Gateway 550 MHz computer. All of the LVDTs and load cells LC4 and LC3 were read and recorded directly by the data acquisition card. The 550 MHz computer was running Labview 5.1 by National Instruments. Labview software uses a graphical programming language to control the data channels and sampling rates, and indicate the signals being measured and recorded. The Labview system converts the voltages into forces or displacements based on calibrations. The Labview system made it possible to read and record data at the rate of three readings (all instruments) per second. The data file generated by Labview was a tab-delimited ASCII text- file. The data was then opened in Microsoft Excel 2000 for reduction.

4.7 Load and Displacement Data Reduction

The voltages from the load cells and LVDTs were read and recorded using a data acquisition card and converted to forces and displacements by a Gateway 550 MHz computer running the Labview operating system as described in the previous section. The data was downloaded to a Microsoft Excel spreadsheet where the data was reduced and initial graphs were made of the applied shear load versus individual LVDT

displacements and load cell forces (see Appendix B and C). This data was then used to obtain additional data such as applied moments and resulting rotations:

4.8 Test Procedure

A typical test involved the following steps:

- 1) Heavy hex leveling nuts were screwed onto the anchors so that the distance between the concrete and the bottom of the plate was 1.5 in. The interior nuts on the anchors that would be experiencing pure compression were machined to an overall thickness of 1/2 into adequately accommodate the load cells:
- 2) The base plate was installed on the anchors until the bottom of the plate was flush with the nuts of the tension anchors and load cells of the compression anchors. The base plate was adjusted until the sides of the anchor bolts were touching the sides of the holes. This reduced the amount of slip due to the applied shear. All of the, compression anchors were fitted with washers and two heavy hex nuts. The tension bolts were fitted with a washer, load cell, another washer and a single heavy hex nut. The heavy hex nuts were hand tightened to a snug fit.
- 3) The LVDTs were attached to the pipe and anchors using the template. The hydraulic ram was set up at the point where the shear load was to be applied. All instruments were connected to the data acquisition unit and Labview was started. All LVDTs and load cells were tested to make sure they were reading and the heavy hex nuts on the anchors with load cells were loosened if they showed a preload.

- 4) Logging on Labview was begun and load was applied by pumping the hydraulic ram at a steady pace.
- 5) When the LVDT at the point of application of load ran out of travel, pumping was discontinued and the LVDT was moved to a higher position. Logging of data was never stopped. The jump in displacement was adjusted during the data reduction. After repositioning the LVDT, the application of load was resumed. This was repeated every time the LVDT ran out of travel.
- 6) When the hydraulic ram ran out of travel, a chain was wrapped around the pipe and attached to an overhead 5-ton crane that was raised until the chain became tight. This held the pipe in position so blocks could be placed under the ram without removing load from the pipe/plate system. When the ram was raised enough such that it just touched the pipe in its lower position, the crane was lowered and loading resumed with the hydraulic ram. As with the LVDT, the logging of data was never stopped. All adjustments were made when the data was reduced.
- 7) Loading continued until a structural failure was evident from the pipe load displacement graph.
- 8) The applied shear load was released. Logging was stopped. Raw data was downloaded from Labview to a Microsoft Excel 2000 spreadsheet where it could be reduced.
- 9) The pipe and plate system was removed from the anchor bolts and inspected for failure and permanent deformations.

CHAPTER 5 TEST RESULTS

5.1 Introduction

This chapter discusses the test observations, a summary of the test results, and typical individual test results. Complete results of all of the tests are provided in the appendices.

5.2 Test Observations

The following subsections contain an account of the observations made during testing on all of the specimens.

5.2.1 Test # 1

The first test was on specimen 8-3/4-10-G. No upper limit was placed on the applied load. Load application was continued until it became obvious a system failure had occurred. Loading was discontinued after a weld failure on the tension side of the pipe/plate connection. A plastic hinge had also developed in the pipe just beyond the connection to the plate.

A minor plate rotation was observed during test 8-3/4-10-G as the plate slightly pulled away from the grout pad in the tension region. No significant cracking or crushing of the grout pad was observed in the compression zone. As loading continued, the tension bolts began to bend slightly downward. The compression bolts did not experience any flexural deformations.

One of the compression load cells, LC2, was not reading data properly during testing. After testing was complete and the load cells were extracted from the grout pad, it was noted that the wiring to load cell LC2 had been detached. Therefore, the data from load cell LC2 was not used in any analysis.

5.2.2 Test #2

The second test was on specimen 8-3/4-10-U. No upper limit was placed on the applied load. Load application was continued until it became obvious a system failure had occurred. Loading was discontinued after a weld failure on the tension side of the pipe/plate connection. A plastic hinge had also developed in the pipe just beyond the connection to the plate.

The initial position of the base plate was vertically straight. As load was applied, the plate started to deform. Plate rotation was characterized by the inward horizontal displacement of the compression side and an outward horizontal displacement of the tension side. The base plate never came into contact with the concrete face. The tension side anchor bolts bent slightly downward as testing progressed (see Figure 5.1). No notable flexural deformations were observed on the compression bolts.

5.3 Summary of Test Results

Both tests revealed larger compression forces in the outermost bolts compared to their respective tension side bolts. After all testing was complete the load cells were recalibrated. The load cells yielded the same calibrations as before the tests. This behavior was not characteristic of the rigid plate behavior previously assumed. The base

plates showed a flexible behavior which caused the neutral axis to shift towards the compression bolts, therefore allowing higher bolt loads in the compression bolts compared to the tension bolts. In order for equilibrium to be maintained, the rows of bolts near the line of symmetry (original neutral axis) must have experienced tension. These bolt loads were not measured based on the previous assumption that the base plates behaved in rigid body rotation. In anchor bolt design, the critical load case for bolts is in tension. Since the higher loads were experienced in the compression bolts rather than the tension bolts, the previous design equations were conservative to use.

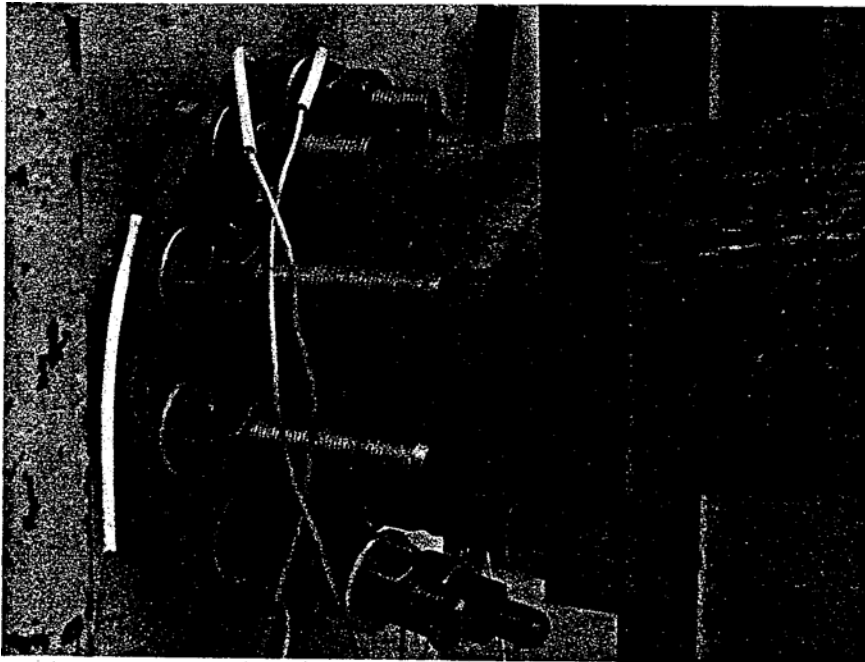


Figure 5.1 Deformation of tension bolts during loading of ungrouted plate

The loads in the compression bolts during both tests were larger than the tension forces in the corresponding tension bolts. This resembles flexible plate behavior that had been previously observed by Cook and Klingner (1989, 1992). The compressive reaction moves inward towards the compressive element of the attached member as the

compressive load increases (see Figure 5.2). The smallest distance between the outermost edge of the compression element of the attached member and the compression reaction, x_{min} is determined by dividing the moment capacity of the rectangular plate calculated across its width by the compressive reaction, C . The design equations found in Chapter 2 still give conservative values based on the data from this research project and will therefore be evaluated in Chapter 6:

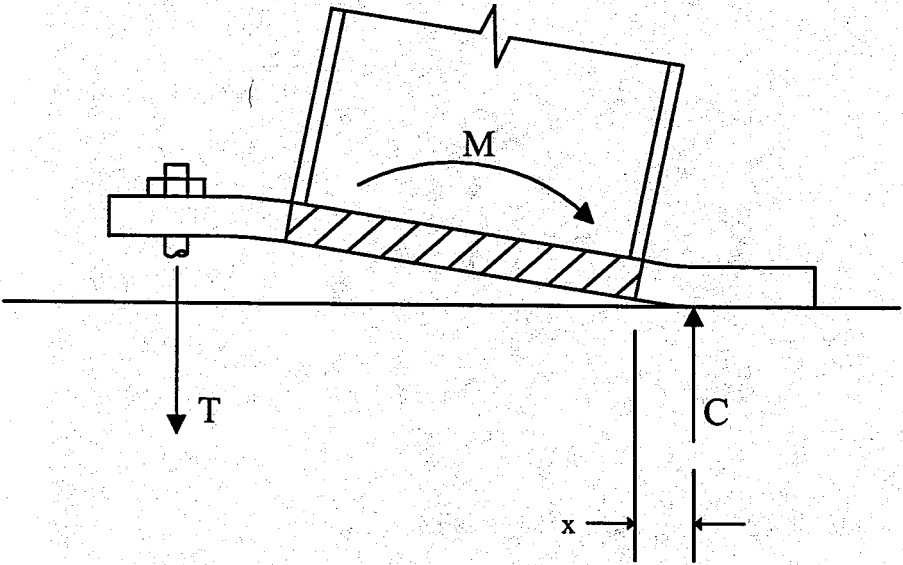


Figure 5.2 Flexible plate behavior

The load displacement graphs for both tests are shown in Figure 5.3. The graphs show loading in the elastic range for comparison purposes. The full-scale load displacement graphs are shown in Figure 5.4.

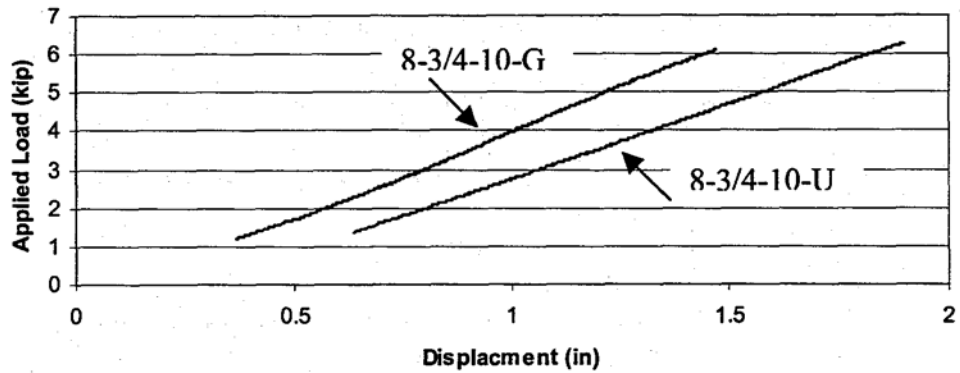


Figure 5.3 Elastic range load-displacement

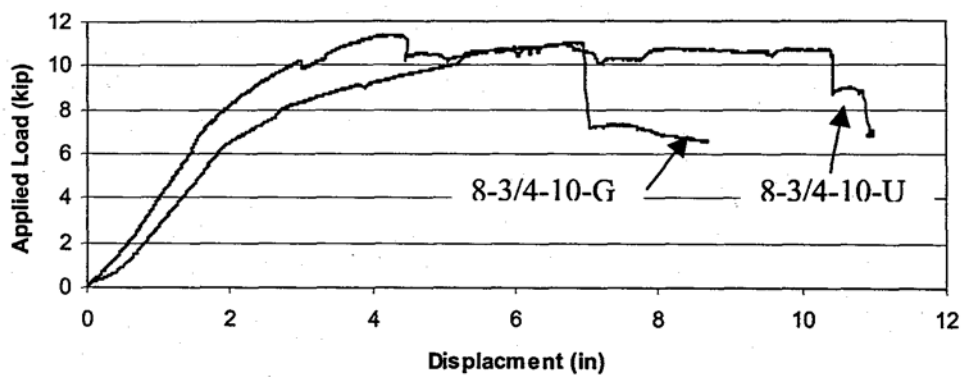


Figure 5.4 Full-scale load-displacement

5.4 Individual Test Results

Appendix A contains cross-sectional views of each plate specimen indicating the numbering and labeling of the LVDT and load cells for the bolts for both tests performed. LVDT and load cell data obtained from all of the tests are presented graphically in Appendices B and C respectively. Appendix D contains load-displacement graphs.

Appendix E contains moment-rotation graphs. The moments for these graphs were obtained by multiplying the applied shear load by the distance from the bottom of the base plate to the point of load application. Subtracting the deflection due to the tube from the total deflection and dividing the resulting value by the distance from the bottom of the base plate to the point of load application determined the rotation. Appendix F contains stiffness evaluations for each test, which are the results of linear regressions applied to the load-displacement plots.

CHAPTER 6

DESIGN CONSIDERATIONS

6.1 Introduction

Performance of annular base plate connections should be evaluated based on strength and serviceability. Both design considerations are discussed in this chapter.

6.2 Strength

Strength considerations are usually related to the yielding of one or more components of a structure. As the annular base plate structures of this test program and previous test programs (Cook et al. (1995) and Cook et al. (2000)) were loaded to failure, yielding typically occurred first in the base plate, followed by yielding of the tubular member, and finally followed by fracture of the weld. This sequence of yield formation (i.e., plate yield followed by yielding of the tubular member) was designed into the test program since the behavior of the annular base plate was the primary concern of the study. Although the anchor bolts did experience flexural deformations as the base plate deformed, the axial load carried by the bolts remained in the elastic range of the bolts.

6.2.1 Base Plate Moment Capacity

Equation (2-9) discussed in Chapter 2 and repeated here was evaluated based on the experimental results of this study and previous studies. The predicted base plate moment capacity (M) resulting from Eq. (2-9) is shown in Table 6.1 compared to the approximate yield moment (M_y) determined from tests.

$$M = F_y t^2 \frac{r_p r_b}{r_b - r_p} \quad (2-9)$$

where:

M = predicted moment capacity of base plate

F_y = yield stress of the base plate

t = base plate thickness

r_p = pipe outside radius

r_b = distance from center of plate to centerline of anchor bolts

Table 6.1 Comparison of measured and predicted moments

Test #	n	t in	r_b in	r_p in	F_y ksi	M_y kip-in	M Eq. (2-9) kip-in	M/ M_y
6-1-4d	4	1.00	5.75	3.31	52.5	350	410	1.17
6-1-4s	4	1.00	5.75	3.31	52.5	350	410	1.17
6-1-6	6	1.00	5.75	3.31	52.5	370	410	1.11
6-1-8	8	1.00	5.75	3.31	52.5	400	410	1.03
6-3/4-4d	4	0.75	5.75	3.31	55.4	200	244	1.22
6-3/4-8	8	0.75	5.75	3.31	55.4	200	244	1.22
8-3/4-4d	4	0.75	5.75	4.31	55.4	400	538	1.34
8-3/4-6	6	0.75	5.75	4.31	55.4	600	538	0.90
8-3/4-8	8	0.75	5.75	4.31	55.4	500	538	1.08
8-3/4-8-G	8	0.75	5.75	4.31	55.3	700	537	0.77
8-3/4-4s-G	4	0.75	5.75	4.31	55.3	800	537	0.67
6-3/4-4sw-GS	4	0.75	5.75	3.31	55.3	460	243	0.53
6-3/4-4s-GS	4	0.75	5.75	3.31	55.3	480	243	0.51
8-3/4-10-G	10	0.75	5.75	4.31	43.5	800	422	0.53
8-3/4-10-U	10	0.75	5.75	4.31	43.5	600	422	0.70
Mean								0.93
Coefficient of variation								0.31

As mentioned above, the initial yielding of the annular base plate system tested involved the base plate. For this reason, the primary consideration for assessing the recommended design model for base plate behavior is based on evaluating how well the model reflects the yield point of the tests and not the ultimate moment. This differs from

the previous studies (Cook et al. (1995) and Cook et al. (2000)), where design models were evaluated based on the ultimate moment exhibited by the test specimen.

As shown by Table 6.1, Eq. (2-9) provides a reasonable fit to all test data based on the mean (0.93) and coefficient of variation (0.31) associated with a comparison to the approximate yield moment (M_y). Appendix H provides moment-rotation graphs for all fifteen tests shown in Table 6.1 with the predicted moment (M) indicated by a solid dot on the graphs. The graphs in Appendix H provide a better indication of predicted strength versus test results since the approximate yield moment shown in Table 6.1 could only be estimated based on the moment-rotation behavior associated with each test.

The underestimation of moment (M) in the last six tests shown in Table 6.1 (four from Cook et al. (2000) and two from this study), is likely due to a combination of the presence of a grout pad in the five tests preceding the last test in Table 6.1 and the fact that in all six of these tests the steel strength was determined from mill test reports rather than coupon testing as performed in the Cook et al. (1995) study. In the tests involving a grout pad (those with a "G" in the test designation), the presence of the grout pad inhibited the formation of the full yield pattern on the compression side of the base plate resulting in an increased strength.

As discussed in Chapter 2, the derivation of Eq. (2-9) is based on the consistent deformation contours exhibited by the six and eight bolt base plates. Although the yield line pattern assumed in the derivation of Eq. (2-9) is not consistent with that observed in

the four bolt tests with both diamond and square bolt patterns, the results shown in Table 6.1 and the graphs in Appendix H indicate that this equation may be used with four bolt arrangements. Although not included here, a comparison of the test results for the four bolt arrangements to Eq. (2-9) and other equations proposed during the course of this study indicate that Eq. (2-9) provides the best fit to the test data based on the coefficient of variation for all of the four bolt tests:

6.2.2 Anchor Bolt Loads

As discussed in Chapter 2, Eq. (2-3) was used by previous studies (Cook et al. (1995) and Cook et al. (2000)) to predict the tension load in the outermost anchor bolts at the maximum load on annular base plate structures. Although Eq. (2-3), is based on an elastic distribution of loads to the anchor bolts, it provided very reasonable results for all test specimens. Based on the results provided in Table 2.5 and Table 2.6, the mean of the ratio of the measured bolt load at ultimate to the predicted bolt load was 1.12 with a coefficient of variation of 0.13 based on thirteen previous annular base plate tests.

$$P_{bolt} = \frac{2M}{nr_b} \quad (2-3)$$

where:

M= applied moment

n = number of bolts

r_b = distance from the center of pipe to the center of bolt

For the ten-bolt annular base plate tests performed in this study, the maximum bolt load calculated by Eq. (2-3) was compared to the actual values measured at ultimate load and are shown in Table 6.2. When the results shown in Table 6.2 are incorporated into the results shown in Table 2.5 and Table 2.6, the mean of the ratio of the measured maximum bolt load to the predicted bolt load is 1.10 with a coefficient of variation of 0.13. This indicates that although the annular base plate behavior may be complex, the actual distribution of load to the anchors may be easily computed using Eq. (2-3). The explanation of why the elastic model for evaluating bolt loads produces an excellent relationship to measured bolt loads likely lies in the fact that in typical annular base plate structures the diameter of the attached tubular member (that acts as a rigid body for rotation at the base plate connection) is not significantly different than the diameter of the anchor bolt pattern.

Table 6.2
Comparison of predicted and measured bolt loads at ultimate

Test #	Maximum Applied Moment kip-in	Measured P_{bolt} kips	Predicted P_{bolt} kips	Measured P_{bolt} / Predicted P_{bolt}
8-3/4-10-G	1094	35.2	38.1	0.92
8-3/4-10-U	1050	39.0	36.5	1.07

6.3 Serviceability

Serviceability is the other primary concern when designing base plates for sign and lighting structures. Serviceability considerations are related to the overall deflection of the sign or lighting structure. The amount of deflection depends on the attached tubular member, thickness and size of the base plate, and flexibility of the anchors.

6.3.1 Stiffness Evaluation

The serviceability of the base plate connection can be evaluated by considering the stiffness of the system. The stiffness of the entire system can be found by determining the slope of the load deflection curve in the elastic range. Then, knowing the stiffness of the tubular member, the stiffness of the connection can be found. The connection stiffness is related to the contribution from the plate and bolts to the overall stiffness.

The overall stiffness of the system was found by applying a linear regression to the elastic region of the load deflection curves of each test. The linear regression was only performed for portions of the recorded data. The regression was not performed on the data in regions with large amounts of scatter. The regions where the test set-up was adjusting to the load, roughly the first 15-20% of loading, also were not included. The resulting slope of the line representing the remaining data was taken to be the overall stiffness of the pipe/plate/bolt system. The results of the linear regression are shown in Figure 6.1.

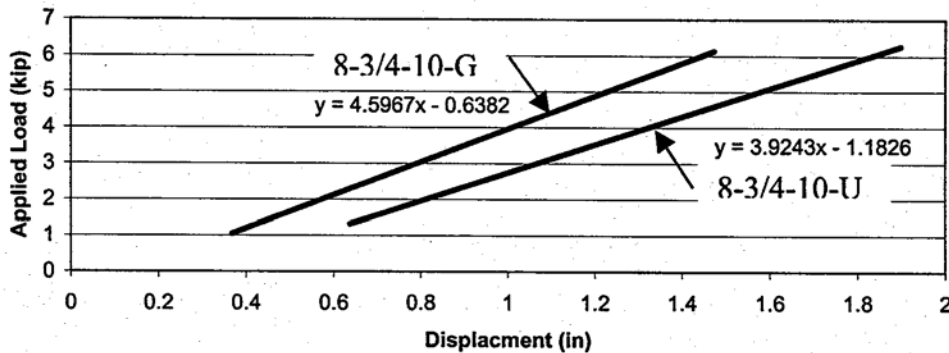


Figure 6.1 Stiffness determination by linear regression analysis

This method of analysis is possible because the tubular member and the base plate connection can be modeled as a system of two springs acting in series. The stiffness of the entire system can be found by:

$$k_{total} = \frac{1}{\frac{1}{k_{pipe}} + \frac{1}{k_{connection}}} \quad (6-1)$$

The stiffness of the base plate connection can be determined by rearranging the terms of Eq. (6-1). Equation (6-2) was used to find the stiffness of the connection.

$$k_{connection} = \frac{1}{\frac{1}{k_{total}} + \frac{1}{k_{pipe}}} \quad (6-2)$$

The stiffness of the pipe was found by assuming that the pipe was a cantilevered member and that the additional deflection comes from the plate and bolts. The equation for the stiffness of the pipe, modeled as a member with a pure fixed end support, was:

$$k_{pipe} = \frac{2EI}{L^3} \quad (6-3)$$

where:

E = modulus of elasticity of the pipe

I = moment of inertia of the pipe section

L = distance from the bottom of the base plate to the point of applied shear

The results of the stiffness calculations are shown in Table 6.3.

Table 6.3 Connection stiffnesses

Test #	Total Stiffness kip/in	Pipe Stiffness kip/in	Connection Stiffness kip/in	Total Stiffness/ Connection Stiffness
8-3/4-10-G	4.60	10.4	8.22	0.559
8-3/4-10-U	3.92	10.4	6.28	0.624

6.3.2 Analysis of Connection Rotation

Calculating the connection stiffness could further be used to quantify the portion of the rotation that comes from the plate and bolts within the elastic loading range. As discussed earlier, the stiffness of the connection can be determined from knowing the stiffness of the tubular member and the overall stiffness: The portion of the deflection that is related to the rotation of the plate connection was:

$$\Delta_{connection} = \frac{P}{k_{connection}} \quad (6-4)$$

where:

P = applied load

$k_{connection}$ = stiffness of the base plate connection

The rotation of the connection was known to be small. Thus, small angle theory was used, and the rotation of the connection was determined by:

$$\theta_{connection} = \frac{\Delta_{connection}}{L} \quad (6-5)$$

where:

L = distance from bottom of base plate to applied load

Rearranging the terms yielded the final equation for calculating the rotation of the connection based on stiffness:

$$\theta_{connection} = \frac{P}{LK_{connection}} \quad (6-6)$$

6.3.3 Serviceability Evaluation

Equation (2-10) was used to evaluate the ungrouted test specimen while Eq. (213) was used to evaluate the grouted test specimen. Both test specimens were evaluated at the same applied moment of 124 kip-in (this was the equivalent of an applied load of 1.29 kips). This load was known to be in the elastic range for both specimens.

$$k_{total} = \frac{2ML_b}{nr_b^2 A_b E_b} + \frac{45M}{Er_b^2 b} \left(\frac{r_b - r_p}{t} \right)^{1.83} \quad (2-10)$$

$$\theta_{bolt+groutedplate} = 0.66\theta_{bolt+plate} \quad (2-13)$$

where:

M = applied moment

L_b = length of bolt from top of plate to head of embedded anchor

n = number of anchor bolts

A_b = cross-sectional area of anchor bolt

E_b = modulus of elasticity of bolt

E = modulus of elasticity of plate

r_b = distance from center of plate to center of bolt

r_p = radius of pipe

t = thickness of base plate

$$b = 2\sqrt{r_b^2 - r_p^2}$$

Table 6.4 Comparison of measured and predicted connection rotations

Test #	Connection Stiffness kip/in	Load for θ Calculations kips	θ_{measured}	$\theta_{\text{calculated}}$ by Eq. (6-9)	$\theta_{\text{measured}}/\theta_{\text{calculated}}$
8-3/4-10-U	6.28	1.29	0.00214	0.00314	0.683
Test #	Connection Stiffness kip/in	Load for θ Calculations kips	θ_{measured}	$\theta_{\text{calculated}}$ by Eq. (6-10)	$\theta_{\text{measured}}/\theta_{\text{calculated}}$
8-3/4-10-G	8.22	1.29	0.00163	0.00213	0.766

Although Eq. (6-9) and Eq. (6-10) over-predict the rotations for both tests, the results are conservative for serviceability considerations.

As discussed in Chapter 2, the second term of Eq. (2-10) was developed based on a rational behavioral model empirically adjusted to reflect analytical results from the finite element analysis reported in Cook et al. (1998). Obviously, the model gives an excellent representation of annular base plate rotation for the configurations used to empirically adjust the rational behavioral model as indicated in Table 2.7. When both terms of Eq. (2-10) (i.e. rotation from both bolt and annular base plate deformations) are used to calculate rotation and the results are compared to the actual rotations measured in tests, there is an over prediction of rotation. This is shown in Table 6.5 for ungrouted base plates. Table 6.5 is simply a combination of the results reported in Table 2.8 combined with the ungrouted base plate test in Table 6.4:

Table 6.5 Evaluation of rotation from anchor bolts and base plate using Eq. (2-10) for ungrouted base plates

Test #	$\theta_{\text{measured}} / \theta_{\text{predicted}}$
8-3/4-8-U	0.388
8-3/4-4s-U	0.651
6-3/4-4sW-U	0.828
6-3/4-4s-U	1.01
8-3/4-10-U	0.683
mean	0.71
COV	0.29

As noted in Chapter 2, test # 8-3/4-8U exhibited an unusually high stiffness that was likely due to bond developed by the anchor bolts (i.e. the anchor bolts did not exhibit deformation over their entire embedded length). When this test is not considered, the results of the ungrouted tests shown in Table 6.5 provide a mean of 0.79 and coefficient of variation of 0.18. The relatively low coefficient of variation indicates that Eq. (2-10) does provide a reasonable fit to the actual test data. Since the second term of Eq. (2-10) was developed to fit multiple base plate configurations based on the finite element study as shown in Table 2.7, it can be assumed that the over estimation of rotation is likely due to the fact that the headed anchor bolts do develop some bond with the concrete and that their effective length may be somewhat less than their full embedded length as assumed in the first term of Eq. (2-10). For design purposes, it seems appropriate to base the contribution of the anchor bolts to the overall rotation on their full embedded length (i.e., top of base plate to the bearing surface on the embedded anchor head).

6.4 Summary- Design Recommendations

The following provides recommended design equations for determining annular base plate thickness, for determining the effective tensile stress area for the anchor bolts, and for performing serviceability checks on annular base plate systems.

6.4.1 Required Base Plate Thickness

As shown in Table 6.1 and Appendix H, Eq. (2-9) provides a reasonable fit to test data for four, six, eight, and ten bolt annular base plate tests. Although Eq. (2-9) was developed based on a yield line analysis consistent with the deformations noted in the six, eight and ten bolt tests, it has also been shown that it provides the best model for the four bolt configurations. Eq. (6-7) is simply a rearrangement of Eq. (2-9) with a capacity reduction factor (ϕ) included for design:

$$t = \sqrt{\frac{M_u (r_b - r_p)}{\phi F_y r_p r_b}} \quad (6-7)$$

where:

t = base plate thickness

M_u = applied moment including load factors

r_b = distance from center of plate to centerline of anchor bolts

r_p = pipe outside radius

ϕ = capacity reduction factor (0.9 suggested)

F_y = minimum specified yield stress of the base plate

6.4.2 Required Effective Anchor Bolt Area

As indicated by Tables 2.5, 2.6, and 6.2, all tests have shown that Eq. (2-3) provides an excellent fit to test data for determining the load in the anchor bolts. Eq. (23) is based on an elastic distribution of the applied moment to the anchor bolts. As discussed in §6:2.2, the reason for this lies in the fact that in typical annular base plate structures the diameter of the attached tubular member (that acts as a rigid body for rotation at the level of the base plate) is not significantly different than the diameter of the anchor bolt pattern.

For design purposes, the force in the anchor bolt should be limited to either the effective tensile area (A_{se}) multiplied by ϕF_y (with a suggested capacity reduction factor ϕ of 0.9) or ϕF_u (with a suggested capacity reduction factor ϕ of 0.75). For consistency with current standards for bolts, the value of ϕF_u (with suggested capacity reduction factor ϕ of 0.75) is used in Eq. (6-8):

$$A_{se} = \frac{2M}{\phi F_u n r_b} \quad (6-8)$$

where:

A_{se} = effective tensile stress area of bolt (0.75 A_o , for threaded bolts)

M_u = applied moment including load factors

ϕ = capacity reduction factor (0.75 recommended when using F_u)

F_u = minimum specified ultimate stress of the anchor bolt

n = number of bolts

r_b = distance from center of plate to centerline of anchor bolts

6.4.3 Serviceability Checks

As discussed in §6.3.3, the contribution to the overall structural deflection of the annular base plate system due to the rotation associated with the annular: base plate and the anchor bolts can be conservatively determined using Eq. (2-10) for ungrouted base plates and Eq. (2-13) for grouted base plates. Eq (2-14) is recommended for grouted base plates with stiffeners.

$$\theta_{bolt+plate} = \frac{2ML_b}{nr_b^2 A_b E_b} + \frac{45M}{Er_b^2 b} \left(\frac{r_b - r_p}{t} \right)^{1.83} \quad (2-10)$$

$$\theta_{bolt+grouted\ plate} = 0.66\theta_{bolt+plate} \quad (2-13)$$

$$\theta_{bok+grouted\ stiffened\ plate} = 0.39\theta_{bolt+plate} \quad (2-14)$$

where:

M= applied moment

L_b =length of bolt from top of plate to head of embedded anchor

n = number of anchor bolts

A_b =cross-sectional area of anchor bolt

E_b = modulus of elasticity of bolt

E = modulus of elasticity of plate

r_b =distance from center of plate to center of bolt

r_p = radius of pipe

t = thickness of base plate

$$b = 2\sqrt{r_b^2 - r_p^2}$$

CHAPTER 7 SUMMARY AND CONCLUSIONS

7.1 Summary

The purpose of this research was to examine the behavior of annular base plates constructed with and without grout pads. The base plates evaluated were modeled after Florida Department of Transportation (FDOT) sign and lighting structures. The loading on those base plates is dominated by moment, as were the plates tested here. The final goal was to recommend strength and serviceability criteria for the design of these structural elements. Two base plates specimens were tested. The test system consisted of a tubular member socket-welded to an annular base plate, which was connected to a concrete test block with ten anchor bolts. One test was constructed with a grout pad while the other was left with a gap between the plate and concrete face. Both tests were evaluated to system failure. Testing consisted of applying an eccentric shear load to the tubular member. Load-displacement data for the anchor bolts and the tubular member at the point of loading were recorded for the tests. Load-displacement data for individual anchor bolts were also recorded.

This research followed two previous experimental studies (Cook et al. (1995) and Cook et al. (2000)) and an analytical study (Cook et al. (1998)) as discussed in Chapter 2. The Cook et al. (1995) study was initiated to evaluate the strength and general behavior of annular base plate connections subjected to an applied moment. The primary purpose of this study was to develop a method to determine the required base plate thickness. The study included tests on ungrouted annular base plates with four, six and eight anchor

bolts. Several behavioral models were investigated during this study including both elastic models based on plate theory and models based on yield line analysis. Overall structural rotations due to deformations of both the anchor bolts and base plate were not a primary consideration during the course of this study. Based on the results of the Cook et al. (1995), it was determined that the overall deflection of the annular base plate structure was dependent on both anchor bolt and base plate deformations as well as that of the attached structural member, this led to the Cook et al. (1998) finite element study. This study investigated annular base plate systems representative of the size of systems typically specified by the FDOT and the size of those tested in the Cook et al. (1995) study. This resulted in recommendations for evaluating the contribution of both the anchor bolt and base plate deformations to the overall displacement of the annular base plate system. In the study reported by Cook et al. (2000), the effect of grout pads relative to both structural behavior and protection from corrosion was investigated. The results of this study indicated that protection from corrosion is significantly improved with the addition of a grout pad. The study also resulted in recommendations for evaluating both the strength and serviceability behavior of ungrouted and grouted annular base plates.

As a result of this study and the previous studies, it can be concluded that both the strength and rotational stiffness of the annular base plate are highly indeterminate. For the determination of the required base plate thickness, several approaches were investigated. The approach providing the best relationship to test data was based on a yield line method developed by Mr. Marcus Ansley, the FDOT Project Manager. For the determination of the distribution of load to the anchor bolts, it was determined that the

assumption of an elastic distribution of load provides an excellent correlation with test results. From a serviceability perspective (i.e., structural rotation due to deformation of both the anchor bolts and annular- base plate), the prediction of rotation is extremely difficult to determine from experimental results due to the fact that the anchors may or may not be debonded over their entire length and that the behavior of the base plate is influenced by the performance of the socket weld between the base plate and the structural member. Cook et al. (2000) presented a recommended method for evaluating the contribution of the annular base plate and anchor bolts to the overall structural deflection that was based on a rationally developed model empirically adjusted to reflect both analytical results and test results. The method recommended in Cook et al. (2000) was used to evaluate the test data for the ten bolt annular base plate systems tested during this study. The results of this evaluation indicated that the recommended method for determining the rotation due to deformations of the anchor bolts and annular base plate was conservative when compared to the test results.

7.2 Conclusions

Based on the results of this research project and previous projects, the following design equations are recommended. The basis of the design equations are presented in Chapter 2 and Chapter 6.

- For determining the required base plate thickness:

$$\text{Eq. (6-7): } t = \sqrt{\frac{M_u (r_b - r_p)}{\phi F_y r_p r_b}} \quad \text{with } \phi = 0.9$$

- For determining the required effective tensile stress area (A_{se}) of the anchor bolts:

$$\text{Eq. (6-8): } A_{se} = \frac{2M_u}{\phi F_u n r_b} \quad \text{with } \phi = 0.75$$

- For evaluating the contribution to overall structural deflection of the annular base plate structure due to rotation resulting from both the anchor bolts and the base plate when ungrouted, grouted, and grouted base plates with stiffeners are used:

$$\text{Eq. (2-10): } \theta_{\text{bolt+plate}} = \frac{2ML_b}{nr_b^2 A_b E} + \frac{45M}{Er_b^2 b} \left(\frac{r_b - r_p}{t} \right)^{1.83}$$

$$\text{Eq. (2-13): } \theta_{\text{bolt + grouted plate}} = 0.66\theta_{\text{bolt+plate}}$$

$$\text{Eq. (2-14): } \theta_{\text{bolt+grouted stiffened plate}} = 0.39\theta_{\text{bolt+plate}}$$

where:

A_b = cross-sectional area of anchor bolt

A_{se} = effective tensile stress area of bolt (0.75 A_b for threaded bolts)

$$b = 2\sqrt{r_b^2 - r_p^2}$$

E = modulus of elasticity of steel

F_y = minimum specified yield stress of the base plate

F_u = minimum specified ultimate stress of the anchor bolt

L_b = length of bolt from top of plate to head of embedded anchor

M = applied moment

M_u = applied moment including load factors

r_b = distance from center of plate to centerline of anchor bolts

r_p = pipe outside radius

t = base plate thickness

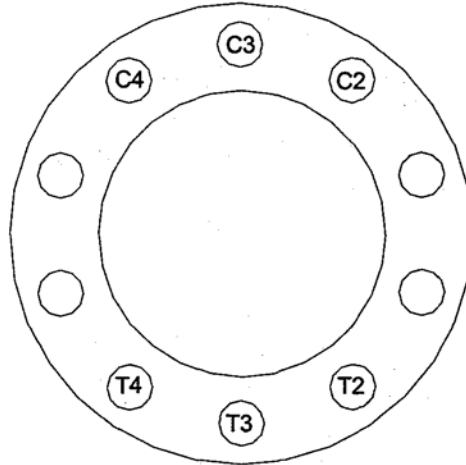
θ = capacity reduction factor

It is also recommended that a flow able grout, installed as shown in Chapter 4, be used to mitigate corrosion (Cook et al. (2000)) and reduce the overall deflection of the annular base plate structure resulting from the flexibility of the annular base plate.

APPENDIX A: INSTRUMENTATION NUMBERING AND ORIENTATION

8-3/4-10-U

LVDT Placement



Note: LVDT P1 is located over load point on pipe

Load Cell Placement

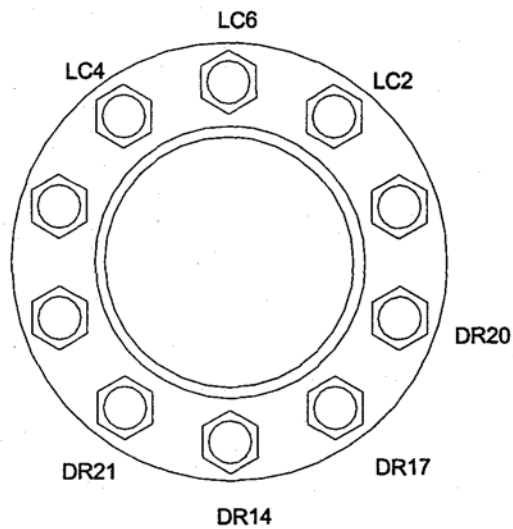
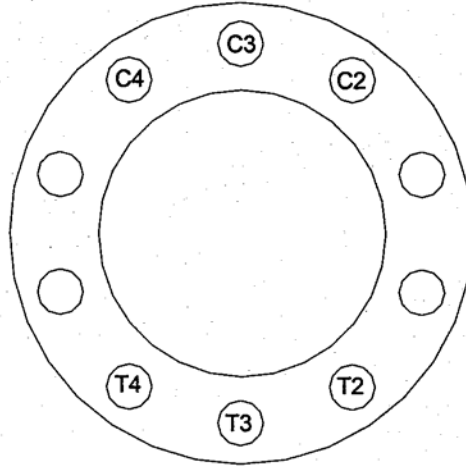


Figure A1.2 Instrumentation placement for Specimen #2, Test 8-3/4-10-U

8-3/4-10-G

LVDT Placement



Note: LVDT P1 is located over load point on pipe.

Load Cell Placement

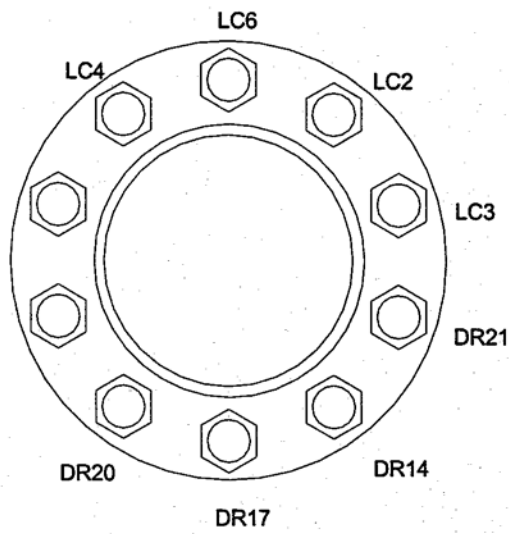


Figure A1.1 Instrumentation placement for Specimen #1, Test 8-3/4-10-G

APPENDIX B: LVDT DATA

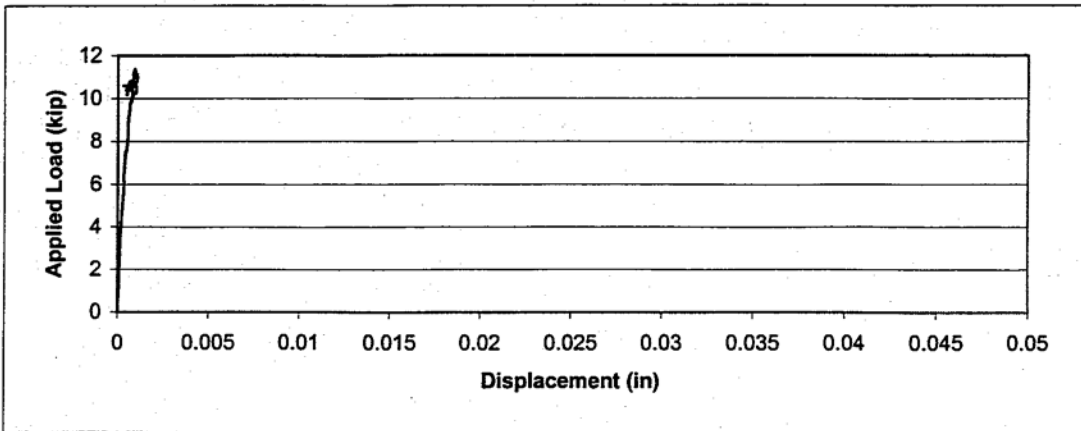


Figure B1.1 Applied Load vs. LVDT C2 (Test 8-3/4-10-G)

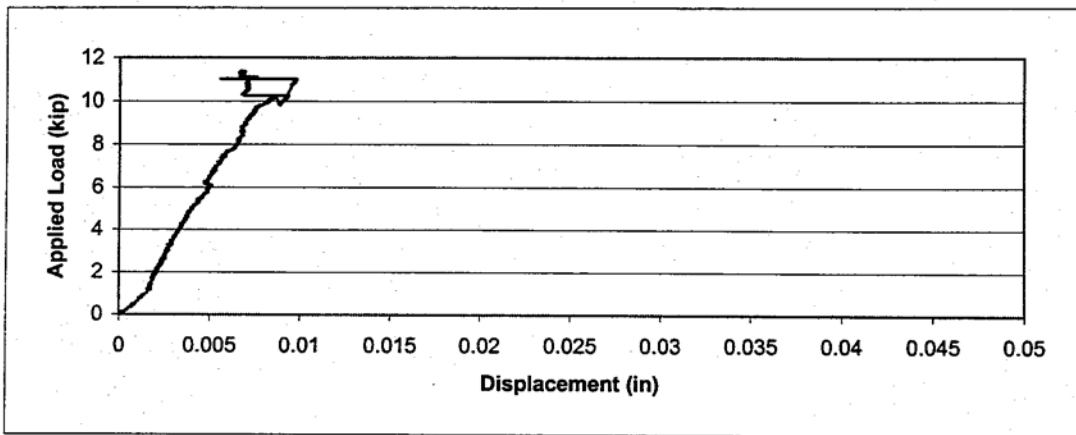


Figure B1.2 Applied Load vs. LVDT C3 (Test 8-3/4-10-G)

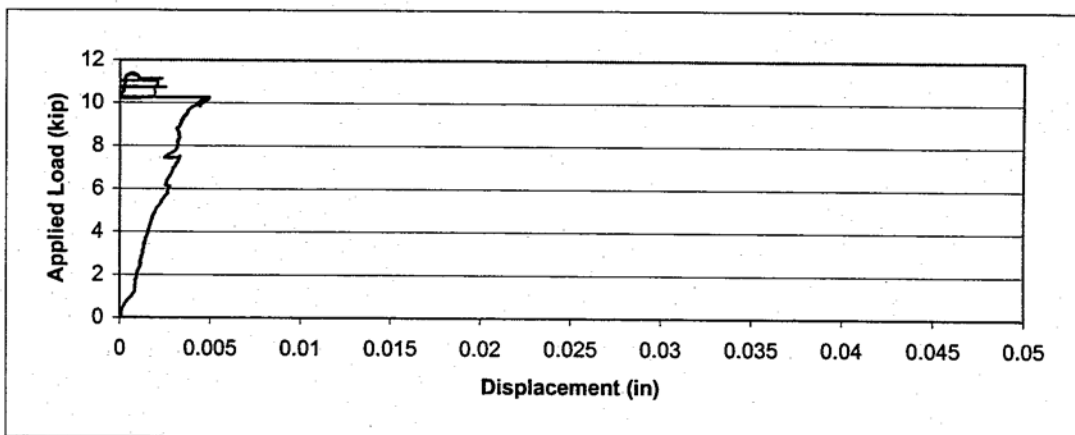


Figure B1.3 Applied Load vs. LVDT C4 (Test 8-3/4-10-G)

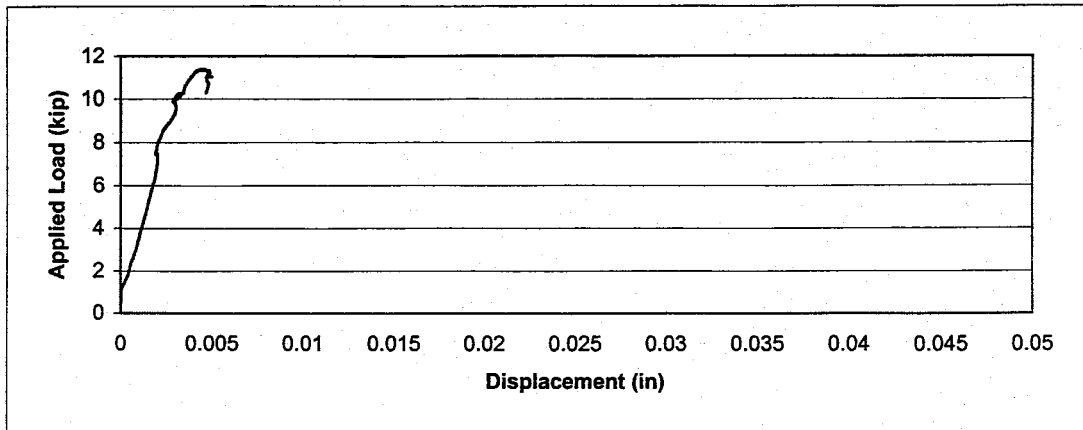


Figure B1.4 Applied Load vs. LVDT T2 (Test 8-3/4-10-G)

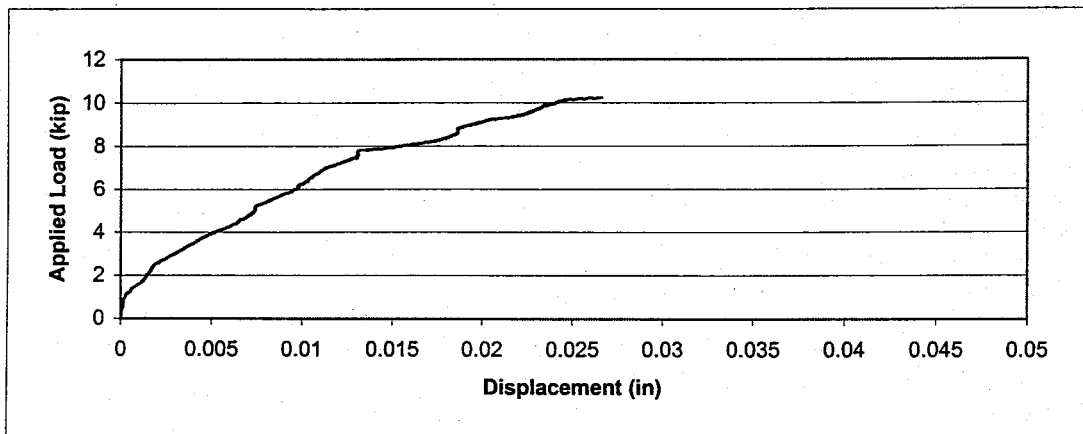


Figure B1.5 Applied Load vs. LVDT T3 (Test 8-3/4-10-G)

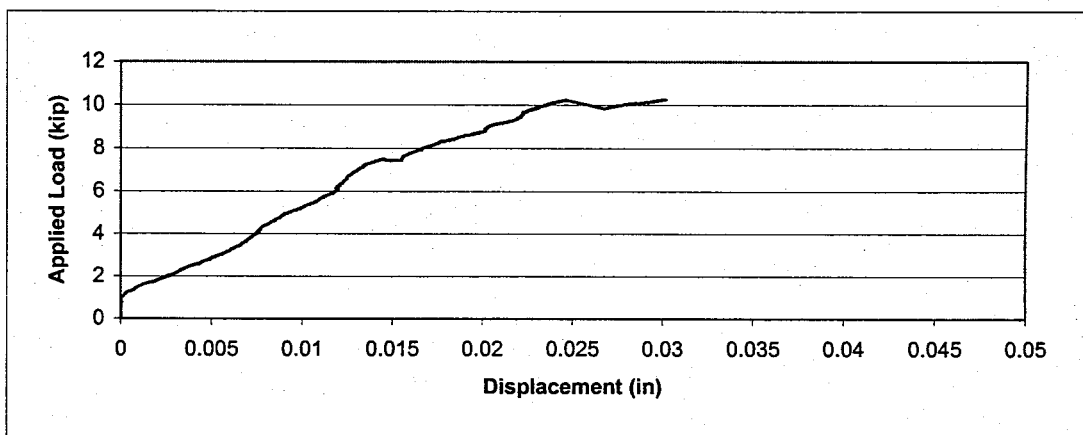


Figure B1.6 Applied Load vs. LVDT T4 (Test 8-3/4-10-G)

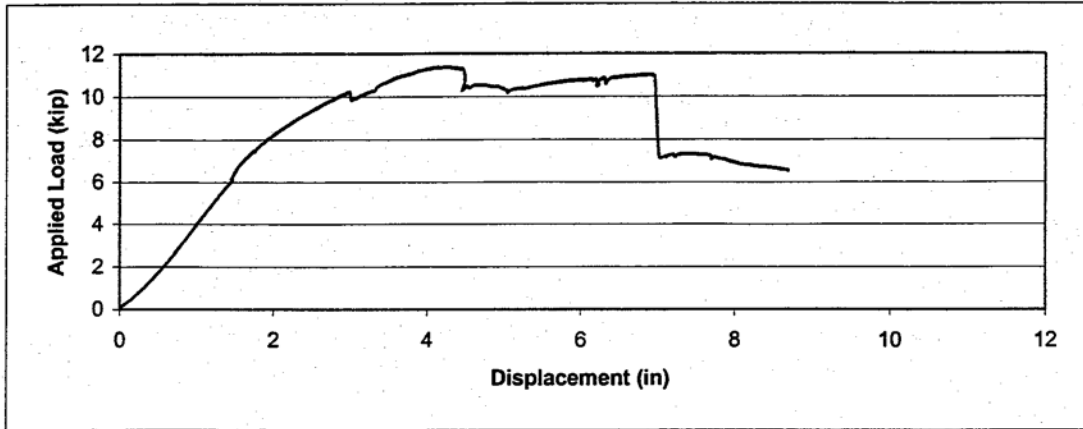


Figure B1.7 Applied Load vs. LVDT P1 (Test 8-3/4-10-G)

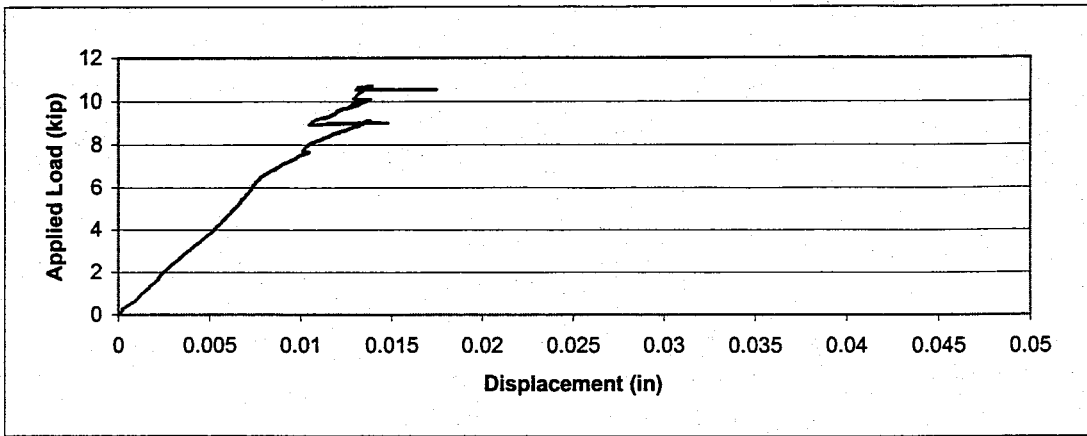


Figure B2.1 Applied Load vs. LVDT C2 (Test 8-3/4-10-U)

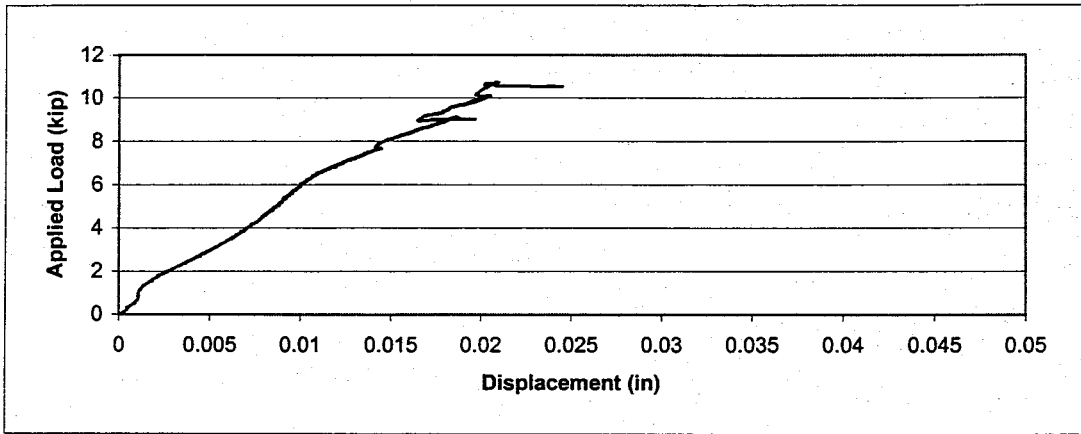


Figure B2.2 Applied Load vs. LVDT C3 (Test 8-3/4-10-U)

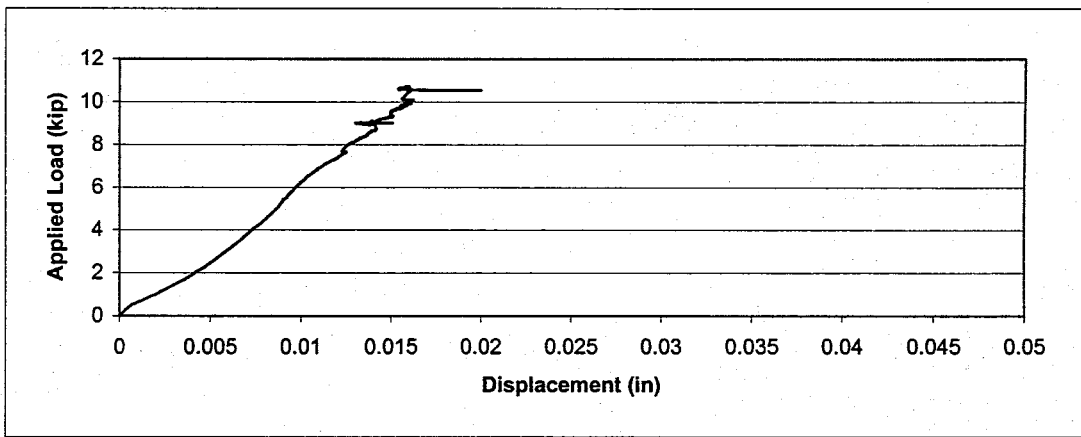


Figure B2.3 Applied Load vs. LVDT C4 (Test 8-3/4-10-U)

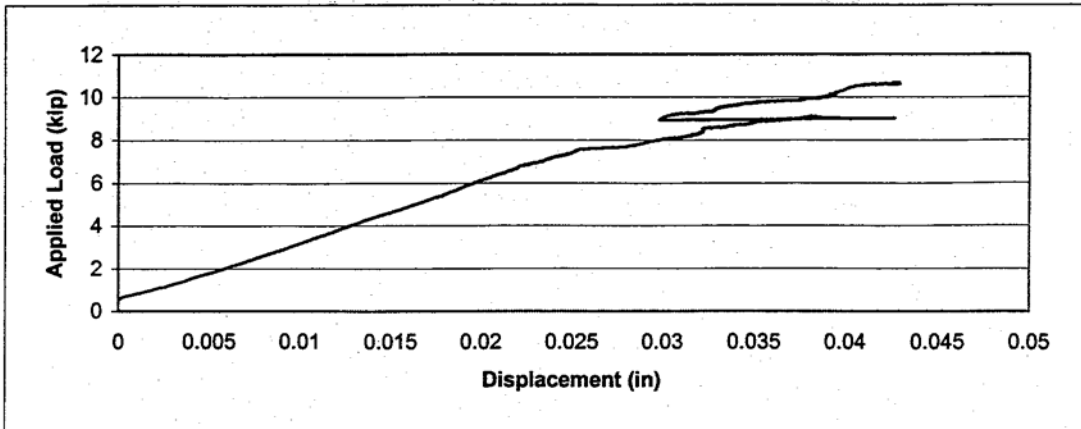


Figure B2.4 Applied Load vs. LVDT T2 (Test 8-3/4-10-U)

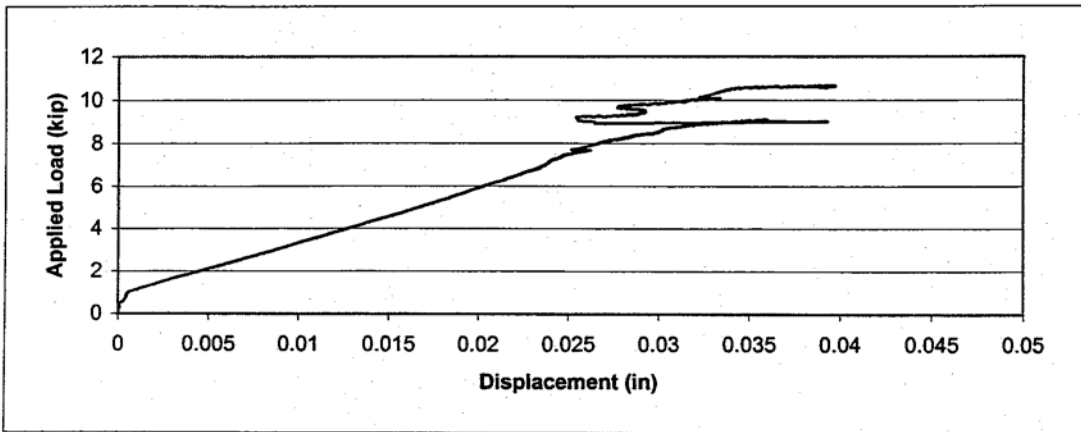


Figure B2.5 Applied Load vs. LVDT T3 (Test 8-3/4-10-U)

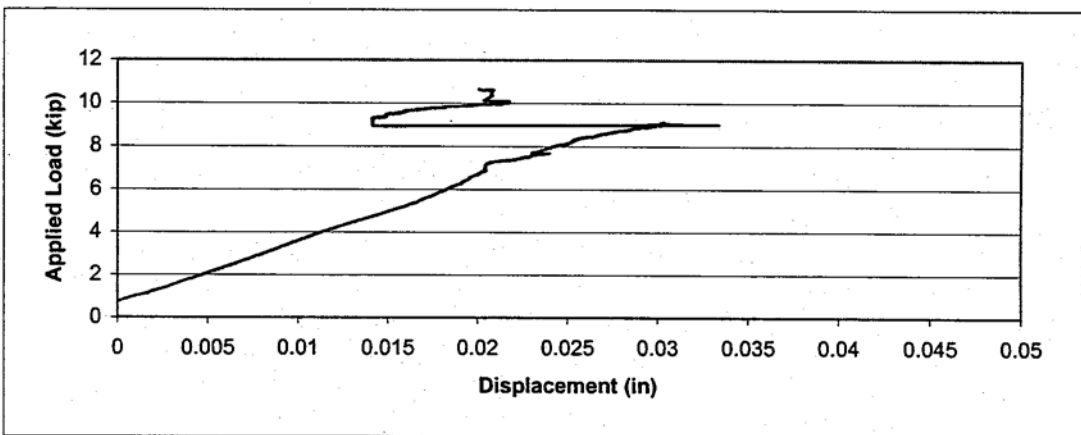


Figure B2.6 Applied Load vs. LVDT T4 (Test 8-3/4-10-U)

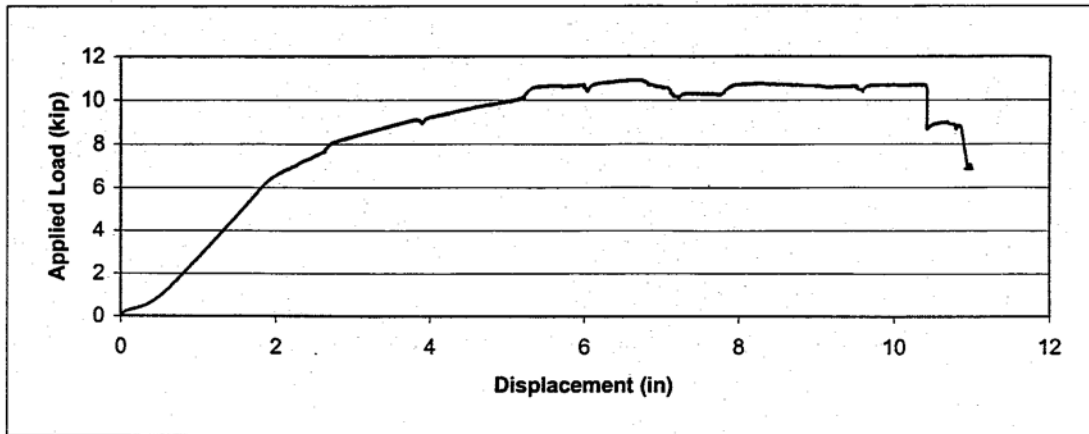


Figure B2.7 Applied Load vs. LVDT P1 (Test 8-3/4-10-U)

APPENDIX C: LOAD CELL DATA

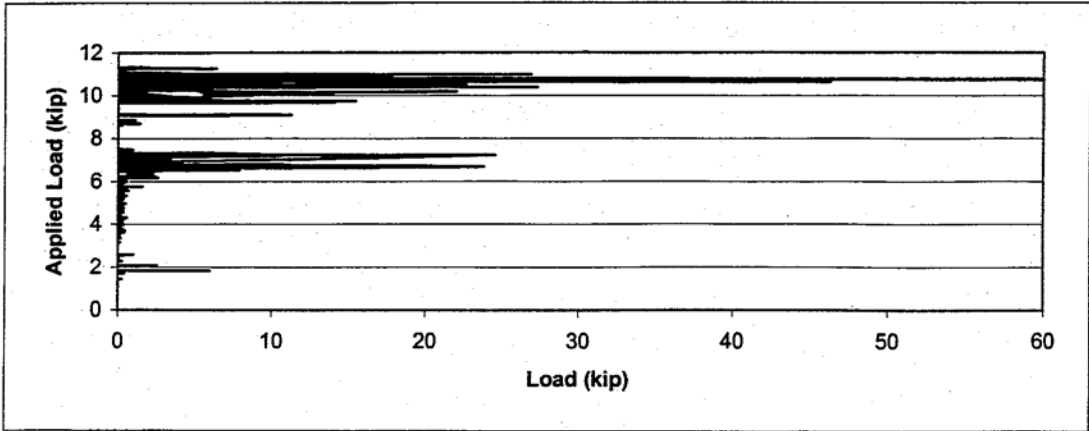


Figure C1.1 Applied Load vs. Load Cell LC3 (Test 8-3/4-10-G)

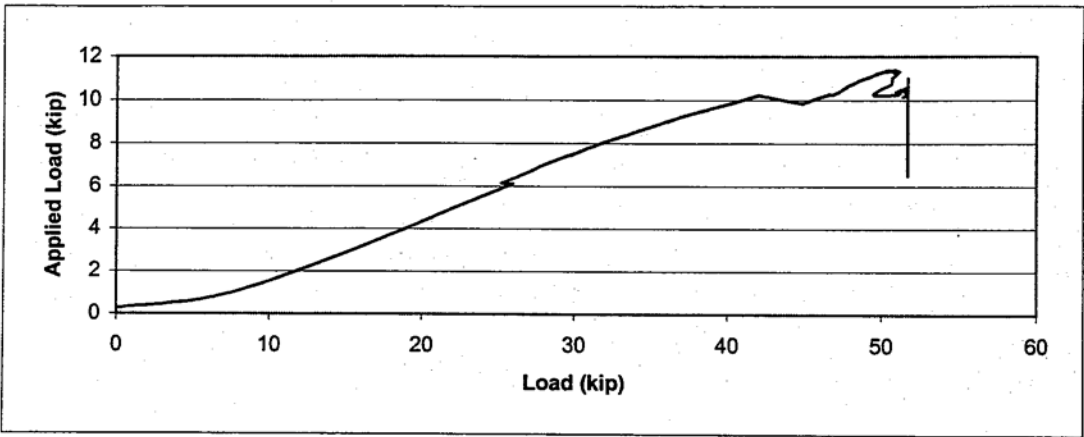


Figure C1.2 Applied Load vs. Load Cell LC2 (Test 8-3/4-10-G)

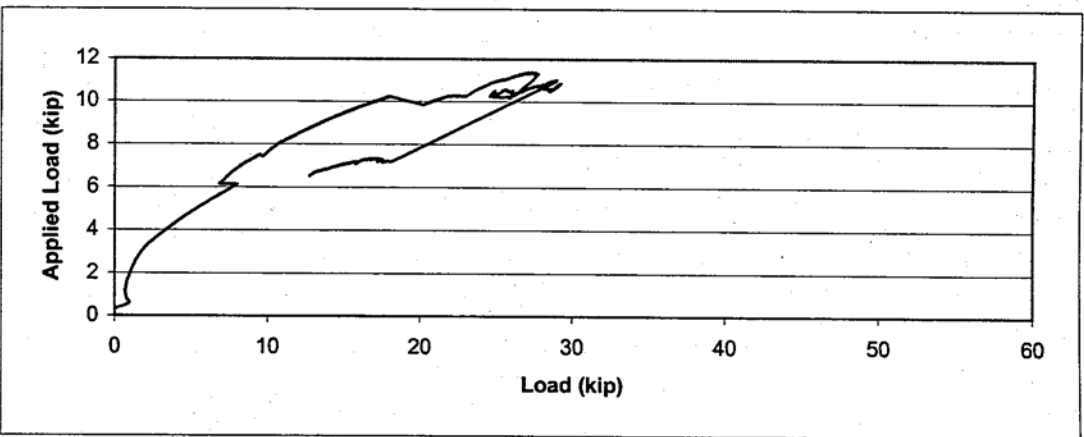


Figure C1.3 Applied Load vs. Load Cell LC6 (Test 8-3/4-10-G)

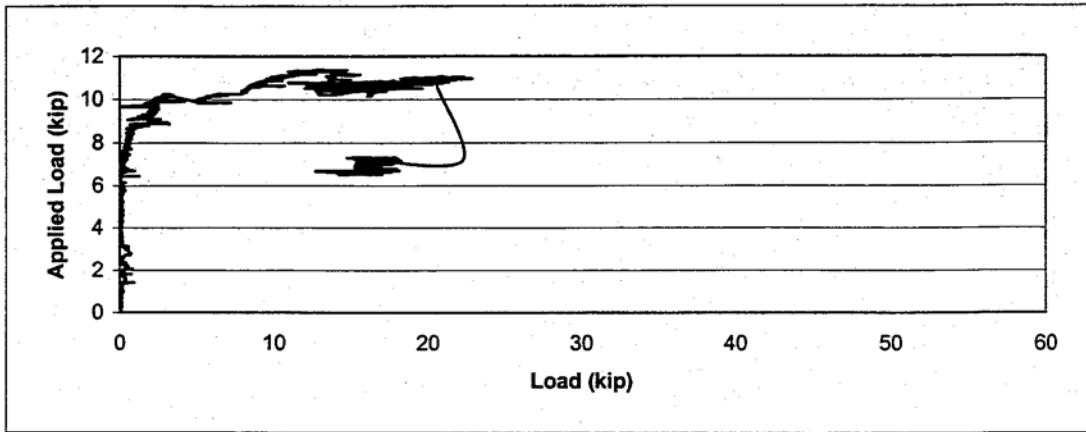


Figure C1.4 Applied Load vs. Load Cell LC4 (Test 8-3/4-10-G)

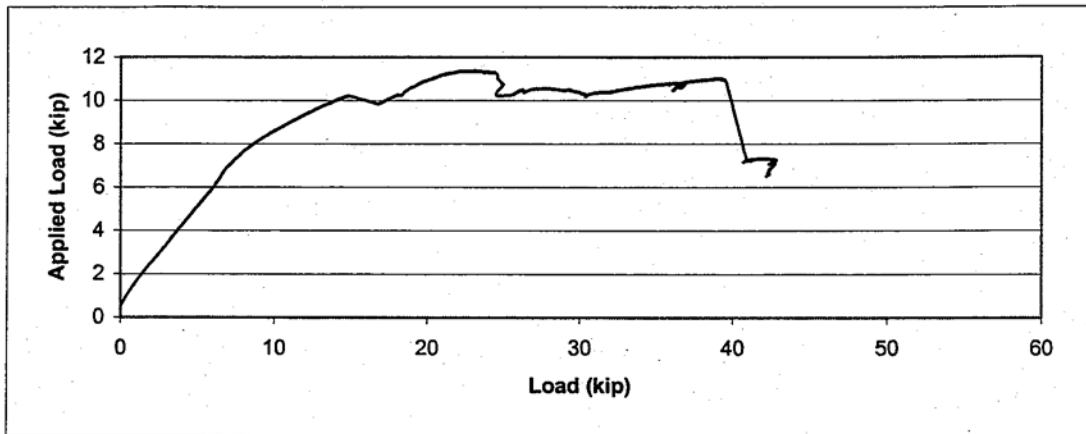


Figure C1.5 Applied Load vs. Load Cell DR21 (Test 8-3/4-10-G)

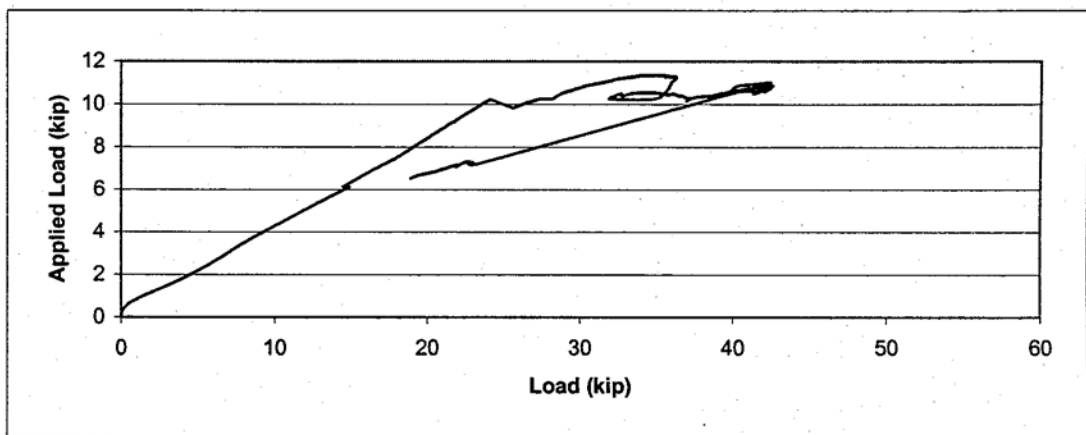


Figure C1.6 Applied Load vs. Load Cell DR14 (Test 8-3/4-10-G)

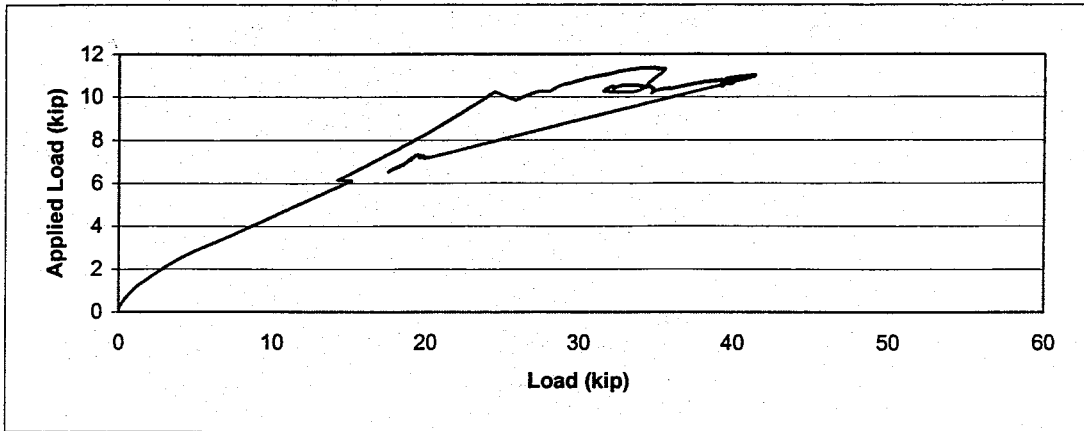


Figure C1.7 Applied Load vs. Load Cell DR17 (Test 8-3/4-10-G)

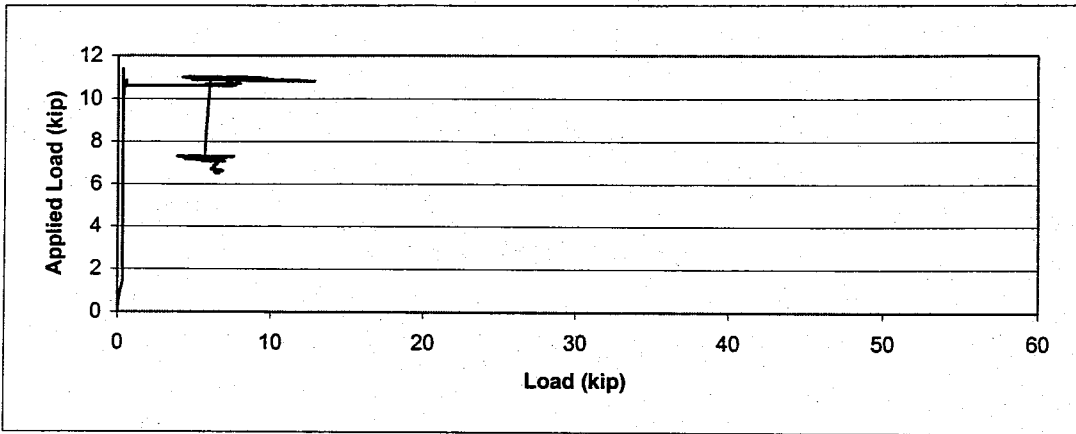


Figure C1.8 Applied Load vs. Load Cell DR20 (Test 8-3/4-10-G)

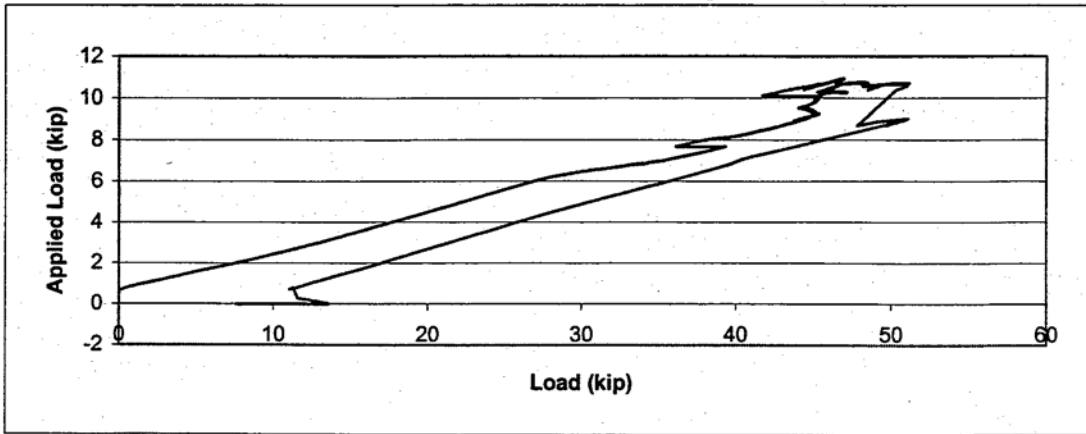


Figure C2.1 Applied Load vs. Load Cell LC2 (Test 8-3/4-10-U)

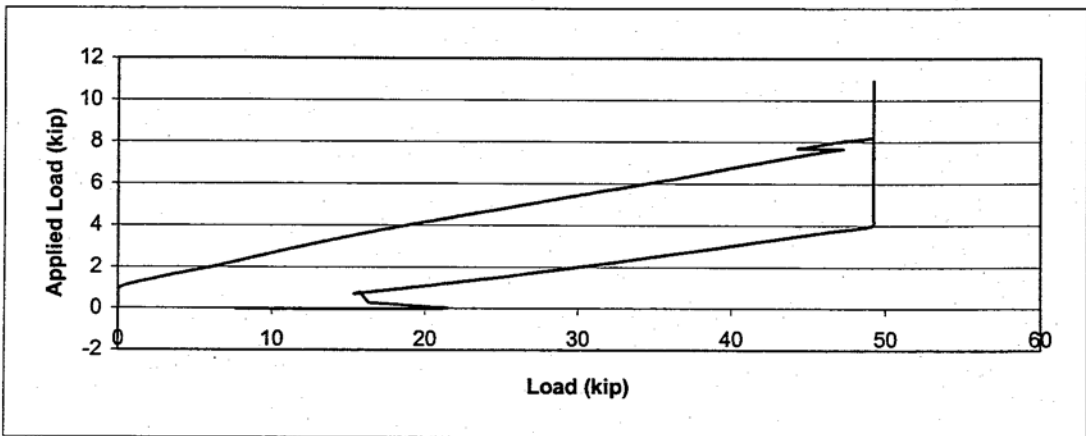


Figure C2.2 Applied Load vs. Load Cell LC6 (Test 8-3/4-10-U)

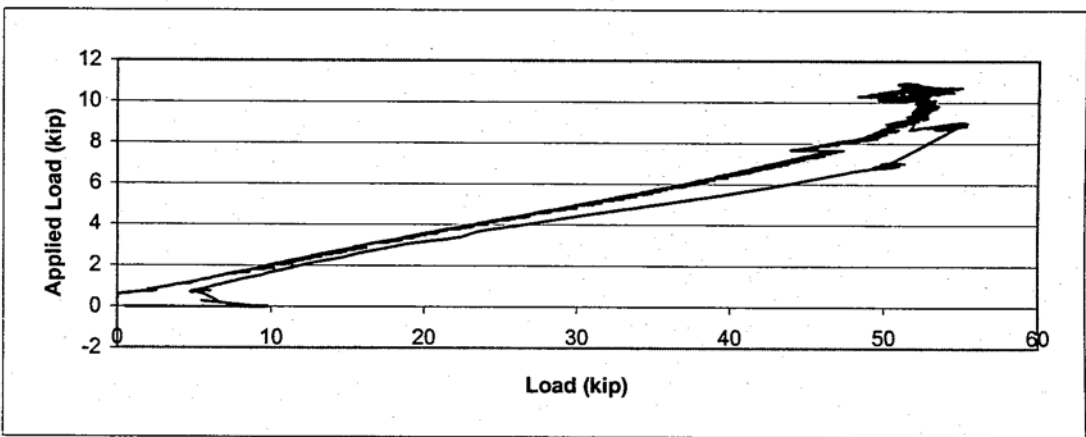


Figure C2.3 Applied Load vs. Load Cell LC4 (Test 8-3/4-10-U)

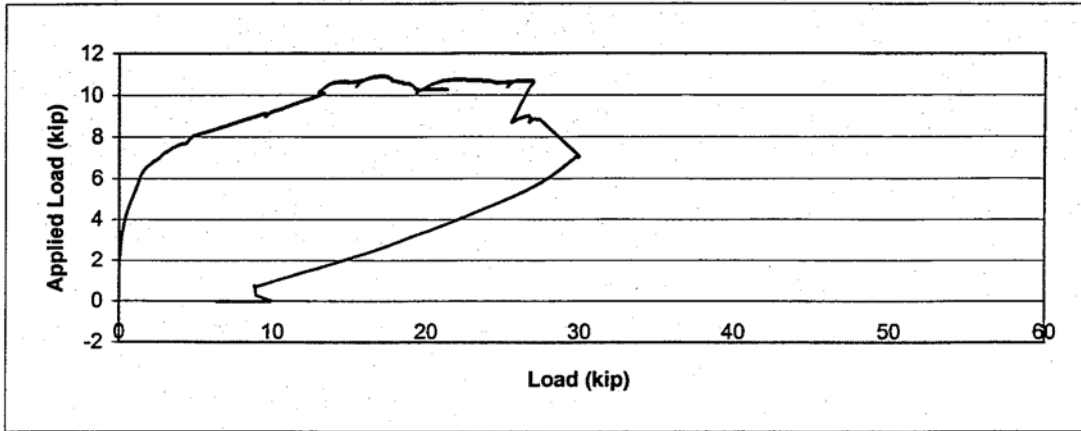


Figure C2.4 Applied Load vs. Load Cell DR20 (Test 8-3/4-10-U)

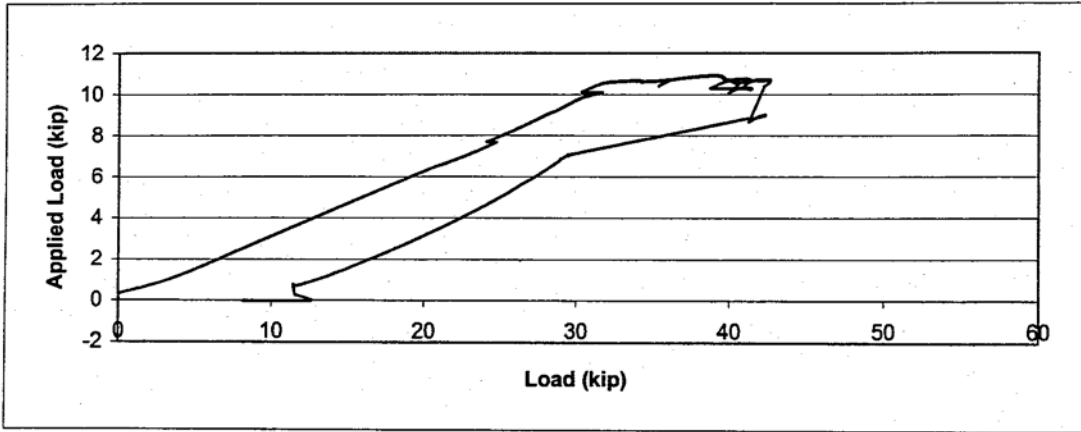


Figure C2.5 Applied Load vs. Load Cell DR17 (Test 8-3/4-10-U)

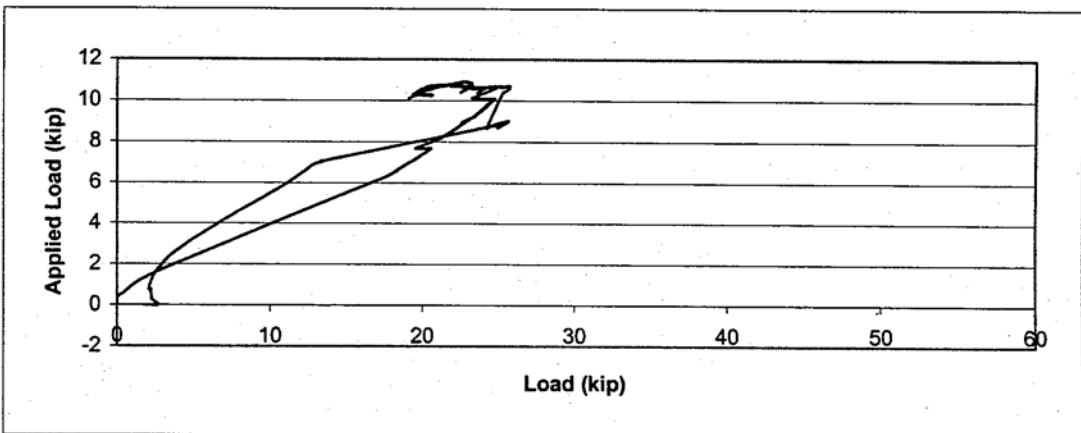


Figure C2.6 Applied Load vs. Load Cell DR14 (Test 8-3/4-10-U)

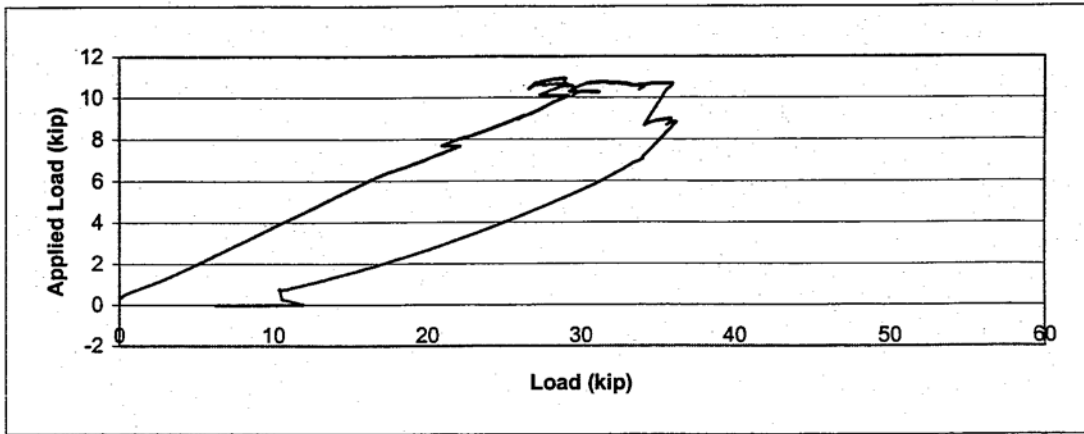


Figure C2.7 Applied Load vs. Load Cell DR21 (Test 8-3/4-10-U)

APPENDIX D: LOAD-DISPLACEMENT GRAPHS

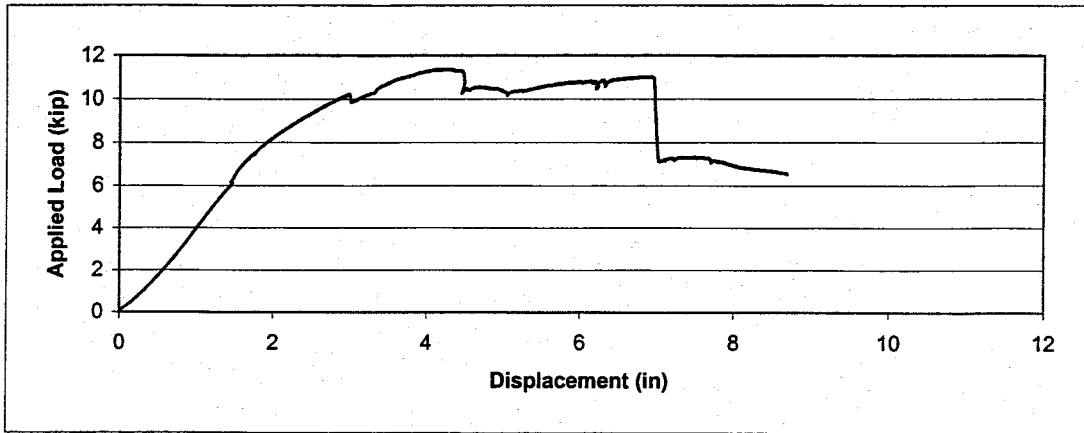


Figure D1 Load-displacement curve for 8-3/4-10-G

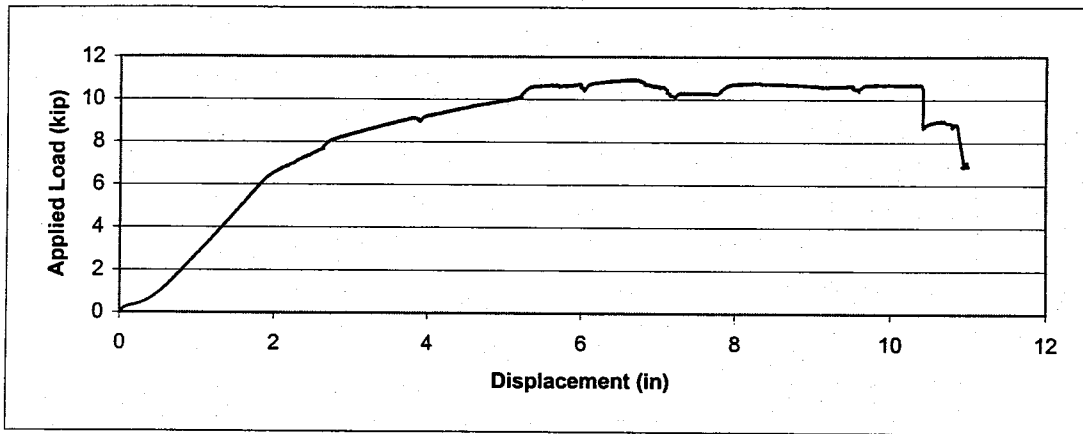


Figure D2 Load-displacement curve for 8-3/4-10-U

APPENDIX E: MOMENT-ROTATION GRAPHS

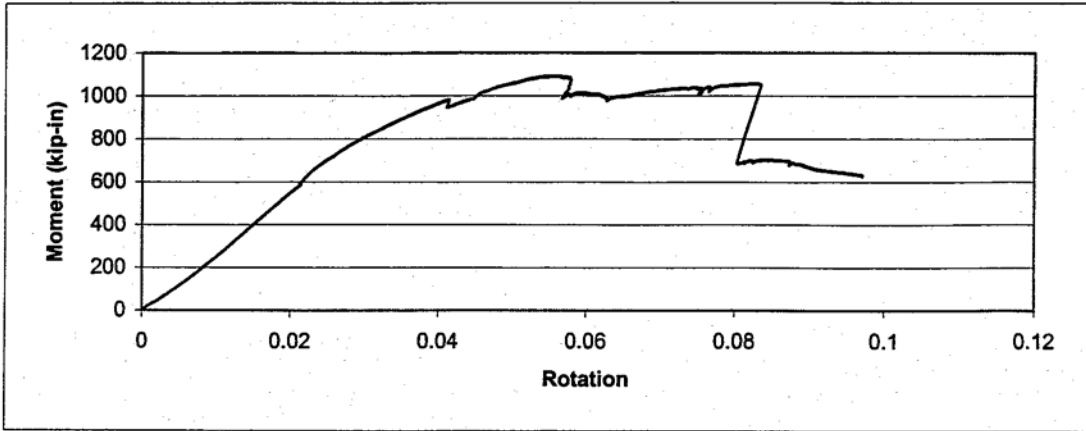


Figure E1 Moment-rotation curve for 8-3/4-10-G

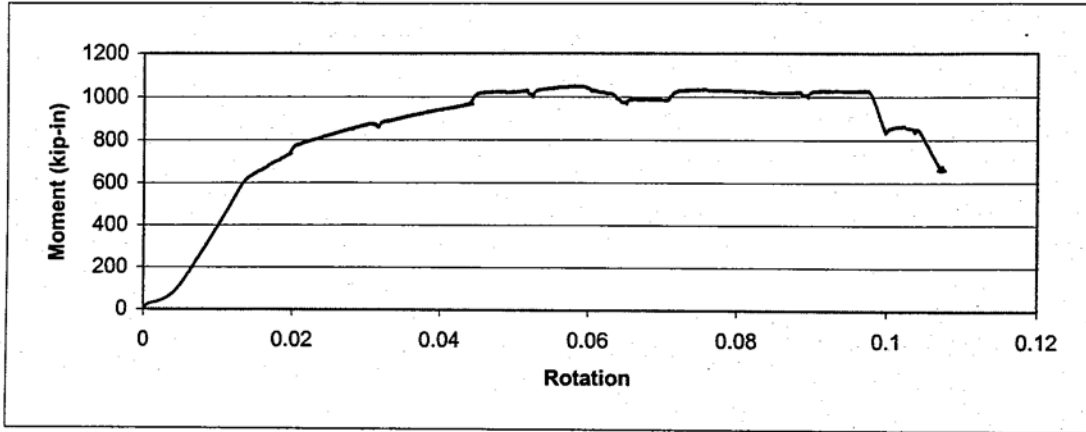


Figure E2 Moment-rotation curve for 8-3/4-10-U

APPENDIX F: STIFFNESS

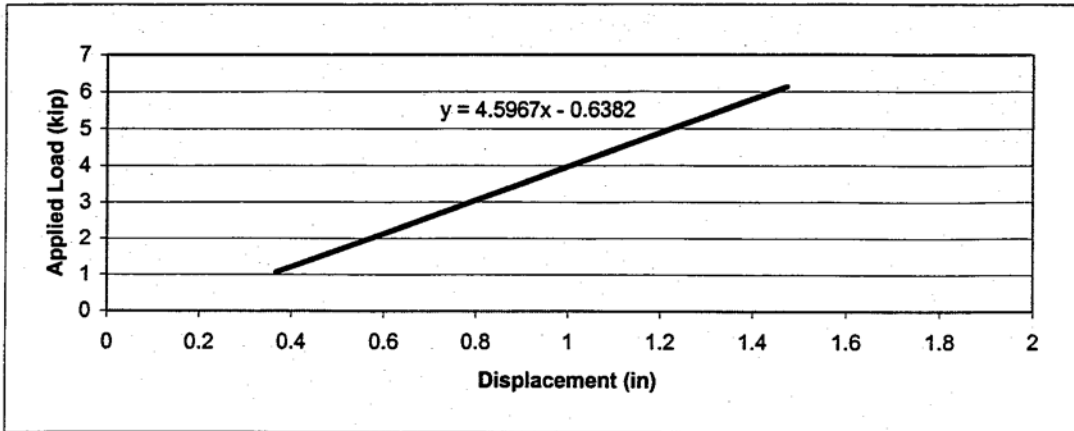


Figure F1 Stiffness plot for 8-3/4-10-G

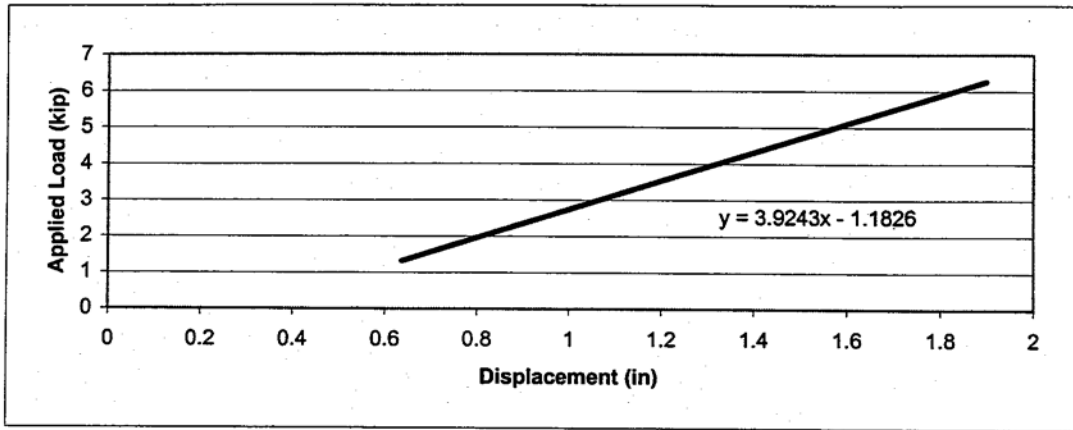
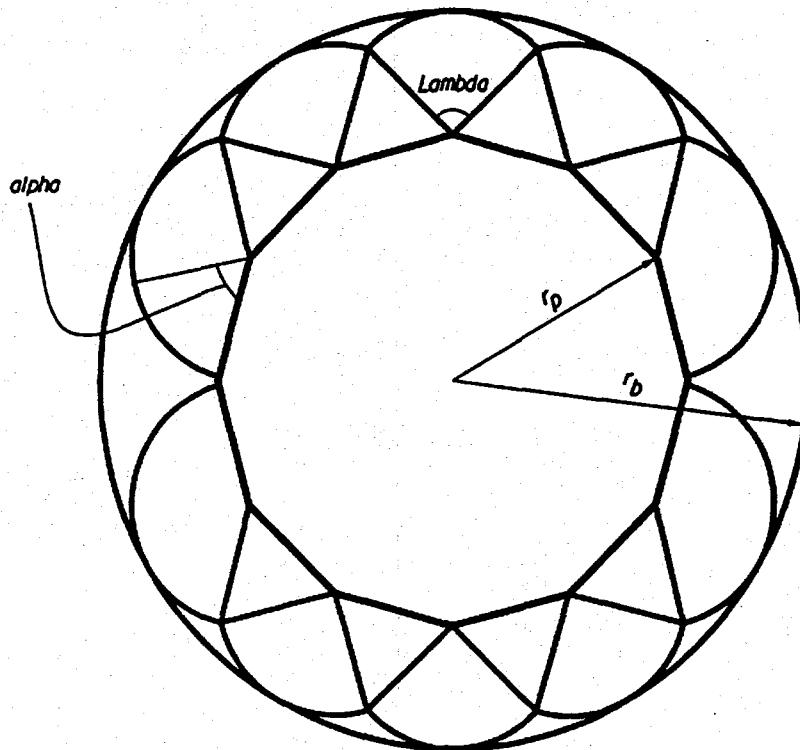


Figure F2 Stiffness plot for 8-3/4-10-U

APPENDIX G: DERIVATION OF EQ. (2-9)

Base Plate Yield Line Mechanism

kip := 1000-lbf



$$\alpha := \arccos \left[\frac{r_p \cdot \sin\left(\frac{\pi}{p}\right)}{(r_b - r_p)} \right]$$

$$\lambda := 2 \cdot \pi - \left[\left(\frac{p-2}{p} \right) \cdot \pi + 2 \cdot \arccos \left[\frac{r_p \cdot \sin\left(\frac{\pi}{p}\right)}{(r_b - r_p)} \right] \right]$$

$$\delta := r_p \cdot \theta$$

Internal Work for 1/2 of Fan

$$M_p \cdot r_p \cdot \theta \cdot \frac{1}{2} \cdot \left[2 \cdot \pi - \left[\left(\frac{p-2}{p} \right) \cdot \pi + 2 \cdot \arccos \left[\frac{r_p \cdot \sin\left(\frac{\pi}{p}\right)}{(r_b - r_p)} \right] \right] \right]$$

Work done by 1/2 of λ fan at top

$$\sum_{n=1}^{\frac{p-1}{4}} \left[M_p \cdot r_p \cdot \theta \cdot \cos\left(\frac{2 \cdot \pi \cdot n}{p}\right) \cdot \left[2 \cdot \pi - \left[\left(\frac{p-2}{p}\right) \cdot \pi + 2 \cdot \operatorname{acos} \left[\frac{r_p \cdot \sin\left(\frac{\pi}{p}\right)}{(r_b - r_p)} \right] \right] \right] \right]$$

Work done by remaining λ fans.
The reduction for δ is obtained by
multiplying by $\cos\left(\frac{2 \cdot \pi \cdot n}{p}\right)$

$$M_p \cdot r_p \cdot \theta \cdot \cos\left[\frac{2 \cdot \pi \cdot \left(\frac{p-1}{4}\right)}{p}\right] \cdot \operatorname{acos} \left[\frac{r_p \cdot \sin\left(\frac{\pi}{p}\right)}{(r_b - r_p)} \right]$$

Work done by α fan

External Work

$$M \cdot \theta$$

Calculate Total Internal Work by Multiplying the 1/2 fan Components by 4 and Eliminate θ by Setting Equal to External Work Such that:

$$M = 4 \cdot \left[\begin{aligned} & M_p \cdot r_p \cdot \frac{1}{2} \cdot \left[2 \cdot \pi - \left[\left(\frac{p-2}{p}\right) \cdot \pi + 2 \cdot \operatorname{acos} \left[\frac{r_p \cdot \sin\left(\frac{\pi}{p}\right)}{(r_b - r_p)} \right] \right] \right] \dots \\ & + \sum_{n=1}^{\frac{p-1}{4}} \left[M_p \cdot r_p \cdot \cos\left(\frac{2 \cdot \pi \cdot n}{p}\right) \cdot \left[2 \cdot \pi - \left[\left(\frac{p-2}{p}\right) \cdot \pi + 2 \cdot \operatorname{acos} \left[\frac{r_p \cdot \sin\left(\frac{\pi}{p}\right)}{(r_b - r_p)} \right] \right] \right] \dots \\ & + M_p \cdot r_p \cdot \cos\left[\frac{2 \cdot \pi \cdot \left(\frac{p-1}{4}\right)}{p}\right] \cdot \operatorname{acos} \left[\frac{r_p \cdot \sin\left(\frac{\pi}{p}\right)}{(r_b - r_p)} \right] \end{aligned} \right] \dots$$

Find the result for round by letting p go to ∞

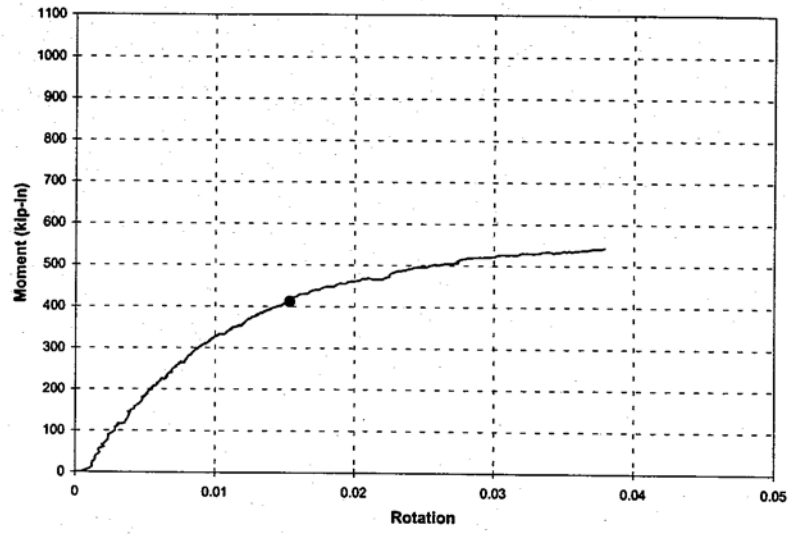
$$\lim_{p \rightarrow \infty} 4 \cdot \left[\begin{aligned} & M_p \cdot r_p \cdot \frac{1}{2} \cdot \left[2 \cdot \pi - \left[\left(\frac{p-2}{p}\right) \cdot \pi + 2 \cdot \operatorname{acos} \left[\frac{r_p \cdot \sin\left(\frac{\pi}{p}\right)}{(r_b - r_p)} \right] \right] \right] \dots \\ & + \sum_{n=1}^{\frac{p-1}{4}} \left[M_p \cdot r_p \cdot \cos\left(\frac{2 \cdot \pi \cdot n}{p}\right) \cdot \left[2 \cdot \pi - \left[\left(\frac{p-2}{p}\right) \cdot \pi + 2 \cdot \operatorname{acos} \left[\frac{r_p \cdot \sin\left(\frac{\pi}{p}\right)}{(r_b - r_p)} \right] \right] \right] \dots \\ & + M_p \cdot r_p \cdot \cos\left[\frac{2 \cdot \pi \cdot \left(\frac{p-1}{4}\right)}{p}\right] \cdot \operatorname{acos} \left[\frac{r_p \cdot \sin\left(\frac{\pi}{p}\right)}{(r_b - r_p)} \right] \end{aligned} \right] \rightarrow -4 \cdot M_p \cdot r_p \cdot \frac{r_b}{(-r_b + r_p)}$$

Which can be expressed as

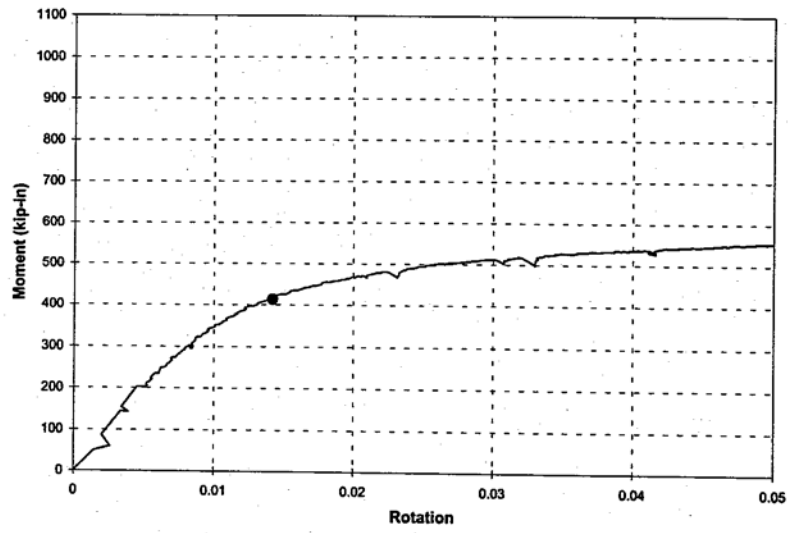
$$4 \cdot M_p \cdot r_p \cdot \frac{r_b}{r_b - r_p}$$

APPENDIX H: MOMENT-ROTATION GRAPHS WITH EQ. (2-9)

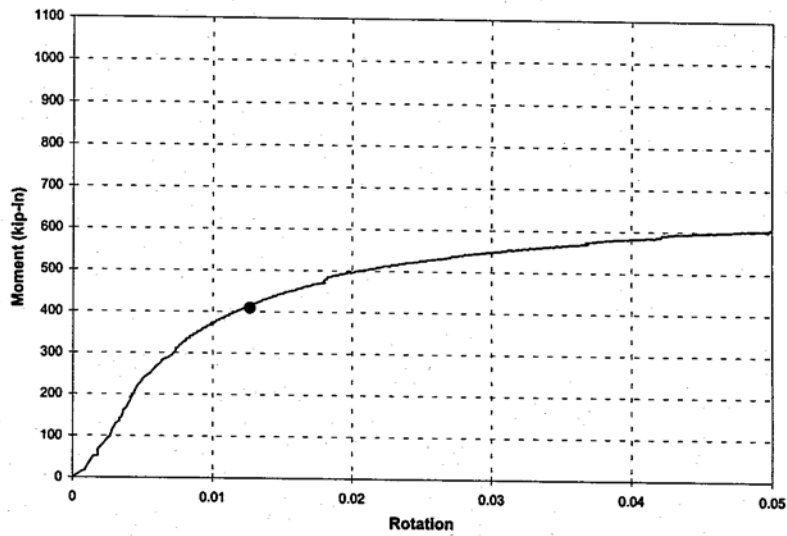
6-1-4d



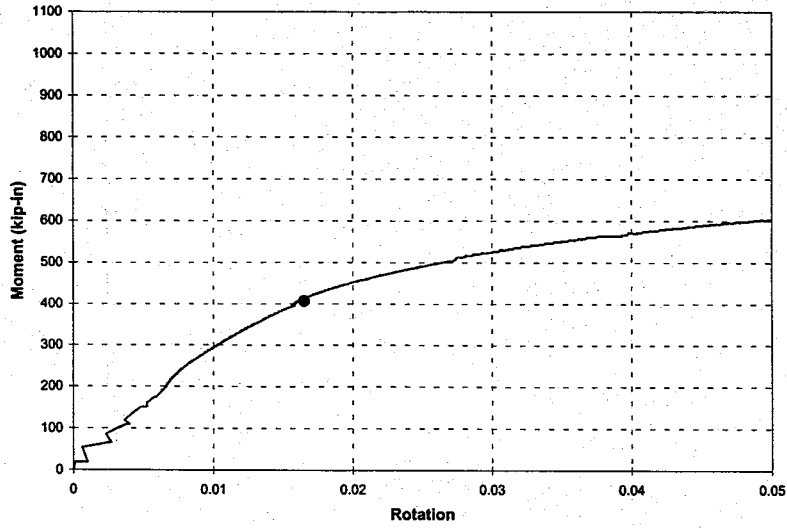
6-1-4s



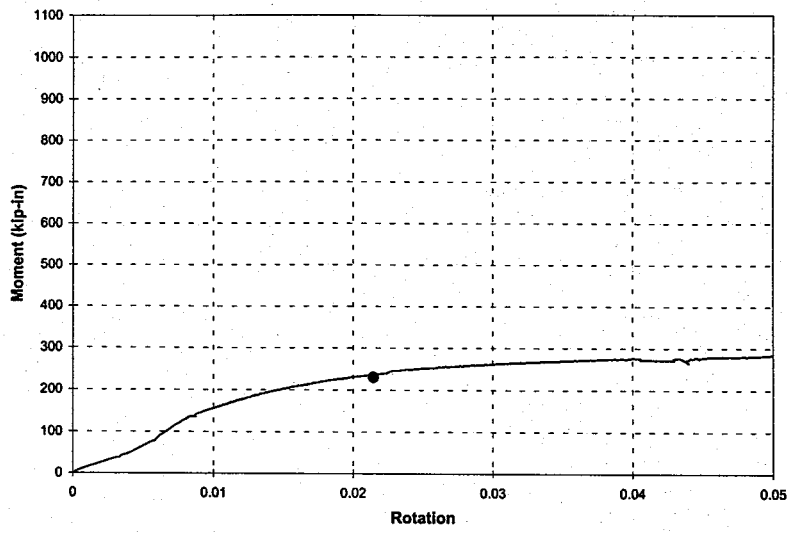
6-1-6



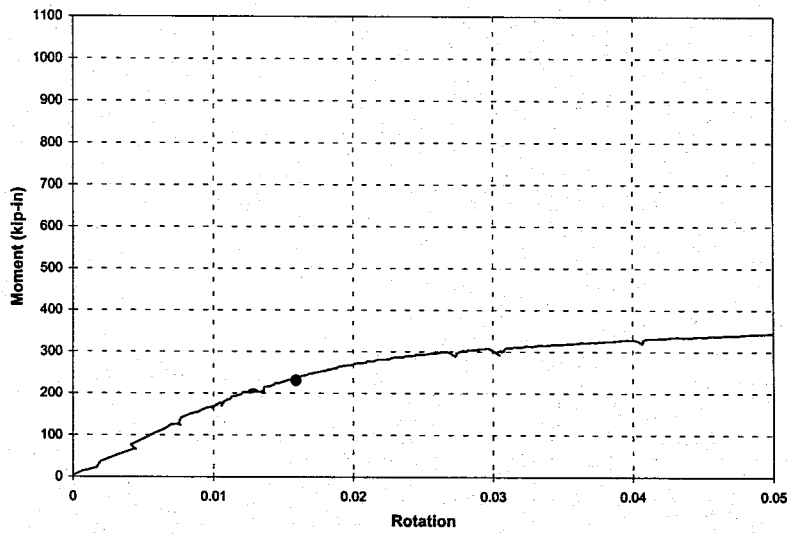
6-1-8



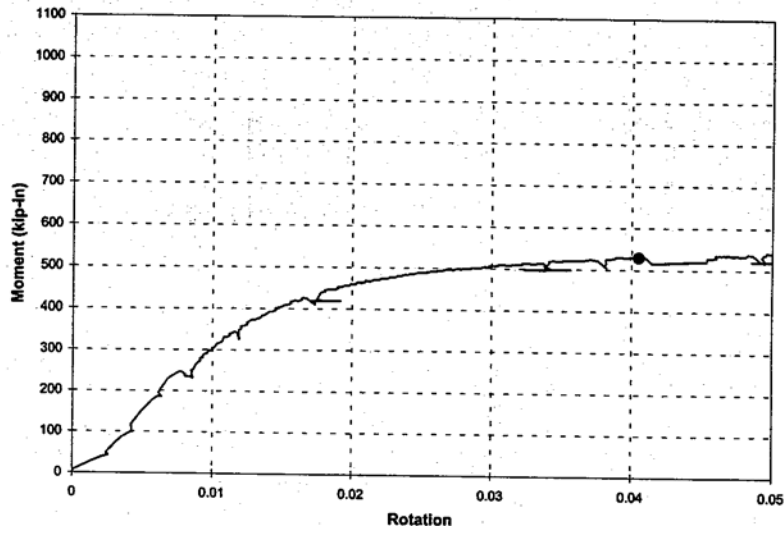
6-3/4-4d



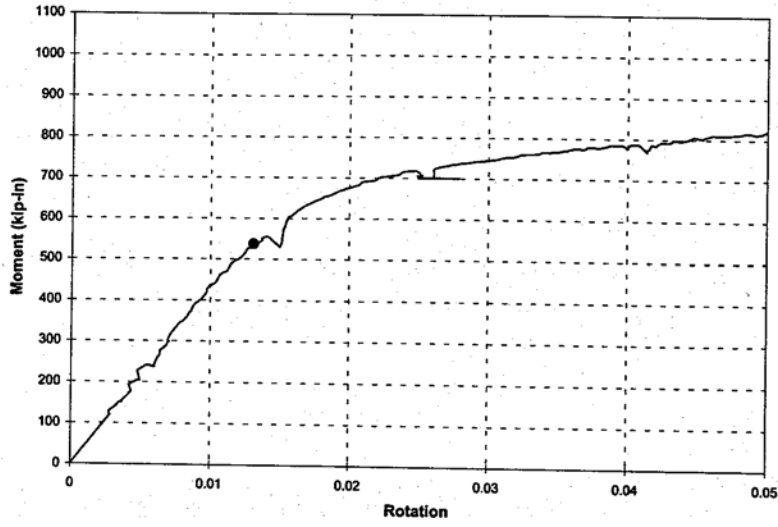
6-3/4-8



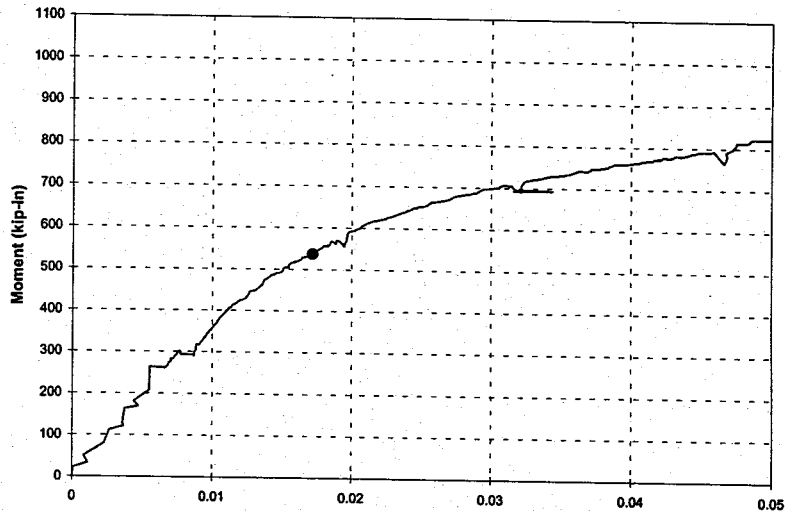
8-3/4-4d



8-3/4-6

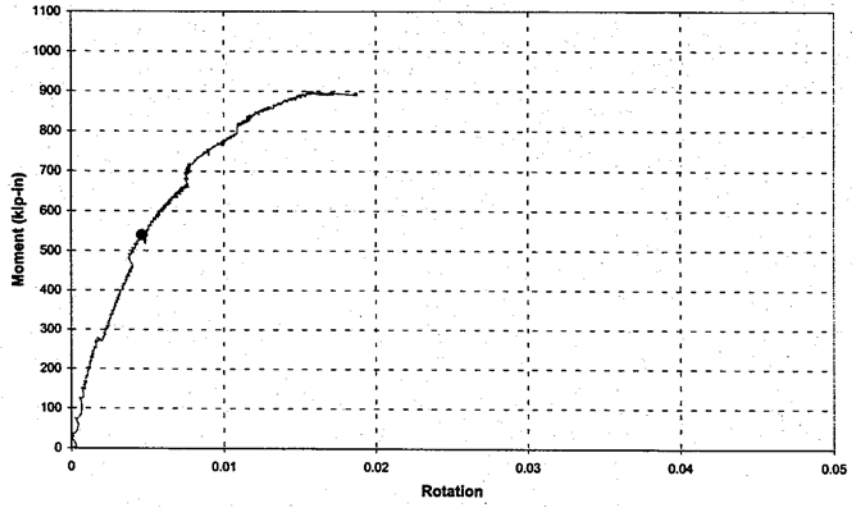


8-3/4-8

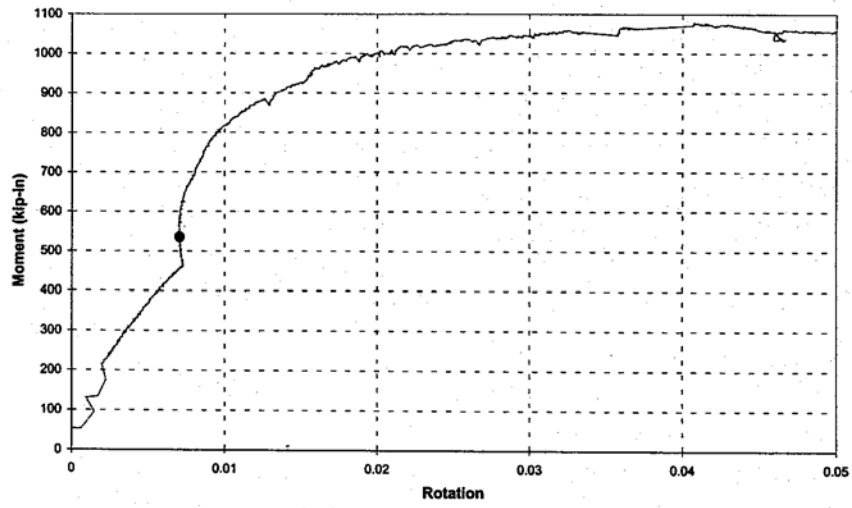


Rotation

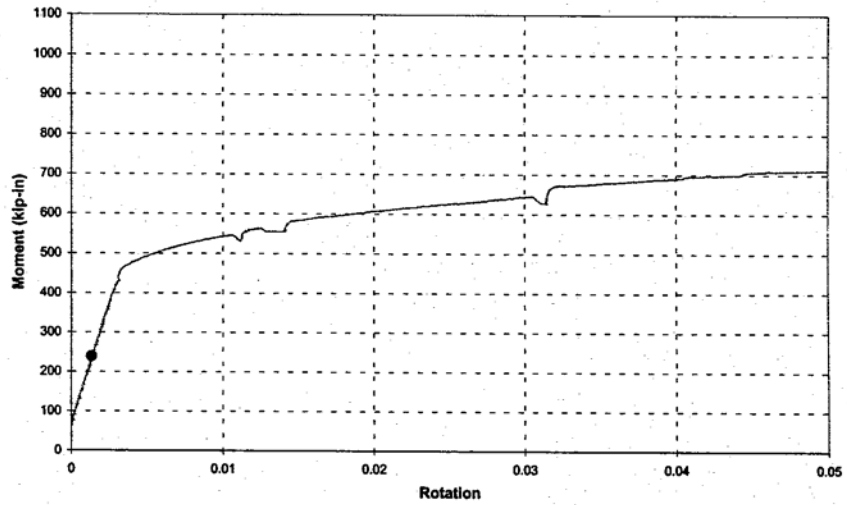
8-3/4-8-G



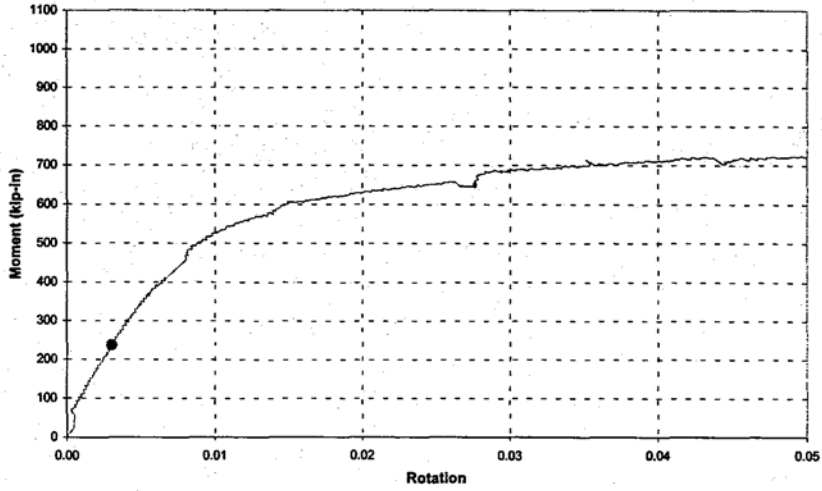
8-3/4-4s-G



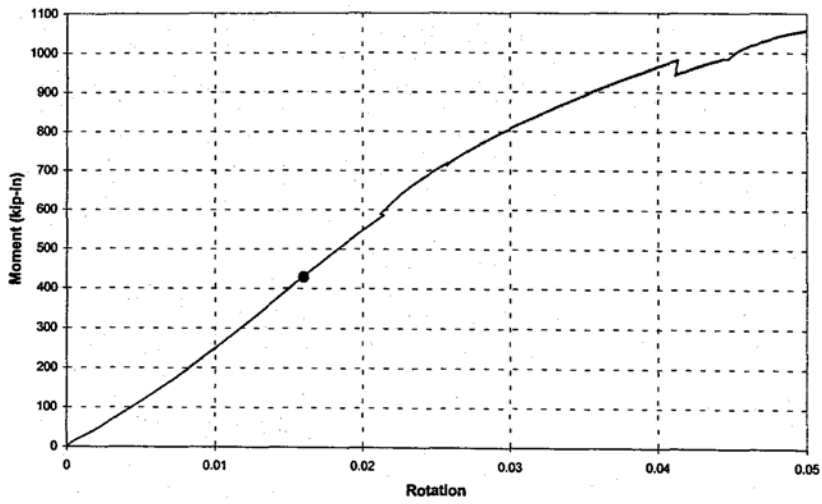
6-3/4-4sW-GS



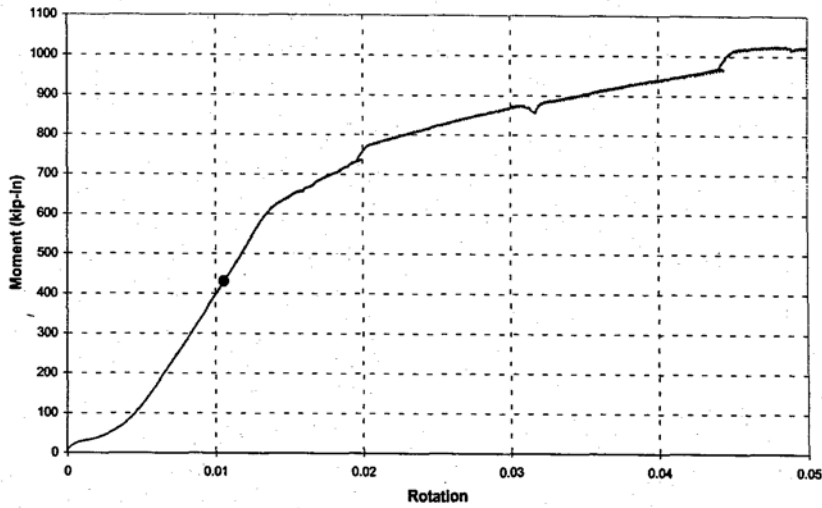
6-3/4-4s-GS



8-3/4-10-G



8-3/4-10-U



LIST OF REFERENCES

- AISC Manual of Steel Construction Load & Resistance Factor Design, Second Edition, American Institute of Steel Construction, Inc., USA, 1995.
- Building Code Requirements for Structural Concrete (ACI 318-95) and Commentary (ACI 318R-95), American Concrete Institute, Farmington Hills, MI, 1995.
- Cannon, R. W., "Flexible Baseplates: Effect of Plate Flexibility and Preload on Anchor Loading and Capacity," *ACI Structural Journal*, American Concrete Institute, V. 89, No. 3, May-June 1992, pp. 315-324.
- Cook, R. A., Ellifritt, D. S., Schmid, S. E., Adediran, A., and Beese, W., "Design Procedure for Annular Base Plates," Research Report No. 95-4, Engineering and Industrial Experiment Station, University of Florida, Gainesville, Florida, 1995.
- Cook, R. A., Hoit, M. I., and Nieporent, S. B., "Deflection Calculation Model for Structures with Annular Base Plates," Research Report No. 98-1, Engineering and Industrial Experiment Station, University of Florida, Gainesville, Florida, 1998.
- Cook, R. A., Tia, M., Fischer, K. B., Darku, D. D., "Use of Grout Pads for Sign and Lighting Structures," Research Report No. BB-512, Engineering and Industrial Experiment Station, University of Florida, Gainesville, Florida, 2000.
- Cook, R.A., and Klingner, R.E., "Behavior and Design of Ductile Multiple-Anchor Steel-to-Concrete Connections," *Research Report No. 1126-3*, Center for Transportation Research, University of Texas at Austin, Austin, Texas, 1989, pp.16-26, 111-112.
- Cook, R.A., and Klingner, R.E., "Ductile Multiple-Anchor Steel-to-Concrete Connections," *Journal of Structural Engineering*, American Society of Civil Engineers, V. 118, No. 6, June, 1992, pp. 1645-1665.
- DeWolf, J.T., Design of Column Base Plates, American Institute of Steel Construction, Chicago, Illinois, 1991, pp. 2-3, 18-24.
- DeWolf, J.T., and Sarsley, A., "Column Base Plates with Axial Loads and Moments," *Journal of the Structural Division*, American Society of Civil Engineers, V. 106, No. ST11, November, 1980, pp. 2167-2184.
- Specifications for Cantilever Signal Structures, Florida Department of Transportation Structures Design Office, Tallahassee, 1996.

Standard Specifications for Structural Supports for Highway Signs, Luminaries, and Traffic Signals (draft), AASHTO, Birmingham, Alabama, 1997.

Targowski, R., Lamblin, D., and Guerlement, G., "Baseplate Column Connection under Bending: Experimental and Numerical Study." *Journal of Constructional Steel Research*, Elsevier Science Publishers Ltd., V. 27, 1993 pp. 37-54.

Thambiratman, D.P., and Paramasivam, P. "Base Plates Under Axial Loads and Moment," *Journal of Structural Engineering*, American Society of Civil Engineers, V. 112, No. 5, May, 1986, pp. 1166-1181.

Westergaard, H. M., "Computation of Stresses in Bridge Slabs Due to Wheel Loads," U.S. Bureau of Public Roads, V. 11, No. 1, March 1930, pp. 1-23.